Veðurstofa Íslands

Design-flood estimates from daily runoff simulations using the Icelandic Reanalysis (ICRA): estimating extremes in gauged and ungauged areas.

Andréa-Giorgio R. Massad
Bergur Einarsson
Tinna Þórarinsdóttir
Matthew J. Roberts

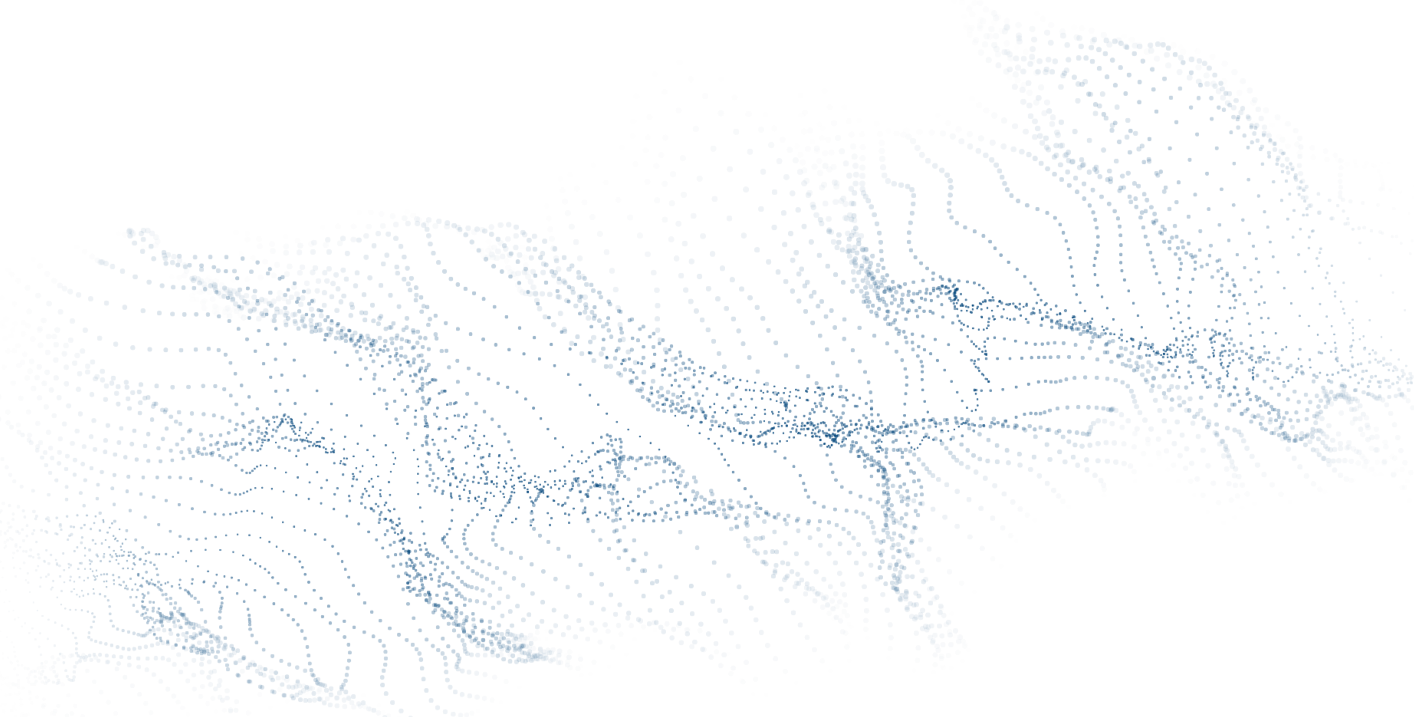

Skýrsla

VÍ 2024-011

Veðurstofa Íslands

Design-flood estimates from daily runoff simulations using the Icelandic Reanalysis (ICRA): estimating extremes in gauged and ungauged areas.

Andréa-Giorgio R. Massad
Bergur Einarsson
Tinna Þórarinsdóttir
Matthew J. Roberts

Veðurstofa Íslands
Bústaðavegur 7–9
105 Reykjavík

+354 522 6000
vedur@vedur.is

Skýrsla
VÍ 2024-011

Lykilsíða

Skýrsla nr.: 2024-011

Dags.: 31 Dec 2024

ISSN: 1670-8261

Dreifing: Opin ☒ Lokuð ☐

Skilmálar:

Upplag: Rafræn útgáfa

Fjöldi síðna: 81

Heiti skýrslu:

Design-flood estimates from daily runoff simulations using the Icelandic Reanalysis (ICRA): estimating extremes in gauged and ungauged areas

Framkvæmdastjóri sviðs:

Matthew J. Roberts

Höfundar:

Andréa-Giorgio R. Massad, Bergur Einarsson, Tinna Þórarinsdóttir, Matthew J. Roberts

Verkefnisstjóri:

Tinna Þórarinsdóttir

Verknúmer:

4812-0-0001

Gerð skýrslu/verkstig:

Málsnúmer:

2023-0078

Unnið fyrir:

Rannsóknasjóð Vegagerðarinnar

Samvinnuaðilar:

Útdráttur:

Extreme flood estimates are crucial for designing hydraulic infrastructure, including bridges, culverts, highways, and stormwater drains. This study presents an initial attempt to estimate extreme flood values using simulated runoff from the ICRA reanalysis data. Runoff is first converted into discharge and compared to measurements from 40 streamflow gauging stations across Iceland. A hierarchical cluster analysis identifies groups of stations that cluster similarly based on observed and simulated discharge, and cluster-based corrections are applied to address systematic overestimation in the simulated dataset. An Extreme Value Analysis shows that after correction, return level estimates from simulations align more closely with observations in most cases. The results indicate that, after correction, estimated extreme discharge values based on catchment-accumulated runoff from the ICRA dataset strongly agree with observed extreme discharge. The study's findings are further evaluated on ungauged rivers to estimate flood return levels in locations without measurements, and for additional comparison, flood estimates were also calculated for five rivers using hydrological simulations based on the GR6J model combined with the CemaNeige module.

Lykilorð:

Flood analysis, hierarchical clustering, ungauged rivers, hydrological modelling.

Undirskrift framkvæmdastjóra sviðs:

Matthew Roberts

Undirskrift verkefnisstjóra:

TÞ

Yfirfarið af:

PC

Contents

Samantekt helstu niðurstaðna

Mikilvægt er að geta stuðst við niðurstöður flóðagreiningar við hönnun innviða nærri straumvatni, svo sem brúa, ræsa, vega og fráveitukerfa. Í rannsókninni sem hér er kynnt voru kannaðir möguleikar þess að meta stærð aftakaflóða út frá hermdu afrennsli úr ICRA veðurendurgreiningunni. Í fyrsta skrefi var afrennsli úr endurgreiningunni breytt yfir í rennsli fyrir 40 vatnasvið þar sem samfelldar rennslismælingar eru tiltækar. Stigskipt klasagreining var svo nýtt til að kann klasaskiptingu rennslisraðanna, bæði fyrir mældu og hermdu raðirnar. Næst var leiðréttingarstuðull metinn fyrir hvern klasa, sem leiðréttir ofmat afrennslis í hermdu röðinni. Ofmatið í hermdu röðunum er tilkomið vegna þess að ekki er gert ráð fyrir írennsli í reikningunum á þeim. Að lokum voru bæði mældu og hermdu raðirnar flóðagreindar. Samanburður á niðurstöðum sýnir að í flestum tilfellum bætir notkun klasaháðs leiðréttingastuðuls samræmið á milli niðurstaðnanna sem byggja á mældum og hermdum gögnum. Almennt sýna þessar niðurstöður að hægt er meta aftaka flóð, fyrir gefið vatnasvið, með leiðréttu afrennsli úr ICRA endurgreiningunni. Þessari aðferðafræði er svo beitt í tilraunaskyni til að meta flóðahætti 20 ómældra vatnasviða. Til frekari samanburðar, á mögulegum aðferðum til að meta flóð ómældra vatnasviða, var einnig prófað að flóðagreinar 5 líkanreiknaðar rennslisraðir fyrir mæld vatnasvið. Notast var við GR6J afrennslislíkanið með CemaNeige einingu til að herma snjósöfnun og leysingu. Þetta líkan er hluti af airGR líkan pakkanaum. Flóðagreining þessum á líkanreiknuðu rennslisröðum skilaði einnig ásættanlegum niðurstöðum, samanborið við flóðagreiningu á mældum rennslisröðum af sömu vatnasviðum.

1 Introduction

Extreme flood estimates are important in the design of hydraulic infrastructure, including highways, stormwater drains, bridges and culverts. In Iceland, numerous examples of damaging floods occurred over recent years, including widespread flooding in southeast Iceland in September 2017, or a 50-year flooding in the north of the country in June 2021.

While flood return levels have been calculated, based on measurements from the Icelandic gauging network (Hróðmarsson and Þórarinsdóttir, 2018), most recent research on extremes at IMO have been focussing on precipitation. A recently published study by Massad *et al.* (2020) reassessed precipitation return levels in Iceland, resulting in a new national map of 24-hour precipitation thresholds for a 5-year event. The 2020 study was based on hourly precipitation data made available by the Icelandic reanalysis of atmospheric conditions, known as the ICRA dataset (Nawri *et al.*, 2017). The ICRA dataset was derived from the HARMONIE numerical weather prediction model, providing access to various atmospheric parameters from over 11,000 grid-points at 2.5 km horizontal resolution. The dataset begins in 1979, providing over 38 years of hourly data.

While extreme precipitation such as those calculated for the 1M5 map can lead to notable floods, all events are not necessarily rainfall driven. Therefore, in this study, the runoff estimated from the ICRA dataset is investigated using the same extreme-value approach by Massad *et al.* (2020) and Þórarinsdóttir *et al.* (2021). Defined here as the sum of liquid precipitation and snowmelt minus evaporation, the runoff variable is suggested as a new means for calculating design-flood estimates at any non-glaciated grid-point in Iceland. As the dataset covers the whole country, it would allow flood return-levels to be estimated for ungauged catchments, enabling small-scale engineering assessments of runoff extremes at virtually any location.

Extreme flood estimates from ungauged catchments are challenging. In fact, such estimates represent one of the leading problems in flood hydrology. In several recent studies, IMO has investigated methods for estimating flood return levels in ungauged basins, including simulations using the WaSIM hydrological model in the Westfjords and Tröllaskagi regions (Crochet and Þórarinsdóttir, 2014). An index-flood method was also tested in the Eastfjords, leading to promising initial results (Crochet and Þórarinsdóttir, 2015). With the increasing dependence on Iceland's road infrastructure, combined with the uncertainties of rapid climate change, there is a need to develop updated design-flood methods for rapid and widespread assessments. This project is a first step towards delivering such a methodology.

Building on those previous research projects, the goal of this study is to investigate how accurately can the ICRA runoff estimate flood extremes, and how this variable can be used to derive extreme streamflow values in ungauged areas. The project will follow several steps:

1. Firstly, daily runoff from the ICRA will be extracted for 40 gauged catchments where discharge measurements have been recorded for more than 20 years as well as for 20 ungauged rivers.
2. In a second step, several hierarchical clustering of selected catchments will be presented: one based on the measurement timeseries, and others based on simulated discharge, only for gauged rivers with the aim of determining which catchments cluster similarly in both analyses.
3. Flood extremes will then be calculated based on both datasets using the Block Maxima method.
4. A cluster-based correction will be proposed to improve the extreme streamflow derived from the ICRA data.

5. Finally, these corrections will be applied to the ungauged rivers, based on the clustering results obtained with the simulated runoff data, offering a step towards the estimation of flood extremes in ungauged areas.
6. For further comparison, five gauged rivers will be selected and flood extremes calculated after simulating their discharge with the airGR rainfall-runoff model.

2 Catchment selection

Iceland counts thousands of rivers of various lengths. While discharge in around 200 rivers has been measured for some period, many rivers remain ungauged. For this study, the goal is to mix gauged rivers with ungauged ones, with a focus on catchments in the vicinity of roads and infrastructure.

2.1 Selection of the gauged rivers

Since the first discharge gauging stations were set up in Iceland, the gauging network has expanded to record most of the major rivers in the country. The gauging stations allow for high-resolution measurements down to 10-minute intervals, or even shorter in times of rapid discharge changes.

For this study, only stations with timeseries longer than 20 years were selected, which amounted to a total of 44 rivers (Figure 1). Those stations were previously used for testing and calibrating the hydrologic model airGR (Atlason *et al.*, 2021) as well as for the analogue forecast set up for Vegagerðin (Priet-Mahéo *et al.*, 2020 and 2021). On Figure 1, the gauging stations and their associated catchments are shown on a map of Iceland, with a colour code indicating their river type. This classification of the rivers first appeared in Rist (1990) and was later used by Hróðmarsson *et al.* (2009, 2020) as well as in Hróðmarsson and Þórarinsdóttir (2018). According to that grouping, four kinds of rivers exist in Iceland; although, in reality, they are often a combination of two or three different types. In the North, East and in the Westfjords, direct-runoff rivers (18 catchments, in green on the figure) lie on old, rather impermeable bedrock. On newer bedrock, spring-fed rivers (17 catchments, in blue on the figure) are dominant. Mostly fed by Vatnajökull, seven rivers are classified as glacial rivers (in grey). Finally, two catchments are primarily considered as lake rivers (in orange). Four gauging stations associated with the rivers Skaftá and Kreppa (VHM 70, VHM 183, VHM 233, and VHM 328) are qualified as jökulhlaup rivers, and cannot be forecasted with this method because they are not of meteorological origin. They were therefore discarded in this study, lowering the number of rivers selected to 40. However, it should be noted that those four jökulhlaup rivers are still shown in Figure 1.

Table 1 shows the main characteristics of the gauged catchment areas selected for this study. Included are the area, aspect ratio, longest flowpath, average elevation, as well as percentage of glacial cover, old bedrock (superior to 0.8 million years old), young bedrock, and total bedrock. Catchment areas vary greatly among catchments, ranging from 37 km^2 (VHM 92 – Bægisá) to 7313 km^2 (VHM 30 – Þjórsá). Þjórsá also is the longest river among this selection, with a flowpath above 238 km. Out of the 40 catchments, 16 are partly covered by glaciers, among them eleven have a glacial cover superior to 10%. Eleven catchments have a mean elevation above 700 m.a.s.l., indicating a catchment area spreading into the Highlands. As reflected in Figure 1 by the river classification, old bedrock is mostly present in the watersheds located in the North as well as in the East- and Westfjords. This bedrock, formed in the Tertiary and Early Quaternary, has relatively low permeability, therefore leading to minimal infiltration with most of the precipitation flowing off as surface runoff (Sigurðsson and Einarsson, 1988). For catchments located on younger bedrock (formed in the Late Quaternary), infiltration is higher. In this study, seven catchments contain more than 80% young bedrock.

Table 1 – Main characteristics of the river catchments used for the cluster analysis. Note that the number of significant figures is kept higher in this table than is warranted by the accuracy of the input data, for the sake of completeness or later use for reclassification.

VHM	**Area** *km^2*	**Aspect ratio**	**Longest flowpath** *m.*	**Average Elevation** *m a.s.l.*	**Glacial cover** *%*	**Old bedrock** *%*	**Young bedrock** *%*	**Bedrock** *%*
10	396.1	2.96	55,167	527	0	99.2	0.5	99.7
12	164.7	1.74	31,960	408	0	96.8	0	96.8
19	38.4	1.7	15,040	510	0	100	0	100
26	266.3	3.36	64,555	387	0	61.3	38.7	100
30	7313.5	2.57	247,279	702	13.22	15.5	66	81.5
38	42.8	2.39	20,971	428	0	100	0	100
43	640.7	1.73	50,958	307	0	3.1	96.9	99.9
45	458.3	2.37	58,072	547	0	67.1	32.9	100
48	701.4	1.74	74,306	543	0	48.9	51.1	100
51	299.6	1.87	34,990	723	2.96	97	0	97
59	621.9	2.9	84,104	354	0	0	98.6	98.7
60	419.9	1.92	60,336	572	2.02	0	97.4	97.4
64	5661.9	2.41	169,493	304	11.84	22	62.9	84.9
66	1574.4	2.24	123,017	650	20.3	22.7	53.7	76.4
68	201.1	1.33	35,345	245	0	6.2	93	99.2
81	41.9	2.46	20,560	171	0	38.2	58.5	96.7
83	47.5	1.1	11,878	683	0	100	0	100
92	37.4	1.93	13,904	900	0	77.8	0	77.8
102	5097.1	2.6	189,195	538	28.64	0	71.3	71.3
110	3283	3.31	167,744	878	42.33	44.8	12.6	57.4
116	527.1	1.87	62,858	645	0	1.2	98.8	100
121	183.3	3.6	48,916	209	0	0	100	100
128	513	2.01	58,289	338	0	93.7	1.7	95.4
144	1085.2	1.69	93,866	960	12.88	55.9	28.7	84.6
148	115.1	2.47	28,963	577	0	99.8	0	99.8
149	189.4	3.27	37,033	609	4.83	91	0	91
150	225.9	3.03	45,563	767	40.23	47	12.8	59.8
162	2023.1	2.01	110,507	1,195	56.92	0	43.1	43.1
185	216.8	1.42	31,153	294	0	0	100	100
198	192.9	1.31	31,543	399	0	100	0	100
200	1102.2	3.51	131,238	723	0	97.1	0.4	97.6
204	102.3	2.47	28,106	466	0	100	0	100
205	264.6	2.11	42,434	731	2	82	6	88
206	126.3	2.29	28,303	865	0	100	0	100
218	516.9	1.14	53,731	737	12.22	0	71.7	71.7
238	2163	1.54	118,032	822	4.51	26.5	68.7	95.2
271	1027	2.64	97,404	394	3.35	5	83.3	88.3
400	73.2	1.41	16,634	435	0	100	0	100
408	581.3	1.13	58,363	756	49.27	0	50.7	50.7
411	387.1	3.71	73,405	559	0	97.7	2.3	100

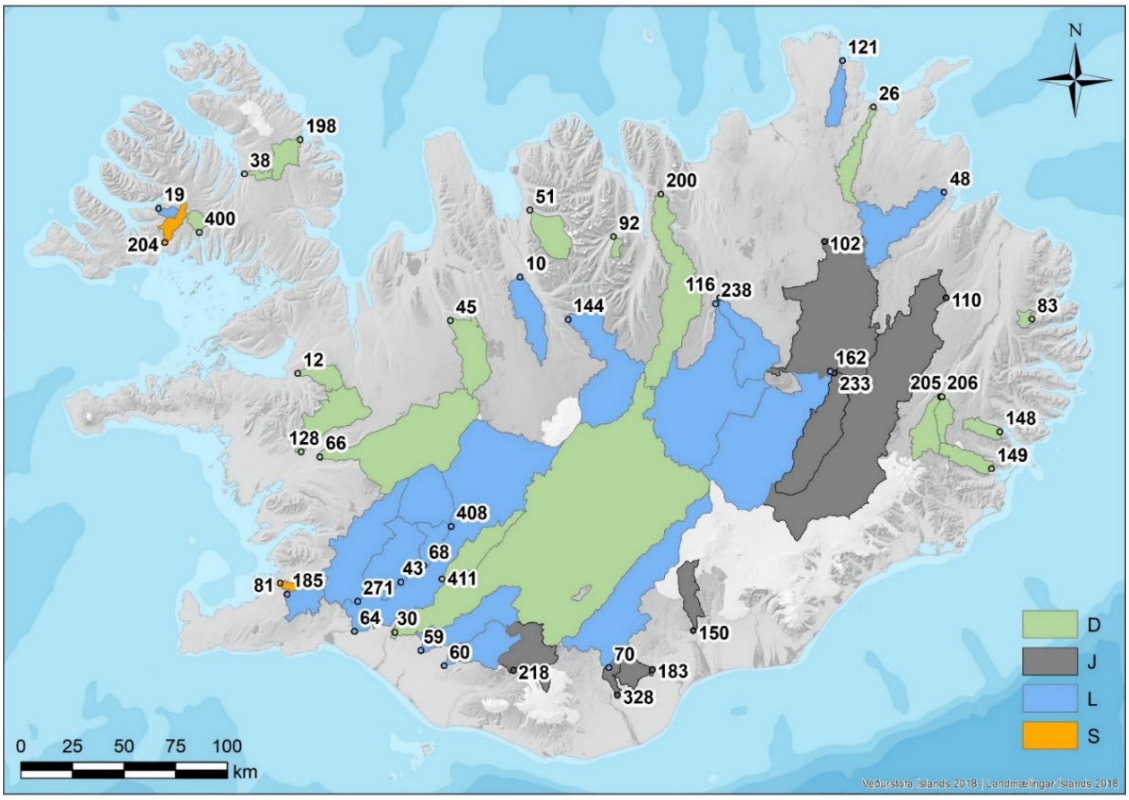

Figure 1 – Location of the gauging stations used in this study, and outlines of the associated catchments. Colour of the catchment areas depends on the type of river: direct-runoff (green), spring-fed rivers (blue), glacial rivers (grey), lake rivers (orange). Map from Atlason et al. (2021).

2.2 Selection of the ungauged rivers

In addition to the 40 gauged rivers presented in Figure 1 and Table 1, 20 ungauged rivers were also selected for this study. Figure 2 shows the location of the 40 gauged rivers in red, and the 20 ungauged rivers in blue. Individual maps were also created for each ungauged catchment and shown in Figure 3.a – 3.d.

These ungauged areas were hand-picked, with the only condition being that they have an area superior to 25 km^2 so that they include at least three grid-points from the ICRA domain. The goal was to cover parts of the country that are currently poorly gauged (Fjarðará, Hellisfljót, Nýjadalsá, Ólafsfjarðará). When possible, rivers which seem of particular interests for Vegagerðin were selected. This is the case for Sléttuá, Flókadalsá and Lágadalsá that are currently flowing under old, one-way bridges. Some others were picked because of new road plans (Steinavötn, in the eastern part of Snæfellsness), or the possibility of future construction plans in the Highland region (Hellisá, Gilsá, Jökulgiskvísl). Overall, Figure 2 shows that combining this selection of gauged and ungauged watersheds leads to a good spatial coverage of the rivers in Iceland.

Table 2 shows the same characteristics as Table 1 for the ungauged catchments. The size of the selected catchments is quite diverse, ranging from 38.4 km^2 (Nýjadalsá) to 730.5 km^2 (Midfjarðará). Three catchments have a mean elevation above 700 m a.s.l. (Hornafjarðarfljót, Jökulgilskvísl, Nýjadalsá), and six are partially covered by glaciers (Hornarfjarðarfljót, Jökulsá í Lóní, Nýjadalsá, Steinavötn, Gilsá, Jökulgilskvísl).

Combining both gauged and ungauged rivers, a total of 61 catchments are used in this study.

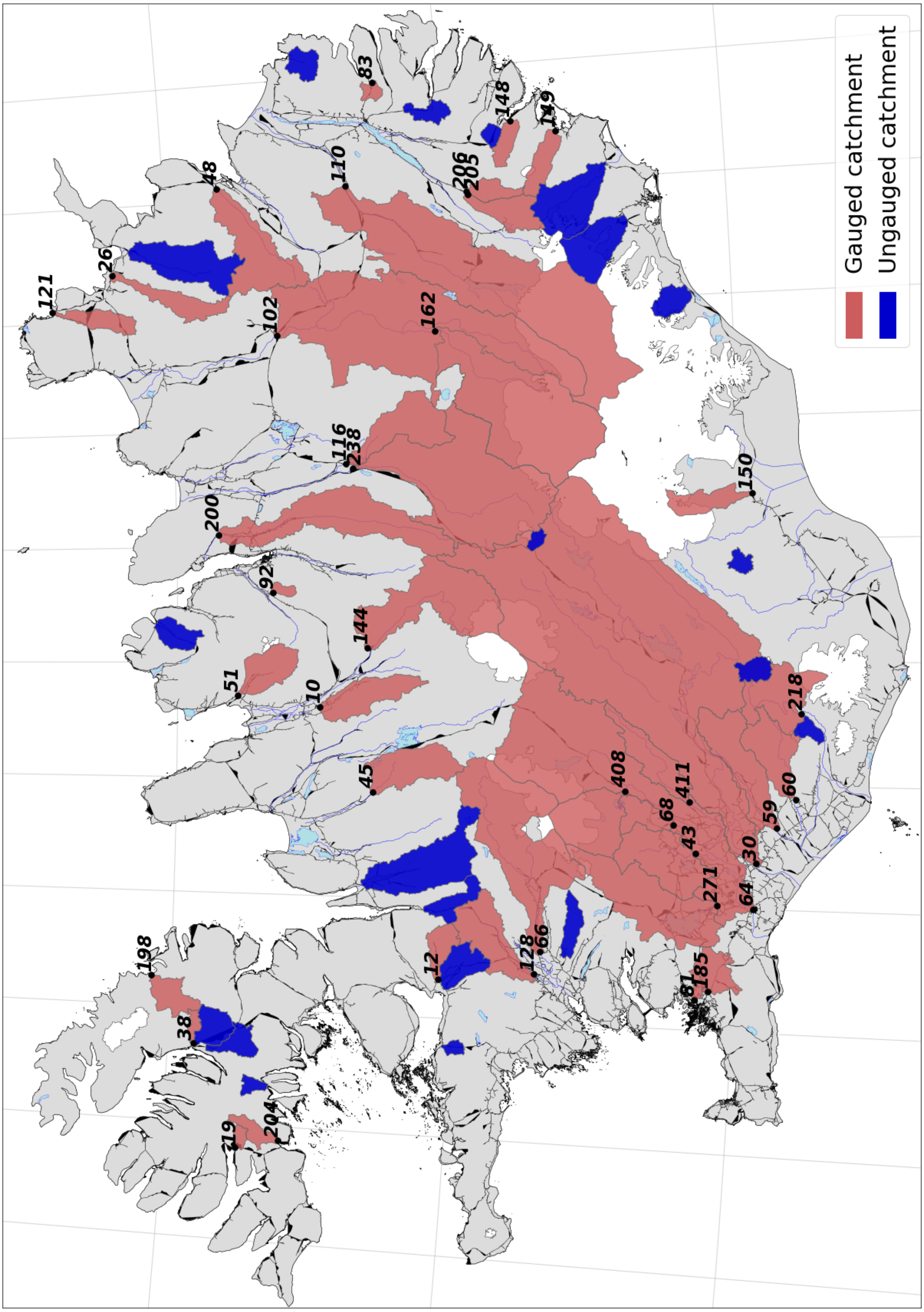

Figure 2 – Catchments selected for this study. Gauged catchments used for the 2022 study are shown in red, ungauged catchments are represented in blue.

Table 2 – Main characteristics of the ungauged catchments used for the cluster analysis. Note that the number of significant figures is kept higher in this table than is warranted by the accuracy of the input data, for the sake of completeness or later use for reclassification.

	Area *km^2*	**Aspect ratio**	**Longest flowpath** *m*	**Average Elevation** *m a.s.l.*	**Glacial cover** *%*	**Old bedrock** *%*	**Young bedrock** *%*	**Total Bedrock** *%*
Berufjarðará	51.3	1.21	15,256	562	0	0	100	100
Fjarðará	126.5	1.06	18,139	361	0	0	100	100
Flókadalsá	141.1	3.22	35,585	357	0.11	72.5	27.4	99.9
Gilsá	70.8	1.43	22,097	622	13.5	78.2	8.4	86.5
Hafralónsá	545.2	2.32	61,735	395	0	14	86	100
Hellisá	64.7	1.19	18,229	542	0	96.3	3.7	100
Hellisfljót	51.4	1.37	14,711	375	0	0	100	100
Hornafjarðarfljót	403.6	1.44	41,579	798	62.1	5.8	31.7	37.5
Hrútafjarðará	160.8	2.07	37,847	329	0	0	100	100
Jökulgilskvísl	107.3	1.49	23,809	816	11	7.7	81.3	89
Jökulsá í Lóni	513.6	1.45	53,786	698	25	3.7	71.3	75
Lágadalsá	179.7	1.06	27,165	390	0	0	100	100
Langadalsá	147.9	1.83	31,086	363	0	0	100	100
Miðá	217.3	1.48	29,833	322	0	4	96	100
Miðfjarðará	730.5	2.2	75,201	326	0	4	96	100
Nýjadalsá	40.7	1.67	14,786	1,128	18.2	78.7	3	81.7
Ólafsfjarðará	155.7	1.7	24,378	493	0	0	98.4	98.4
Sléttuá	105.3	1.85	18,808	564	0	0	100	100
Steinavötn	140.2	1.43	23,484	554	18.1	8.9	73.7	81.9
Svínafossá	38.4	1.52	11,960	156	0	0.5	99.5	100

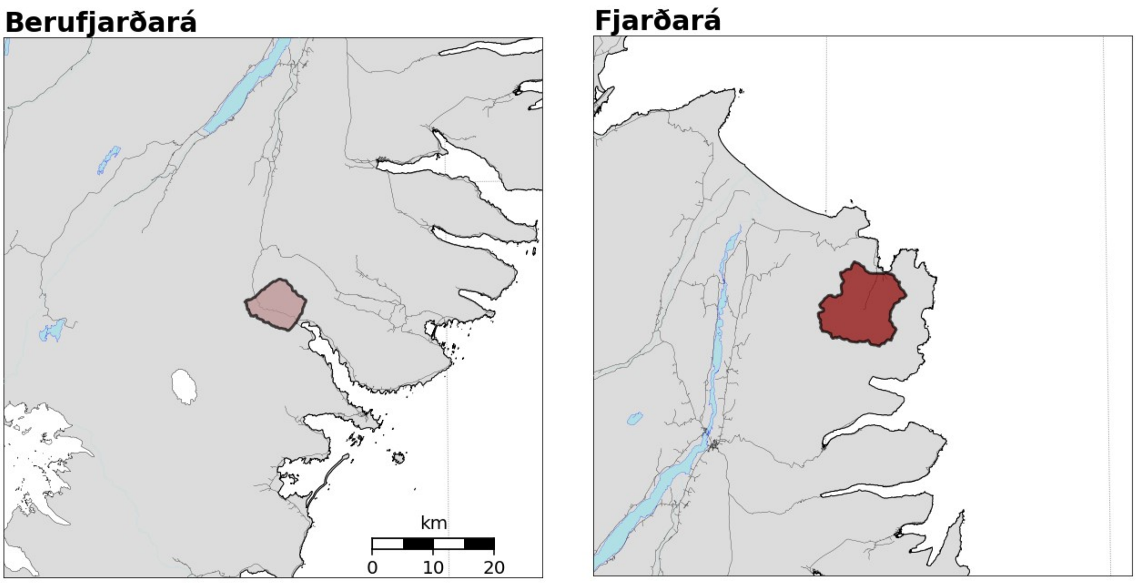

Figure 3.a – Outlines of the ungauged catchments selected for this study (1/4). Scale is only shown for Berufjarðará but is the same for all catchments.

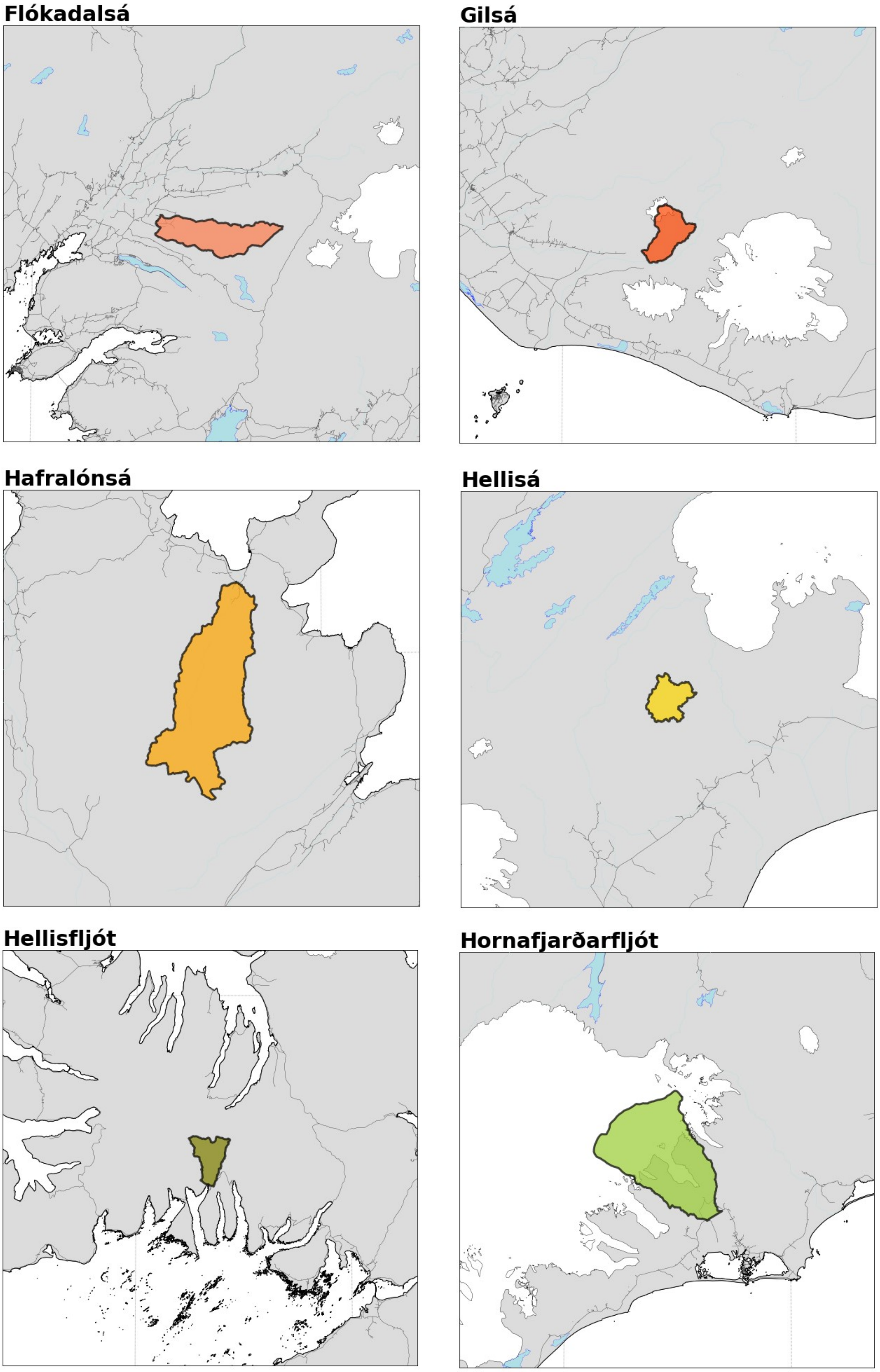

Figure 3.b – Outlines of the ungauged catchments selected for this study (2/4).

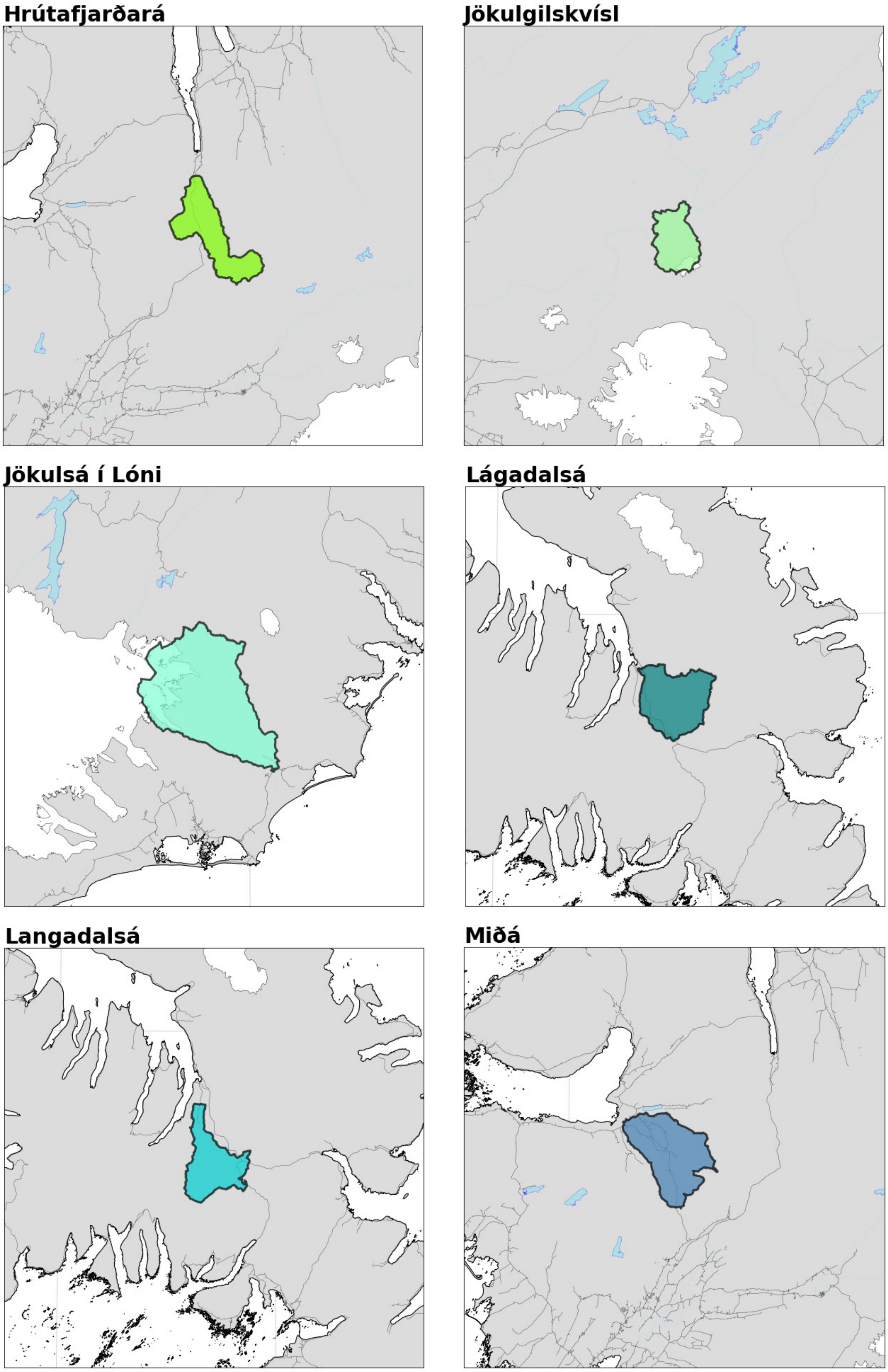

Figure 3.c – Outlines of the ungauged catchments selected for this study (3/4).

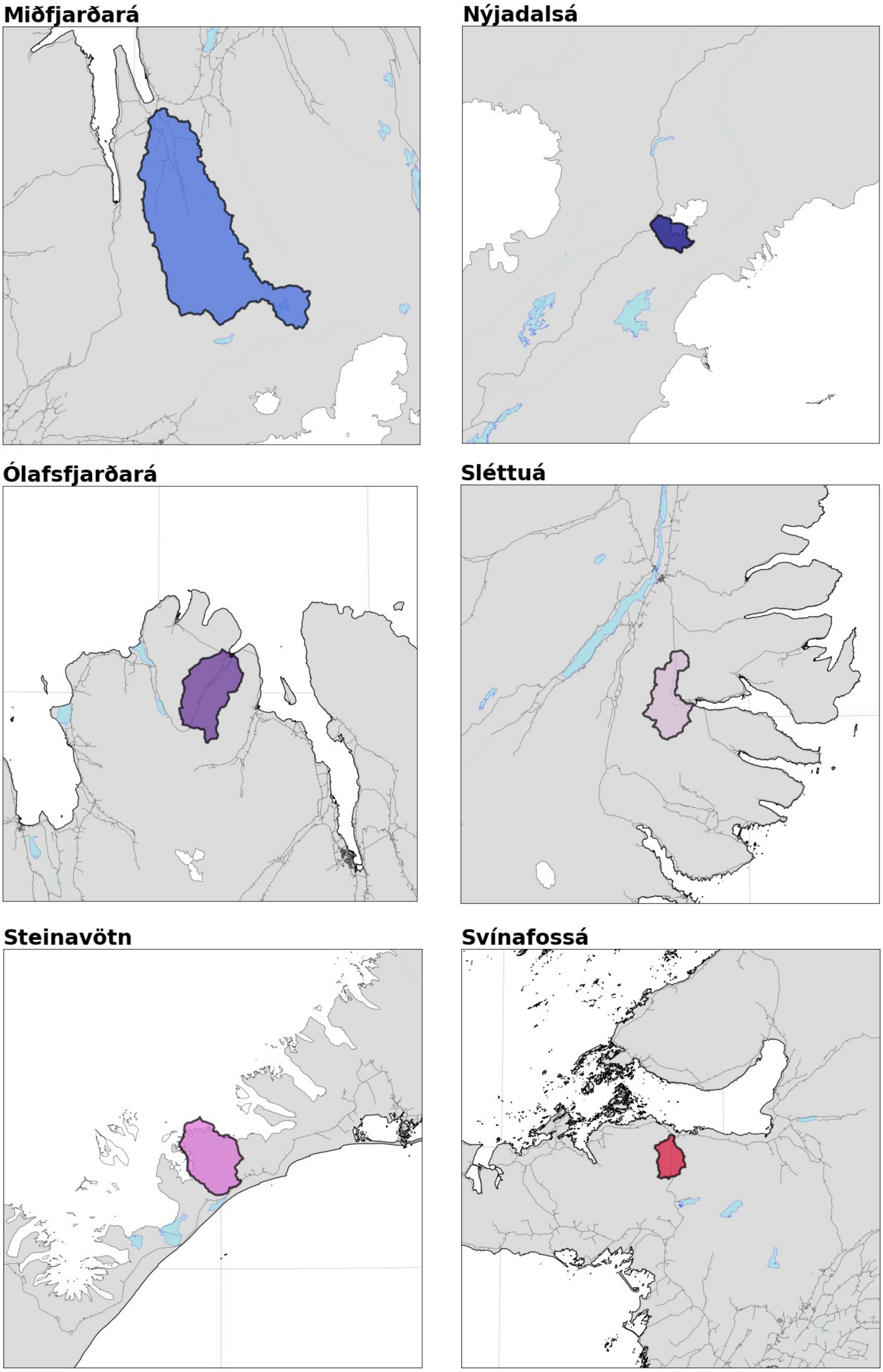

Figure 3.d – Outlines of the ungauged catchments selected for this study (4/4).

3 Data

3.1 Measurements from the gauging station network

As stated in Section 2.1, the gauging network has expanded over the years, now offering high-resolution measurements of all the main Icelandic rivers down to 10-minute intervals. River discharge is not measured directly: the gauges measure the water level, which is then converted into a discharge using flow rating curves. The rating curves are based on discrete discharge measurements that are used to establish the correspondence between water level and discharge. They are quality-checked regularly with discharge measurements, as river path and characteristics may change over time.

Table 3 enlists all the gauged rivers used for this study and indicates the beginning and end year of the observed timeseries along with the number of missing days. Part of the data are flagged as estimation done by specialists at IMO, notably when the rating curves are affected by ice formation in the controlling cross-section of the river. These estimations are assumed to be of acceptable quality and are therefore used in this study.

Only rivers with more than 20 years of data were kept for the analysis. Note that most stations are still recording as of today, but only data until 2017 were needed for this study, to match the reanalysis.

Table 3 – Station list, timeseries available, and number of missing days among that period.

River	Time-period	Missing days	River	Time-period	Missing days
10 – Svartá	1932 – 2017	0	**116 - Svartá**	1985 – 2017	0
12 – Haukadalsá	1950 – 2017	3165	**121 - Ormarsá**	2005 – 2016	0
19 – Dynjandisá	1956 – 2017	789	**128 - Norðurá**	1970 – 2017	1360
26 – Sandá	1965 – 2017	460	**144 - Austari-Jökulsá**	1971 – 2017	0
30 – Þjórsá	1947 – 2017	2564	**148 - Fossá**	1968 – 2017	224
38 – Þverá	1980 – 2017	0	**149 - Geithellnaá**	1971 – 2017	5457
43 – Brúará	1948 – 2017	0	**150 - Djúpá**	1968 – 2017	1
45 – Vatnsdalsá	1948 – 2017	2088	**162 - Jökulsá á Fjöllum**	1984 – 2017	0
48 – Selá	1982 – 2017	0	**185 - Hólmsá**	1980 – 2017	0
51 – Hjaltadalsá	1980 – 2017	0	**198 - Hvalá**	1976 – 2017	1
59 - Ytri-Rangá	1961 – 2015	0	**200 - Fnjóská**	1976 – 2017	0
60 - Eystri-Rangá	2005 – 2017	0	**204 - Vatnsdalsá**	1976 – 2017	4261
64 - Ölfusá	1980 – 2017	0	**205 - Kelduá**	1977 – 2017	2745
66 - Hvítá	1980 – 2017	0	**206 - Fellsá**	1976 – 2017	2956
68 - Tungufljót	1951 – 2017	2023	**218 - Markarfljót**	1982 – 2001	0
81 - Úlfarsá	1956 – 2017	0	**238 - Skjálfandafljót**	1987 – 2017	0
83 - Fjarðará	1958 – 2017	2558	**271 - Sog**	1972 – 2017	0
92 - Bægisá	1980 – 2017	0	**400 - Vattardalsá**	1980 – 2017	0
102 - Jökulsá á Fjöllum	1980 – 2017	0	**408 - Sandá**	1999 – 2017	0
110 - Jökulsá á Dal	1963 – 2017	6194	**411 - Stóra-Laxá**	2000 – 2017	0

3.2 Simulated runoff from the Icelandic Reanalysis

3.2.1 The Icelandic Reanalysis (ICRA), and extraction of the relevant variables

The operational numerical weather prediction (NWP) system used by the Icelandic Meteorological Office (IMO) is the non-hydrostatic HARMONIE–AROME model (Bengtsson *et al.*, 2017). In 2017, the model was used to reanalyse atmospheric conditions in Iceland at hourly time-steps between September 1979 and August 2017. This dataset, known as the Icelandic Reanalysis (ICRA) dataset (Nawri *et al.*, 2017), has a horizontal resolution of 2.5 × 2.5 km and 65 vertical levels, for a total of 66,181 points on land over Iceland.

As in most NWP systems, runoff (*ro*) is not a direct output from the model, but it is a combination of three variables: the rainfall rate (*rf*), the rate of evaporation (*evap*) and the melting (*mlt*). Hourly runoff can therefore be calculated as:

$$ro = rf + mlt - evap$$

It should be noted that the melting variable is also an undirect product of the model resulting from the combination of sleet- and snowfall rates, sublimation, and snow water equivalent. Therefore, in total, six variables need to be extracted from the reanalysis in order to estimate the daily runoff.

Based on the 2.5 km horizontal resolution of the dataset, timeseries were extracted for the watersheds by summing the runoff from all grid-points within the catchment outlines. By summing the runoff for each day, a daily runoff timeseries was created for each catchment, for the nearly 40 years of the reanalysis.

3.2.2 Conversion of runoff into discharge

To compare with the daily discharge timeseries from the gauges, the estimated daily runoff needs to be converted into a simulated discharge for each catchment. The main assumption is that during an extreme hydro-meteorological event, a peak of daily runoff will trigger a peak of daily discharge at the catchment's outlet. In this study, these daily peaks are not necessarily expected to be synchronous, and a lag-time may exist, depending on the catchment's characteristics and the type of flood event.

In order to take into account infiltration and other processes taking place on the catchment, extreme daily runoff is converted into extreme daily discharge as follows:

$$Q(m^3s^{-1}) = C * \frac{runoff(mm) * 0.001 * cell\ area(m^2)}{60 * 60 * 24}$$

This formula is close to the rational equation (Roberson *et al.*,1998), that has been used to estimate design floods from simple rainfall-runoff relationships. Here, the extreme runoff coefficient *C* varies with catchment characteristics. It is not determined right away: first simulated discharge are calculated using this formula without the correction coefficient. *C* is later evaluated by comparing the 5% highest converted runoff values to the 5% highest discharge values measured by the gauge at the catchment's outlet. This runoff coefficient serves as a correcting factor, and is usually expected to be lower than 1, except perhaps in large groundwater-fed rivers where it could be greater than 1. The values taken by this coefficient will be calculated later in this study.

4 Cluster Analysis

4.1 Methodology

Over the years, several types of classifications have been developed with the aim of grouping rivers together according to their type. In 2014, rivers were classified based on the geology of the catchments and the presence of lakes and bogs (Stefánsdóttir *et al.,* 2014), while Rist (1990), and Hróðmarsson and Þórarinsdóttir (2018) based their classification on observations made over more than 50 years of field measurements. More recently, a hierarchical cluster analysis has been used to categorize rivers in groups that share more similarities than with a river from other groups. This analytic method was previously used by Crochet (2012) and was adapted for Icelandic rivers in two previous Vegagerðin-funded projects (Priet-Mahéo *et al.*, 2019 and 2021). According to Demirel and Kahya (2007), the Ward's method based on Euclidean distances is well suited when performing a cluster analysis for hydrological data and is therefore used here.

In this research, the dataset used for clustering is comprised of discharge timeseries and several independent catchment characteristics listed in Tables 1 and 2. For the discharge timeseries: both measurements and simulated discharge as calculated from the ICRA runoff without correcting factor *C* are used, and only values between 2007 and 2017 are kept in order to work with a homogeneous set of data. These data are then combined in three different ways, each method reflecting a different behaviour of the river:

- *Seasonality.* Discharge is averaged over the whole timeseries by Julian day, emphasizing the seasonal pattern of each river. For each catchment, only monthly-averaged discharge is kept so that only the general trend is kept in the analysis, as weekly variations are unrelated to the type of river and rather reflective of punctual weather conditions.
- *Flow-duration curves*. Discharge is ranked decreasingly and then plotted against 10% exceedance steps to create flow-duration curves. Those graphs express how often a discharge level is exceeded, providing a good indication of the river's power potential.
- *Mass curves*. Discharge is averaged over the whole timeseries by Julian day and then summed cumulatively over day of year. Monthly differences are then computed between cumulated discharge. Constant values would be obtained if the discharge remained constant all year long or the difference in values will indicate the seasonality in the mass curve.

An example of each discharge plot is shown in Figure 4 for the river Dynjandisá (VHM 19), in the Westfjords. On the top panel, the seasonality plot is shown based on daily-averaged values (grey line) and monthly-averaged values (black line). For the cluster analysis, as mentioned previously, only the monthly values were used. Contrarily to those figures, it should also be noted that discharge timeseries were normalised between 0 and 1 before being processed, in order to facilitate the comparison between rivers with different average discharge.

Additionally, the various catchment characteristics from Tables 1 and 2 were added to complete the analysis, including the area, aspect ratio, longest flow-path, mean elevation, and geological properties.

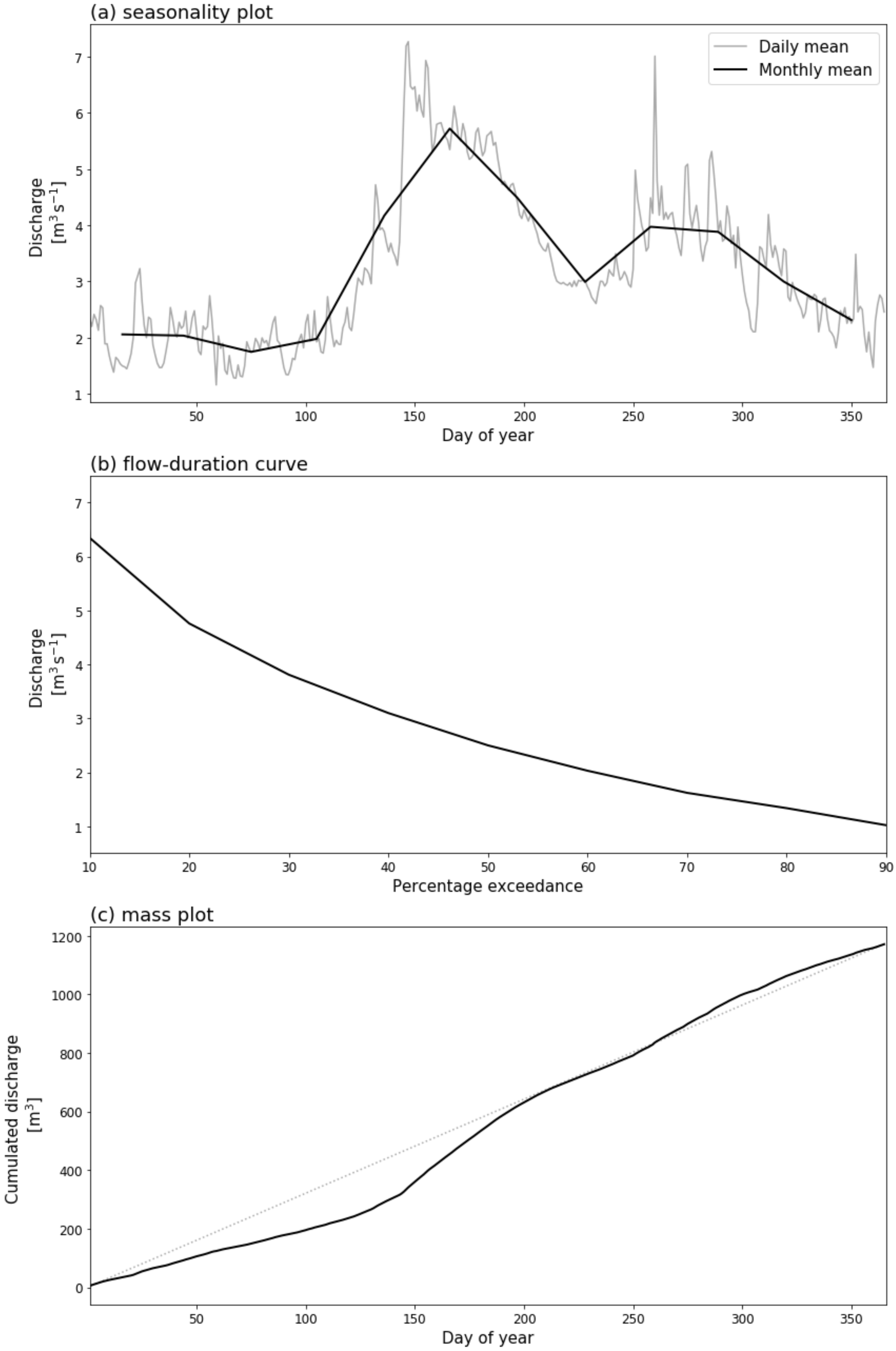

Figure 4 – Discharge timeseries for station VHM 19 as used in the cluster analysis: (a) seasonality plots, shown for both daily-averaged discharge (grey line), and monthly-averaged discharge (black line). (b) flow-duration curve with 10% exceedance steps. (c) mass curve (black line) showing daily-averaged cumulated discharge over the year, with the grey-dashed line indicating values if the discharge was constant.

The cluster analysis was performed both based on measurements, and on simulated discharge (before adjustment with coefficient *C*), to analyse the difference between clustering within both datasets. Results are presented on two dendrograms, shown in Figure 5. For both datasets, the cophenetic distances are close, with a value around 0.8. The cophenetic distance is an indicator of the correlation between distance and cophenetic matrices resulting from the cluster analysis. As it approaches the value of 1, it can be concluded that in the two analyses, data were clustered successfully.

In the figure, it is decided to keep five clusters, and vertical bars are drawn on the dendrograms at a distance value of 2.5 and 2.8. The following stations belong to the same clusters in both analyses:

- *Cluster A:* VHM 43, VHM 59, VHM 68, VHM 81, VHM 185, VHM 271
- *Cluster B:* VHM 19, VHM 38, VHM 51, VHM 83, VHM 92, VHM 148, VHM 149, VHM 198, VHM 200, VHM 204, VHM 205, VHM 206, VHM 400
- *Cluster C:* VHM 10, VHM 12, VHM 45, VHM 128, VHM 411
- *Cluster D:* VHM 102, VHM 110, VHM 150, VHM 162, VHM 408
- *Cluster E:* VHM 116, VHM 48, VHM 238

Those stations were generally classified according to river types, and weather conditions. Cluster A mostly gathers groundwater-fed rivers, some of them partly of a glacial origin and located on the southwestern part of Iceland. In Cluster B, most of the rivers are direct runoff, influenced by snowmelt, and located in the northern half of Iceland. Cluster C is more difficult to describe and quite mixed, with rivers located in the western part of the country, sometimes controlled by small ponds and lakes. Cluster D comprises glacial rivers, and all watersheds are partially covered by glaciers. Finally, in Cluster E, rivers are mainly groundwater-fed, which accounts for a large part of the baseflow. Difference with Cluster A comes from the geographical location of these rivers: in the northeastern quadrant for Cluster E, and in the southwestern part of Iceland for Cluster A.

For further insights into the clustering process, normalised seasonality plots (similar to Figure 4.a) are shown for each cluster, based on measured (Figure 6.a) and simulated (Figure 6.b) discharge. Normalisation was done by scaling the values between 0 and 1. Within each cluster, mean monthly values are drawn with a solid line, and the minimum-maximum interval is shown with a shaded area. For each cluster, the seasonality plots show very distinctive trends, indicating that river with the same behaviour were successfully clustered together by the analyses. For instance, in Cluster A, maximum discharge for all stations reaches its peak during the winter months, and a low point in August. The trend is completely different for Cluster D, with maximum discharge reached at the end of the summer. This is typical of glacial rivers: melting increases over the summer months due to the decreased albedo of snow, temperature rise, and exposure of glacial ice from beneath the winter snow. The discharge in the river therefore slowly increases. For Cluster C and E, the trends are similar in both analyses, with two peaks being reached: one in springtime and the other one in the fall. The general pattern for stations belonging to Cluster B differ between both analyses, which might be attributed to the fact that it is the largest cluster with 13 rivers. Another hypothesis could be that processes such as infiltration and water retention by the snowpack in winter months are not taken into account by the formula that convert runoff into discharge and can account for the differences between rivers in this cluster.

Eight of the 40 selected rivers did not cluster in the same way in both analysis: VHM 26, VHM 30, VHM 60, VHM 64, VHM 66, VHM 121, VHM 144, and VHM 218. It should be noted that VHM 30, VHM 60, VHM 64, VHM 121, and VHM 218 belong to Cluster E while using the measured discharge, but they all belong to Cluster A when the analysis is based on the simulated discharge. According to both dendrograms, Cluster A and E are quite distant from one another.

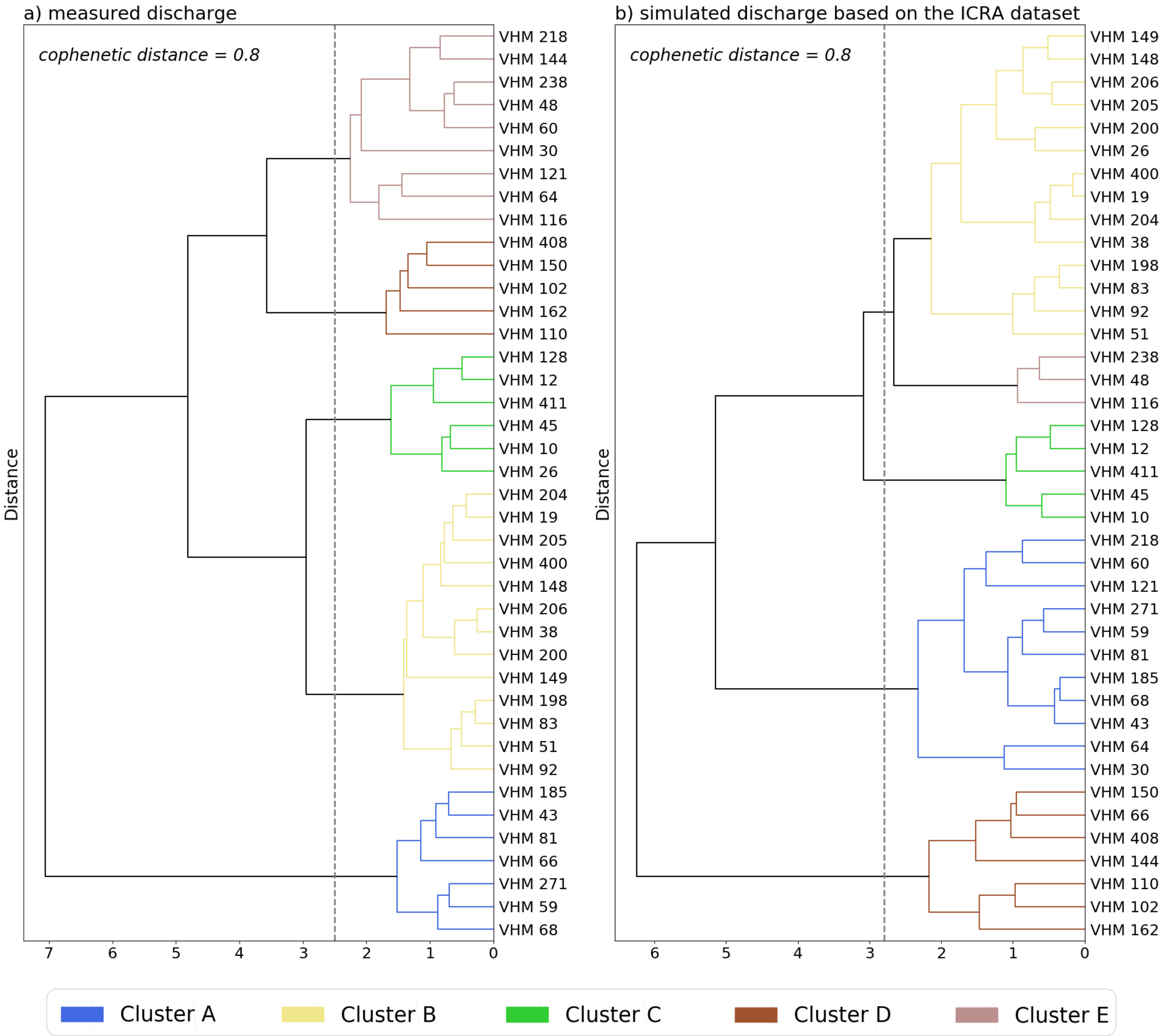

Figure 5 – Dendrograms resulting from the cluster analysis on measured (left, a) and simulated (right, b) discharge timeseries.

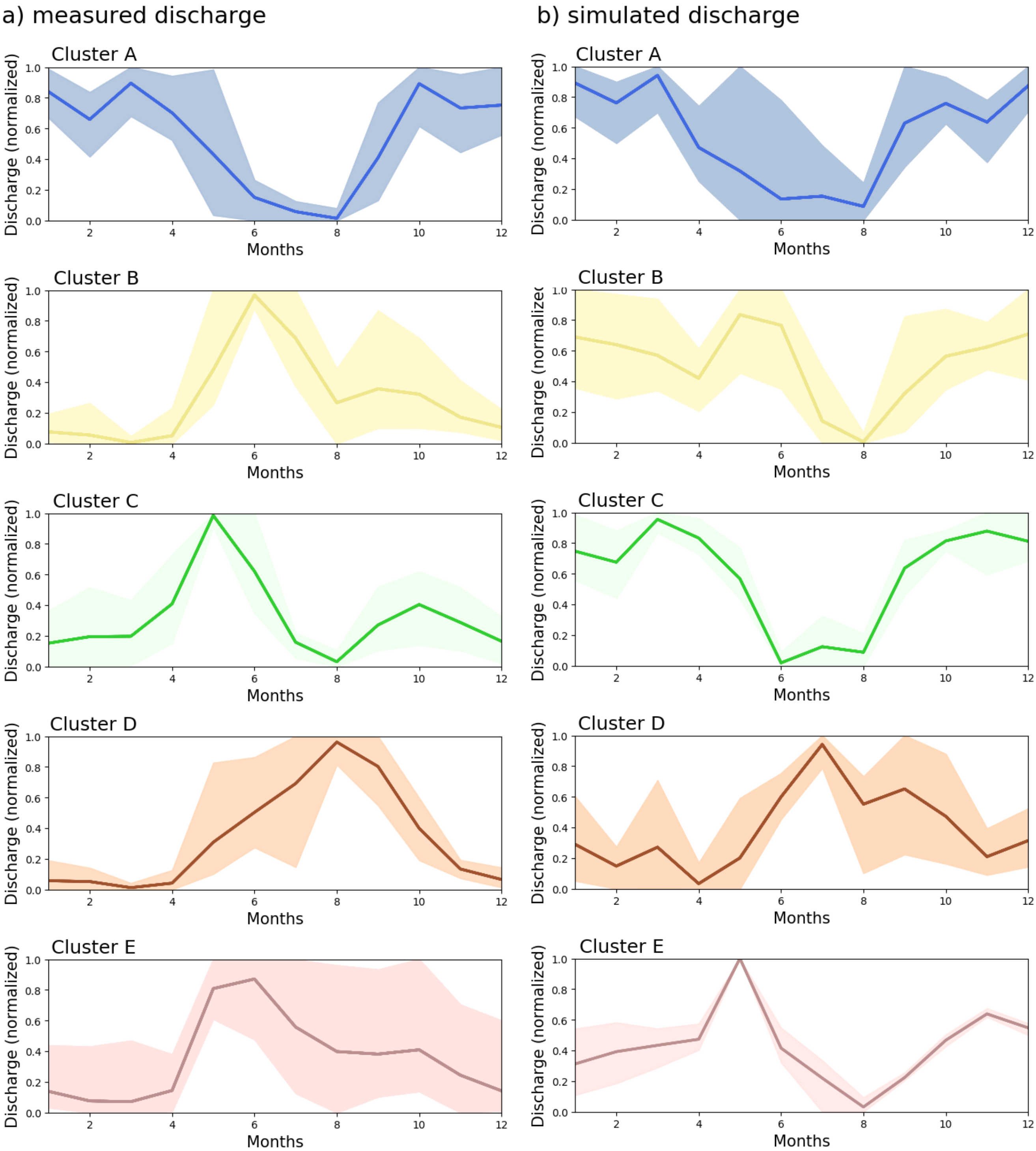

Figure 6 – Seasonality plots for each cluster, based on normalised discharge timeseries from measurements (left, a) and simulated by the ICRA dataset (right, b). For each cluster, mean monthly values among all the stations belonging to the same cluster are shown with the solid lines, and the minimum-maximum intervals are shown with the shaded area.

4.2 Results including the ungauged catchments

After obtaining discharge timeseries from the ICRA dataset for the 20 ungauged rivers, the same methodology was carried out to include the ungauged catchments in the analysis: flow-duration and mass curves, as well as seasonality timeseries were obtained, and added to the cluster analysis with the 40 simulated discharge timeseries from the gauged rivers. Additional catchment information as shown in Table 2, were combined to the characteristics from the gauged catchment (Table 1), and the hierarchical cluster analysis performed. Results from the dendrogram are shown in Figure 7. In this case, the cophenetic distance reach a value of 0.7. To be consistent with Figure 5, it was decided to only keep five clusters:

- *Cluster A:* VHM 185, VHM 68, VHM 43, VHM 271, VHM 59, VHM 81, VHM 60, VHM 121, VHM 64, VHM, 30, and the ungauged rivers Miðfjarðará, Hrútafjarðará, Svínavötn, Miðá, Langadalsá, Hellisfljót, Lágadalsá.
- *Cluster B:* VHM 149, VHM 148, VHM 206, VHM 205, VHM 200, VHM 26, VHM 400, VHM 19, VHM 204, VHM 38, VHM 411, VHM 45, VHM 10, VHM 128, VHM 12, and the ungauged rivers Flókadalsá, Hellisá, and Gilsá.
- *Cluster C:* VHM 51, VHM 198, VHM 83, VHM 92, VHM 144, and the ungauged river Nýjadalsá.
- *Cluster D:* VHM 408, VHM 66, VHM 150, VHM 102, VHM 110, VHM 162, and the ungauged rivers Hornafjarðarfljót, Steinavötn, Jökulsá í Lóni and Jökulgilskvísl.
- *Cluster E:* VH 218, VHM 48, VHM 238, VHM, 116, and the ungauged rivers Sléttuá, Berufjarðará, Ólafsfjarðará, Fjarðará, and Hafralónsá.

When changing the number of members in the cluster analysis, the new groups are inevitably different from those, although catchments seem to cluster similarly for the most part. Catchment change from one cluster to the next usually when they were in close vicinity with the next hierarchical cluster in the first place. This is the case for VHM 198, VHM 83, VHM 51, and VHM 92 that now constitute Cluster C but were all parts of Cluster B before (Figure 5). Similarly, catchments that belonged to Cluster C on the previous dendrograms (VHM 128, VHM 12, VHM 411, VHM 45, and VHM 10) now belong to Cluster B.

This passage from one cluster to the next is also illustrated by the maps on Figure 8. On the top map, results from the cluster analysis based on the ICRA dataset are shown for the gauged catchments only (see dendrogram from Figure 5.b), with the catchment of the ungauged rivers shown in purple. Results from the cluster analysis based on both gauged and ungauged rivers are shown in the bottom map, with the ungauged area appearing with black borders for emphasis. As stated previously, Cluster A mostly gathers spring-fed rivers, some of them being partly glacier-fed. While most gauged rivers in this cluster are located on the southwestern part of Iceland (especially notable for the top map), that does not apply to the ungauged rivers, which are for example in the Westfjords. On the dendrogram, Cluster B and C are quite close, and it is reflected by the type of stations that belong to them. These are mostly mountainous or heathland catchments, many direct-runoff catchments, but some with more storage than others. New catchments like Nýjadalsá for instance fits correctly into that category. Cluster D comprises glacial rivers, and all watersheds are partially covered by glaciers, which is also the case of the ungauged rivers (Jökulsá í Lóni, Jökulgilskvísl, Steinavötn, Hornafjarðarfljót). Cluster E is more difficult to estimate, especially after adding the ungauged catchments. The gauged ones tend to have a groundwater-fed component which is not as clear after the ungauged catchments have been added to the cluster analysis. The timing of the seasonal discharge peak could be the reason the catchments clustered together, although it should also be noted that this cluster contains more ungauged catchments than gauged rivers.

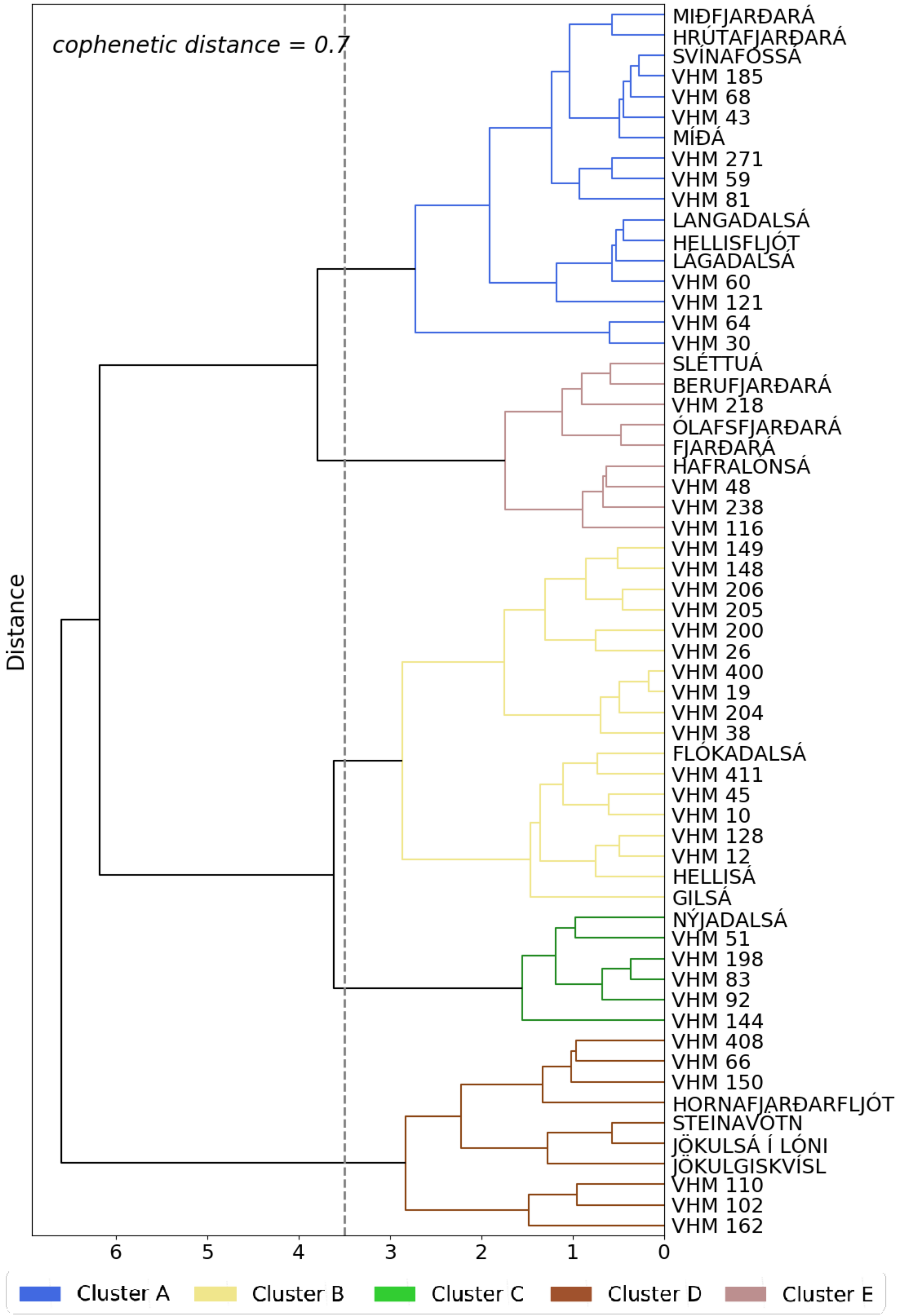

Figure 7 – Dendrograms resulting from the cluster analysis of simulated discharge timeseries for all the rivers, gauged and ungauged.

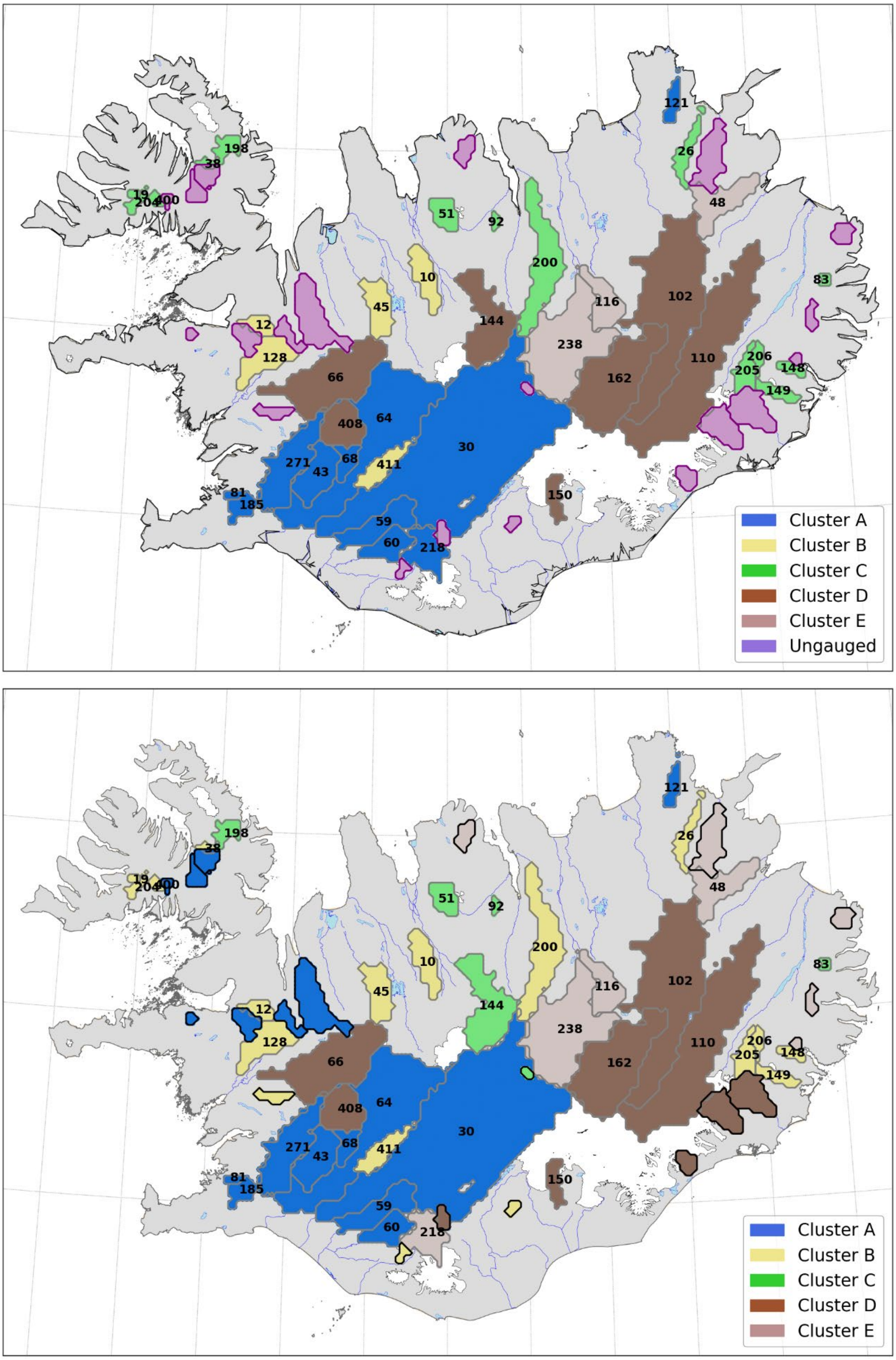

Figure 8 – Maps of Iceland including catchments that clustered similarly after analysis of the simulated discharge for (top) the gauged rivers from the 2022 study, and (bottom) for all the rivers, gauged and ungauged.

5 Extreme Value Analysis

5.1 Methodology

Extreme Value Analysis (EVA) is a statistical discipline used to predict the occurrence of rare events by assessing their frequency from the most extreme values of a dataset. EVA allows the calculation of return levels associated with periods that can be much longer than the length of the timeseries available for the analysis. Two approaches exist: the Peak-over-Threshold method and the Block Maxima method. In this study, only the latter method is used, as in recent hydrological projects at IMO (Pagneux *et al.,* 2017, 2018 and 2019; Þórarinsdóttir *et al.*, 2021).

The Block Maxima approach consists of dividing the timeseries into non-overlapping periods of equal size and retaining only the maximum values within each period. When dealing with hydrological data, it is common to use the maximum daily values from each calendar year. A new timeseries that includes only the maxima is thus generated and referred to as an Annual Maxima Series (AMS). Under extreme value conditions, the AMS follows a General Extreme Value (GEV) family of distribution:

$$G(z) = exp\left\{-\left[1 + \xi\left(\frac{z-\mu}{\sigma}\right)\right]^{-1/\xi}\right\}$$

where z is the extreme value and μ, σ and ξ are the three parameters of the GEV model *G(z)*, defining location, scale and shape parameters, respectively. Three types of GEV distribution exist, depending on the value of the shape parameter ξ. In this study, for consistency with previous work for flood analysis, a GEV distribution of type I (Gumbel) is used to fit the AMS, with ξ set to zero:

$$G(z) = exp\left\{-exp\left[-\left(\frac{z-\mu}{\sigma}\right)\right]\right\},$$

The return level r associated with the return period $1/p$ can finally be estimated with the formula:

$$r = \mu - \sigma log\{-log(1-p)\}$$

and r is defined as the value expected to be exceeded on average once every $1/p$ year.

For more details, see Coles (2001).

5.2 Comparison between simulated and observed discharge

5.2.1 Flow-duration curves

To assess the quality of the simulated discharge based on the ICRA dataset, the timeseries are compared to the measurements from the gauged stations. For comparison purposes, the timeseries are identical for each station and days with no observations are also discarded in the reanalysis. For both datasets, highest daily values are ranked and plotted decreasingly for each river, using only values above the 95^{th} percentile. Examples for each cluster are shown in Figure 9, on plots that are very similar to flow-duration curves, even though the x-axis shows the number of days instead of a percentage exceedance. Results show that the simulated discharge is much higher. While the general distribution of the flow-duration curves is very similar, the simulated discharge needs to be scaled by a correcting factor that corresponds to the runoff coefficient C to match the observations. These results can be extended to most of the stations, as the simulations show an overestimation in the vast majority of cases (38 out of the 40 stations). This is not surprising, as no infiltration is considered in the absence of the correcting factor C, leading to a larger amount of runoff pouring straight into the rivers.

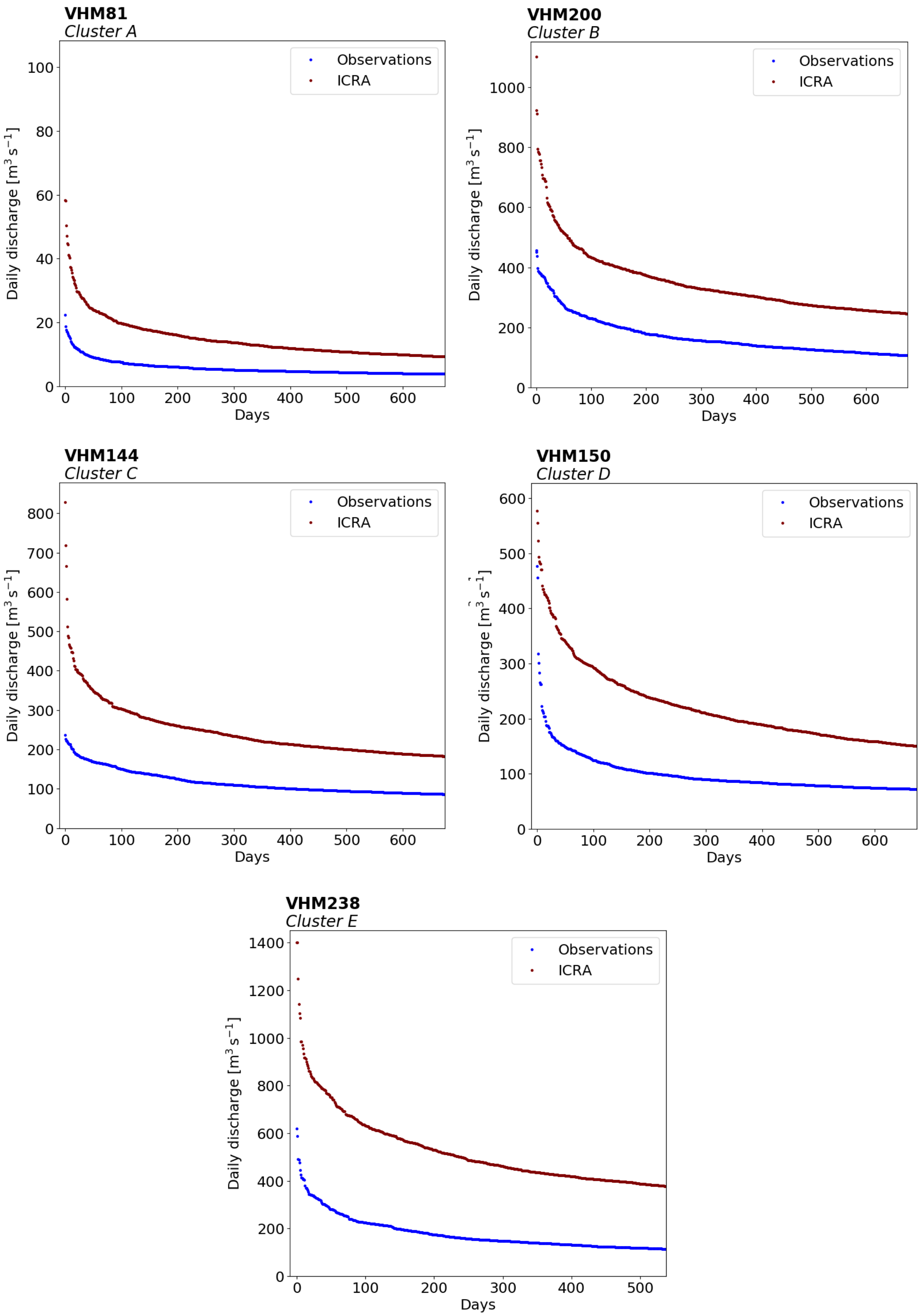

Figure 9 – Flow-duration curves for five gauged rivers including the 5% highest values. Discharge values are based on observations (blue), and on the ICRA runoff (brown).

5.2.2 Correction of the simulated discharge

In order to correct the discharge bias noted in most simulated flow-duration curves of the 5% highest values (as seen in Figure 9), the difference between simulated and observed discharge is quantified using a coefficient of proportionality. This coefficient will then be used as the correcting factor *C* from the formula presented in 3.2.2 to improve the match between measured and simulated discharge. For each station, the coefficient of proportionality is calculated by comparing the mean daily discharge above the 95th percentile between observations and the ICRA dataset. These coefficients are then averaged over all the stations that clustered together.

This method assumes that if a river belongs to one group from the cluster analysis, it is likely that the correction needed when the discharge is calculated from the ICRA runoff is comparable to the other rivers from that group. For instance, for a cluster that is comprised of groundwater-fed rivers where a large part of the runoff infiltrates, the scaling factor is likely to be smaller than for direct-runoff catchments where most runoff goes directly into the river.

Values of those coefficients are shown in Figure 10, in the form of histograms. On the figure, each cluster is represented by a panel, and within a cluster, values of the coefficients of proportionality are shown individually for each station. For this study, the values of these coefficients are based on the daily discharge above the 95th percentile. Corrections based on daily discharge above the 75th and 90th percentiles were also tested but not shown here as they shown similar results. A coefficient of proportionality equal to 1 means there is no difference between mean simulated and observed discharge. Above 1, the mean observed values are higher than the simulations; under 1, the mean simulated values are higher than the measurements.

Mean cluster values are distributed between 0.33 (Cluster E) and 0.58 (Cluster B). It can be noted that for Clusters C and E, the coefficients of proportionality are quite homogeneous for all the stations. This is not the case for Cluster A, B, and D, where some stations appear as outliers. For instance, within Cluster A, the small value of the coefficient calculated for VHM 185 can be explained: the catchment is very porous and leading to a lot of water infiltrating, justifying why only a small portion of the simulated runoff ends up in the river. The opposite effect can be seen in VHM 68 where a lot of groundwater, originating outside of the surface catchment, is emerging in springs within the catchment (Sigurðsson, 1990). In Cluster B, two rivers stand out compared to the other stations: VHM 205 and VHM 206. This can be explained by the fact that these two catchments are quite small, direct-runoff rivers that imply a more straight-forward conversion of the ICRA runoff into a discharge. Moreover, when analysing their flow-duration curves, for both stations the all-time maximum daily discharge values are outliers when compared to the other high values, which consequently influences the large value of their individual correcting factor.

5.2.3 Scaled flow-duration curves

To adjust the simulated high discharge for each station to better fit the measurements, daily discharge values calculated from the ICRA runoff are multiplied by the mean coefficient of proportionality *C* from the belonging cluster. This scaling is shown in Figure 11 on the flow-duration curves of five gauged rivers, one from each cluster. Again, only the 5% highest daily values are shown in the figure. For each plot, flow-duration curve is shown in blue when based on the measurements, in brown when based on the non-corrected simulated discharge, and in red after applying the mean scaling factor. Therefore, to obtain the corrected ICRA values, the ICRA runoff is multiplied by 0.35 for the stations belonging to Cluster A, 0.58 for stations from Cluster B, and so on.

It was decided to show in Figure 11 both stations that have an individual coefficient close to the mean value of its cluster of belonging (VHM 48 and VHM 83), and stations with an individual coefficient far from the mean value (VHM 185, VHM 205 and VHM 408). Results for stations VHM 48 and VHM 83, after scaling down the simulated discharge, give values extremely close to the flow-duration curve based on the measurements. For VHM 185 and VHM 498, even though their individual scaling factors are quite far from the mean values of their respective clusters (0.08 against 0.35, and 0.09 against 0.43, respectively), scaling down the simulated discharge still leads to significant improvement. The only two stations that do not benefit from the scaling are VHM 205 and VHM 206. As stated earlier, these two smalls direct-runoff catchments have a simulated discharge matching the measurements very well, and do not need any correction. It is illustrated for VHM 205 on Figure 11, with the red curve reaching much lower values than what was measured. Those catchments are small valleys far inland where precipitation in the NPW could be underestimated, therefore explaining why the simulated discharge does not need to be scaled down. Another reason could be that these rivers are partly fed by wind drift of snow from outside the catchment and into the valleys.

Overall, most rivers (38 out of 40) benefit from scaling down the simulated discharge from the ICRA runoff. It is therefore expected that using the same factor to correct the discharge from the ungauged areas will lead to results that are closer to reality, in the absence of any measurements to validate the results. Simulated discharge was multiplied by 0.35 for rivers Miðfjarðará, Hrútafjarðará, Svínavötn, Miðá, Langadalsá, Hellisfljót and Lágadalsá; by 0.58 for rivers Flókadalsá, Hellisá and Gilsá; by 0.49 for river Nýjadalsá; by 0.38 for rivers Hornafjarðarfljót, Steinavötn, Jökulsá í Lóni and Jökulgilskvísl; and by 0.33 for rivers Sléttuá, Berufjarðará, Ólafsfjarðará, Fjarðará and Hafralónsá. Results for five ungauged rivers (one for each cluster) are shown in Figure 12, with the flow-duration curve based on the original simulated discharge shown in brown, and after applying the scaling factor in red.

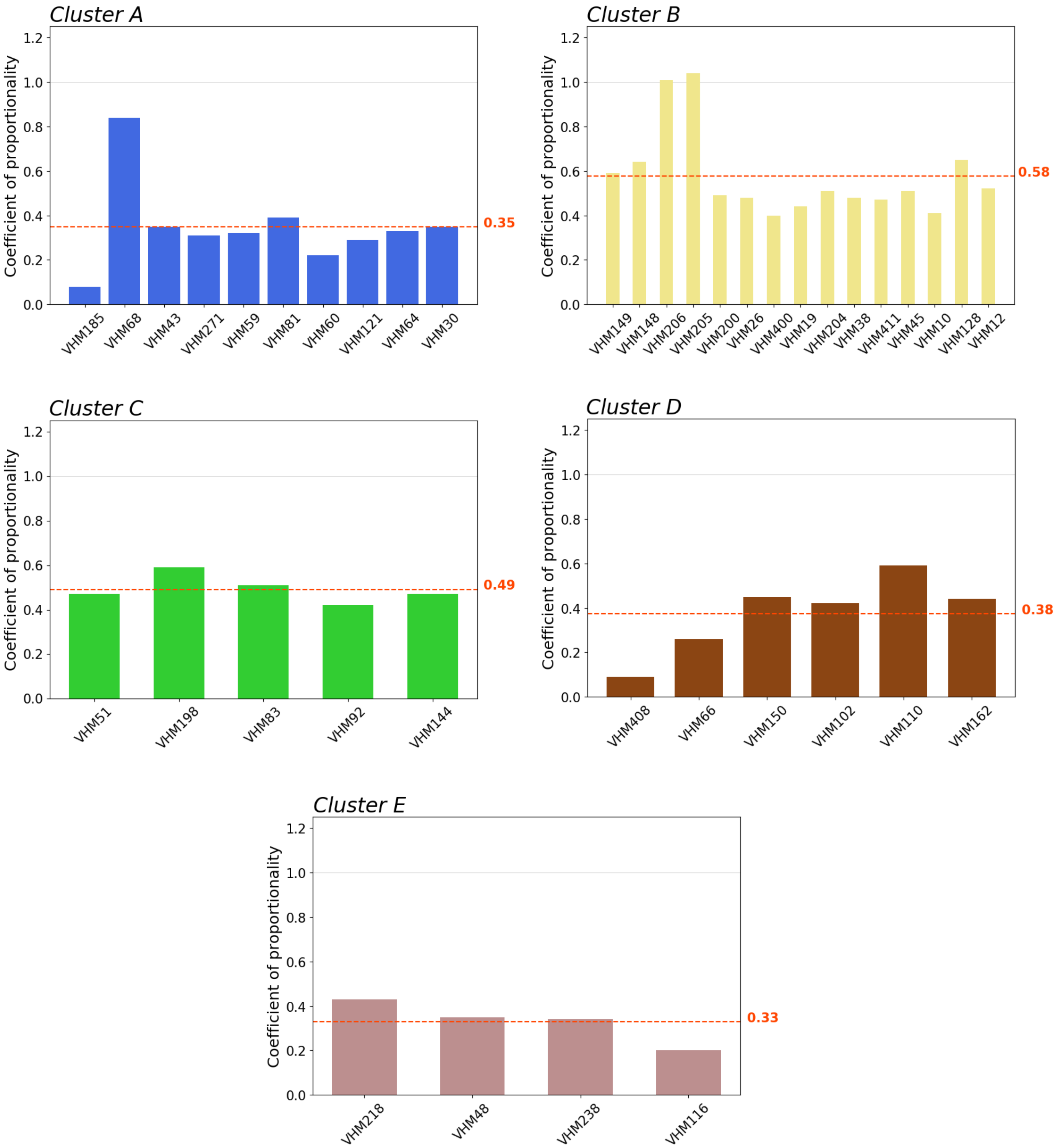

Figure 10 – Histograms showing coefficients of proportionality for each station and based on daily discharge values above the 95th percentile. Stations are shown by cluster, and mean coefficients averaged among all stations are represented by the dashed lines. The colours of the bars were chosen to match the colour of the clusters in Figures 7 and 8.

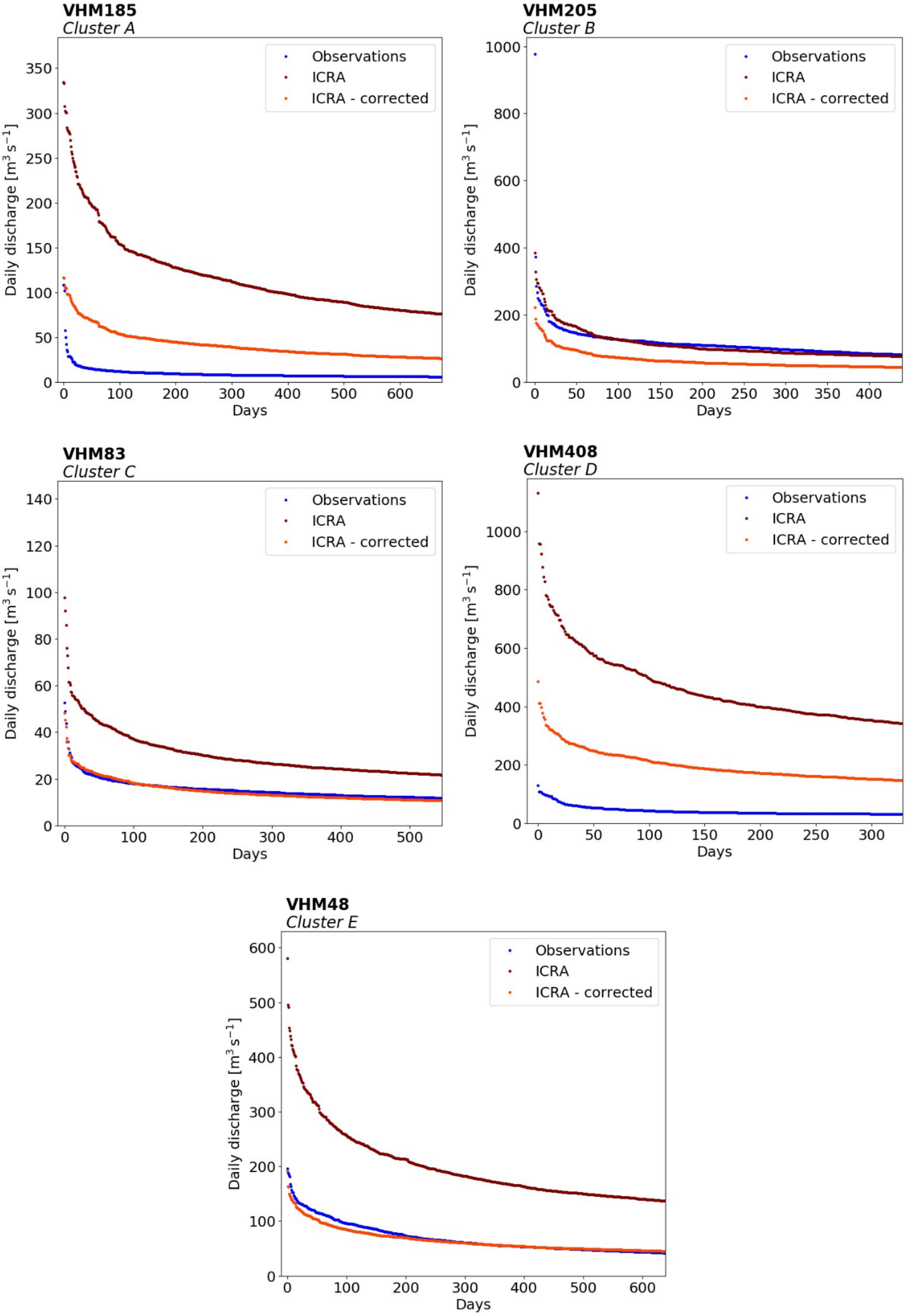

Figure 11 – Flow-duration curves for five gauged rivers including the 5% highest values. Discharge values are based on observations (blue) and on the ICRA dataset before (brown) and after applying the corresponding cluster's scaling factor (red).

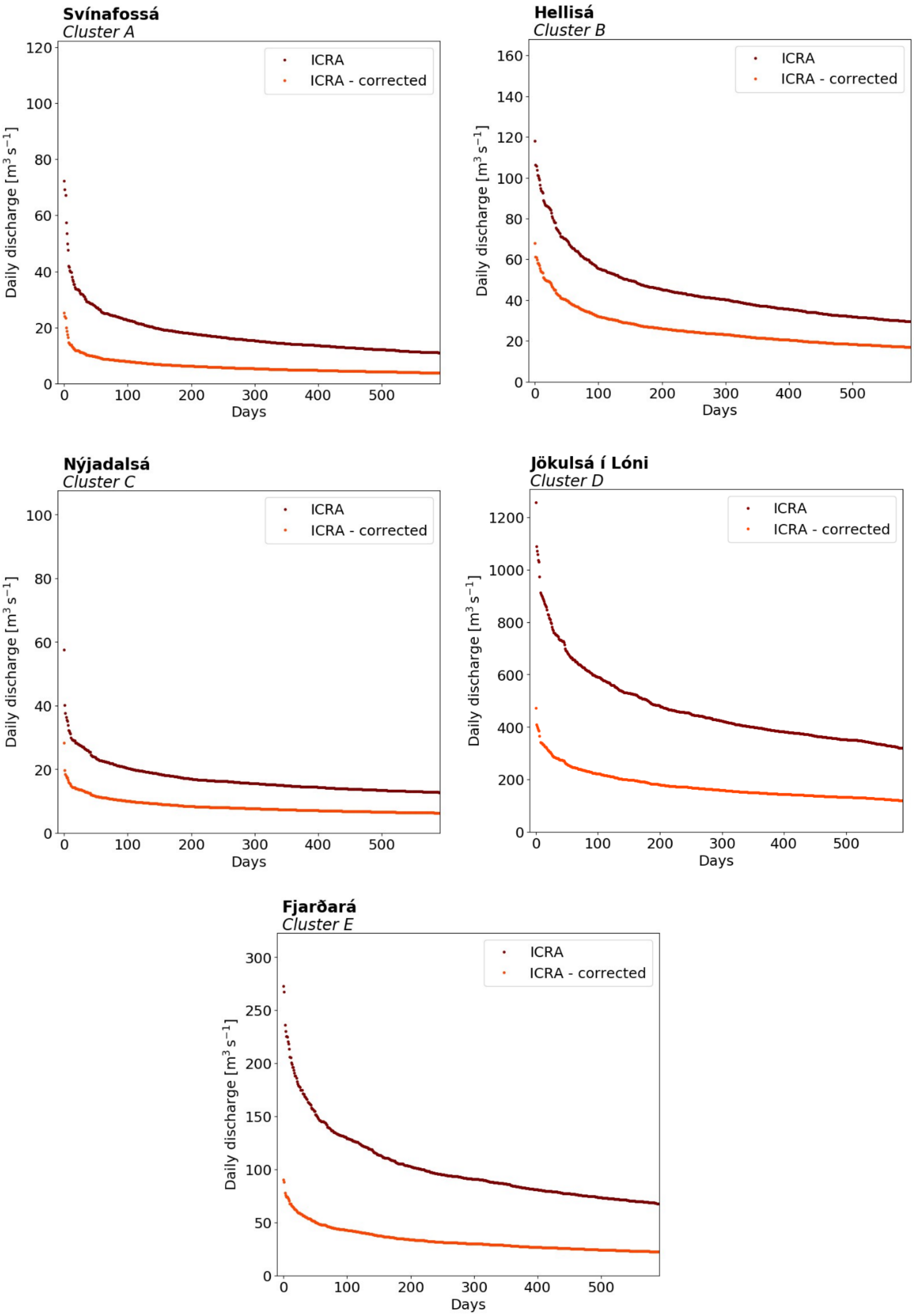

Figure 12 – Flow-duration curves for five ungauged rivers including the 5% highest values. Discharge values are based on the ICRA dataset before (brown) and after applying the corresponding cluster's scaling factor (red).

5.3 Flood analysis

5.3.1 Flood analysis for the gauged catchments

To obtain flood estimates for the gauged rivers, the Block Maxima method is applied both on measured and simulated discharge, before and after applying the correction factor. For each river, the correction coefficient depends on which cluster it belongs to and is applied to the timeseries before the EVA. Daily flood return levels with a 10-, 25-, 50-, 100-, 200-, and 500-year return period are calculated for all gauging stations.

Three examples are shown in Table 4, for stations VHM 83, VHM 185 and VHM 206 (results for other rivers are shown in Appendix I). Those rivers were picked from the histogram for the diversity of results they display. In the case of VHM 83, the mean correcting factor for its cluster of belonging (0.49) is very close to the individual correcting factor (0.51). Therefore, it clearly appears from the table that results after scaling the dataset are very close to the results obtained from the measurements. This is further illustrated by Figure 13 which displays the return-level plot for VHM 83. In those figures, discharge values (y-axis) are plotted against the return periods on a logarithmic scale (x-axis). Here, values from the measured AMS between years 1980 and 2016 are represented by the blue dots. A straight line shows the fit between these data and return periods, and horizontal dashed lines indicate the values for the 25-year flood. The same is done for discharge derived from the ICRA dataset on the top plot in red, and for simulated discharge after correction on the lower plot in orange. In the case of this station, after scaling the data, the value of the daily return level with a 25-year return period is 45 $m^3 s^{-1}$, which is extremely close to the one obtained from the measurements (43 $m^3 s^{-1}$) and more realistic than based on the uncorrected simulated discharge (92 $m^3 s^{-1}$).

VHM 185, as previously discussed, is lacking infiltration when the runoff is converted into discharge without *C*, which explains why its individual correcting factor is so low (0.08), compared to other stations that belong to the same cluster. Therefore, it is expected that the return levels after correction are not as close to the measurements as for VHM 83. This is indeed what can be seen in Table 4 and Figure 14. However, even if the corrected return levels are not lowered enough to reach the values based on the measurements, it is still a considerable improvement from before applying the correcting factor.

VHM 206 serves as a counterexample, as it is, with VHM 205, one of the two stations that do not benefit from rescaling the simulated discharge, as can be seen from Table 4 and Figure 15. In that case, applying the mean correcting factor only lowers the return levels even more, while they were already inferior to the values obtained from the observations in the first place.

Table 4 – Flood return levels ($m^3\ s^{-1}$) for stations VHM 83 (top), VHM 185 (middle), and VHM 206 (bottom). Results are based on the measured discharge, simulated discharge from the ICRA runoff, and simulated discharge from the ICRA runoff after correction. Values are given for a 10-, 25-, 50-, 100-, 200-, and 500-year return period.

VHM 83 - Fjarðará

Return-period	Return levels ($m^3\ s^{-1}$)		
	Observations	**ICRA**	**ICRA, corrected**
10 years	37	78	39
25 years	44	92	45
50 years	50	102	50
100 years	56	111	55
200 years	61	121	60
500 years	68	134	66

VHM 185 - Hólmsá

Return-period	Return levels ($m^3\ s^{-1}$)		
	Observations	**ICRA**	**ICRA, corrected**
10 years	42	313	109
25 years	56	356	124
50 years	65	389	135
100 years	75	421	146
200 years	85	452	157
500 years	97	494	172

VHM 206 - Fellsá

Return-period	Return levels ($m^3\ s^{-1}$)		
	Observations	**ICRA**	**ICRA, corrected**
10 years	120	122	70
25 years	147	145	83
50 years	166	161	93
100 years	186	178	103
200 years	206	195	112
500 years	232	217	125

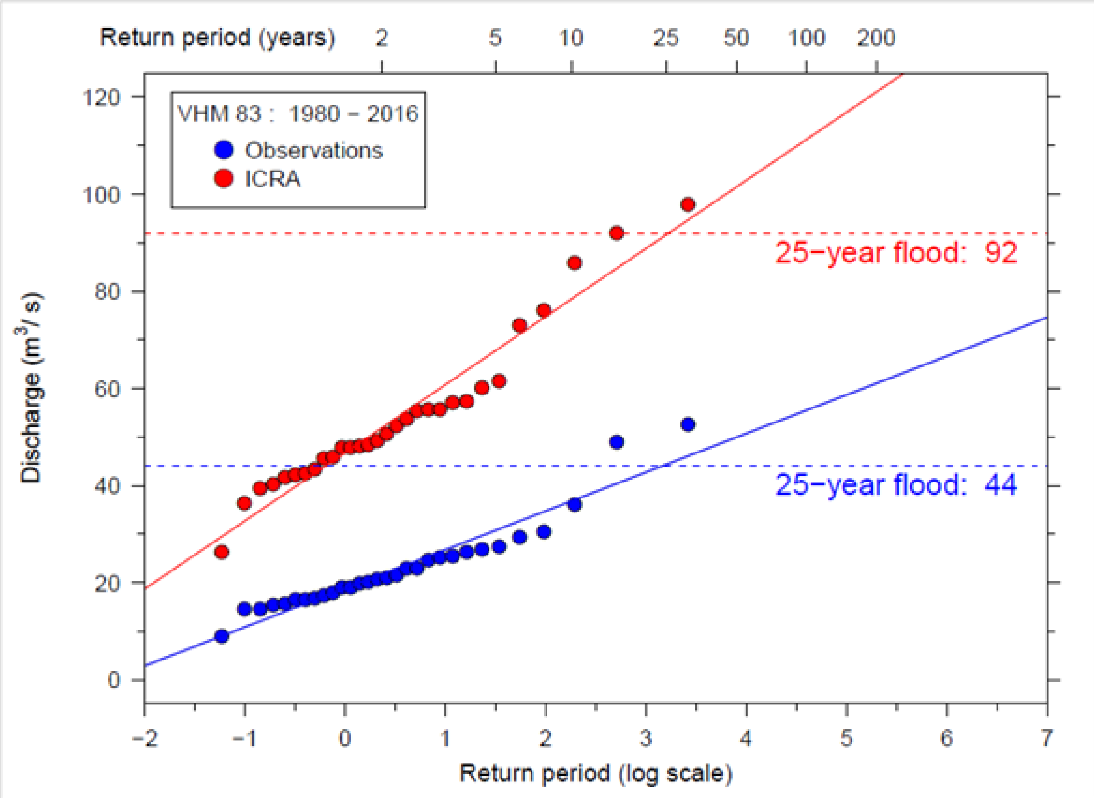

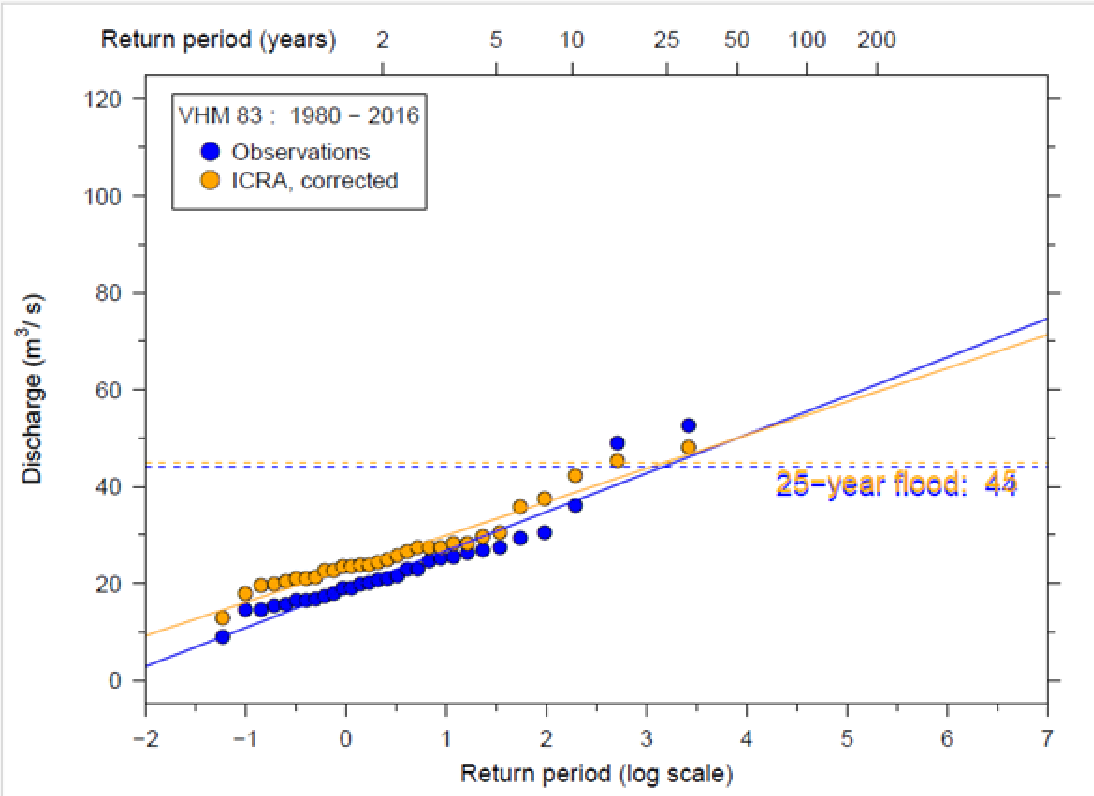

Figure 13 – Return level plot for station VHM 83, based on observations (blue), simulations before (red) and after correction (orange). Dashed-lines show the 25-year return level for the different datasets.

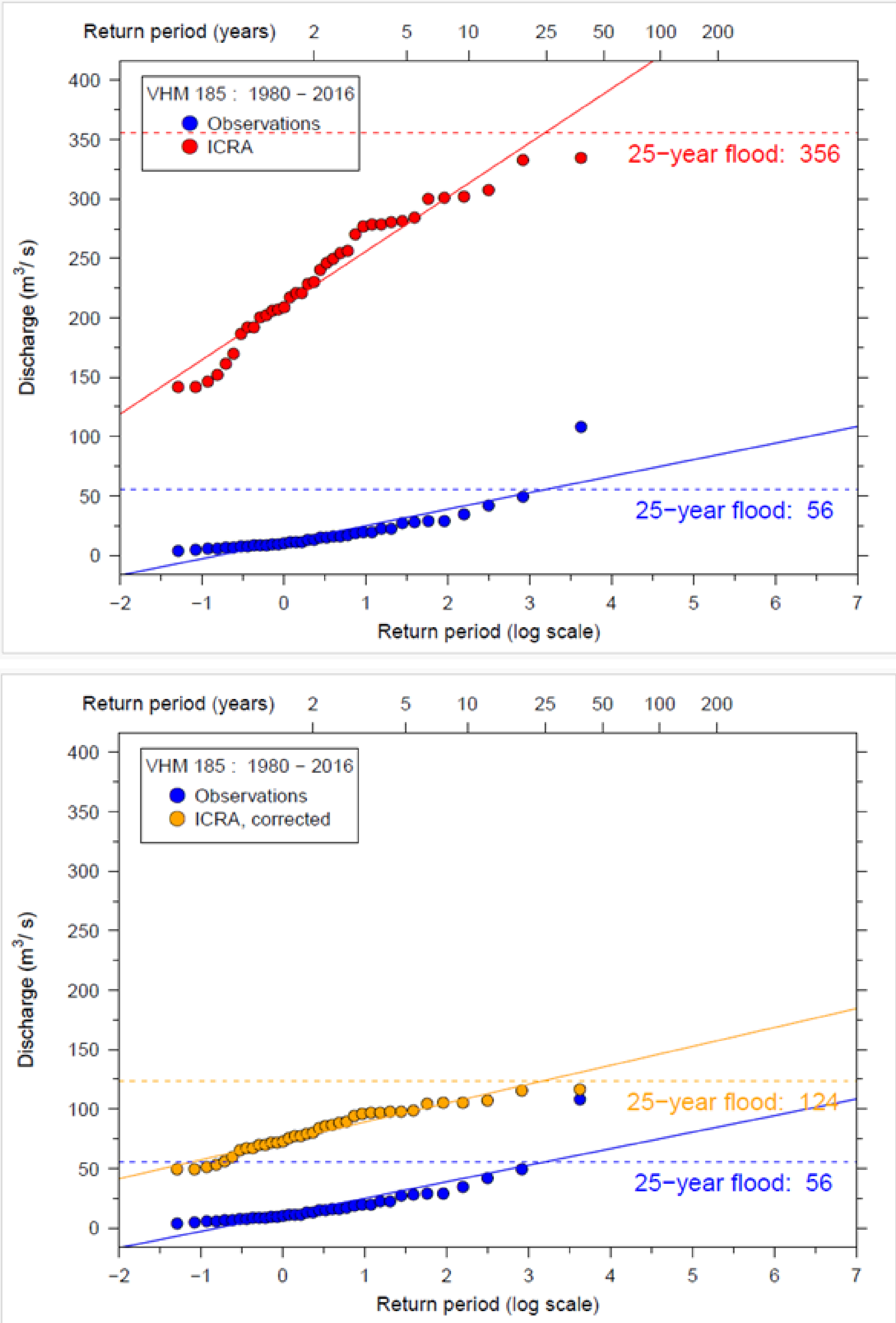

Figure 14 – Return level plot for station VHM 185, based on observations (blue), simulations before (red) and after correction (orange). Dashed-lines show the 25-year return level for the different datasets.

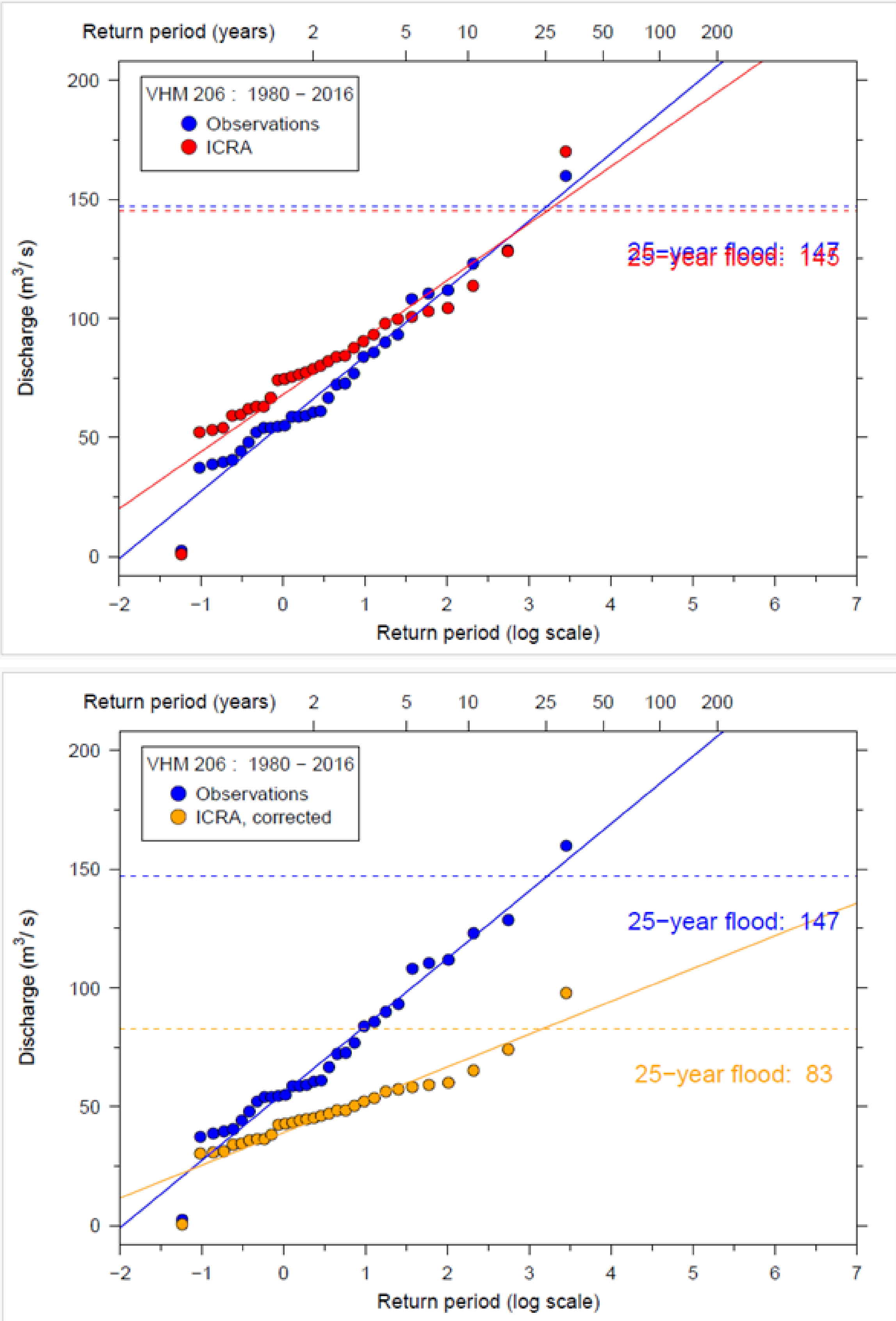

Figure 15 – Return level plot for station VHM 206, based on observations (blue), simulations before (red) and after correction (orange). Dashed-lines show the 25-year return level for the different datasets.

5.3.2 Closeness Coefficient values

To simplify the comparison between observed and simulated extreme discharge values, a Closeness Coefficient (*CC*) is introduced to determine how well the simulated values match the measurements:

$$CC = \frac{\min(obs, sim)}{\max\,(obs, sim)} \times 100$$

This coefficient quantifies simply how close the simulated value is to the observed one, independently of whether the value is higher or lower than the observation. In that sense, *CC* can be used as a percentage match between two values of the same return level.

Coefficients were calculated for all river for the 25-, and 200-year return levels, before and after applying the correction. Results are shown in map form for the 25-year flood only, on Figure 16. On the maps, *CC* are given a colour code according to their values: if the percentage match is below 50%, the value appears on a red circle. If the percentage match is between 50 and 75%, the circle is orange; and if it is higher than 75%, the circle is green. As expected, the values are greatly improved by scaling the simulated timeseries. For the 25-year flood, before applying the correction, 27 *CC* values are inferior to 50%, 7 stations are between 50 and 75%, and 7 stations are superior to 75%. After applying the correction, only 7 stations have a *CC* inferior to 50%, 18 stations have a *CC* between 50 and 75%, and 16 stations have a *CC* superior to 75%. Results for the 200-year flood are exactly the same (not shown here).

Those results are also presented in Table 5, ordered by cluster. To facilitate the reading of the results, the cells are coloured in green when the *CC* value increases after correction, in red when it decreases. Scaling down the ICRA reanalysis leads to closer results between observation and simulation in 33 cases out of 40 for the 25-year flood. Mean *CC* values indicate that overall, all the clusters benefit from the correction. In Cluster A and C, one station (VHM 68 for Cluster A, and VHM 198 for Cluster C) has a lower *CC* after correction. In Cluster B, this concerns five stations (VHM 148, 205, 206, 128, and 411). In Cluster E, all four stations benefit from the scaling. Results are the same for the 200-year flood, except for VHM 150 in Cluster D that has a lower *CC* value after correction of the simulated discharge.

Figure 17 presents another view of these results, this time in the form of histograms. *CC* values are ranked decreasingly before and after correction for the 25-year return level. The bars are coloured according to the cluster of belonging of the station, and horizontal bars show the 10, 25, 50, 75, and 90% *CC* thresholds. Before correcting the simulated dataset, only two stations had a *CC* above 90% for the 25-year flood, while after correction, six stations reach that value. It is however difficult to draw any conclusions whether one particular cluster benefits from the correcting factor more than the others. It should however be noted that all rivers from Cluster A ranks quite low before correction, and much higher after it.

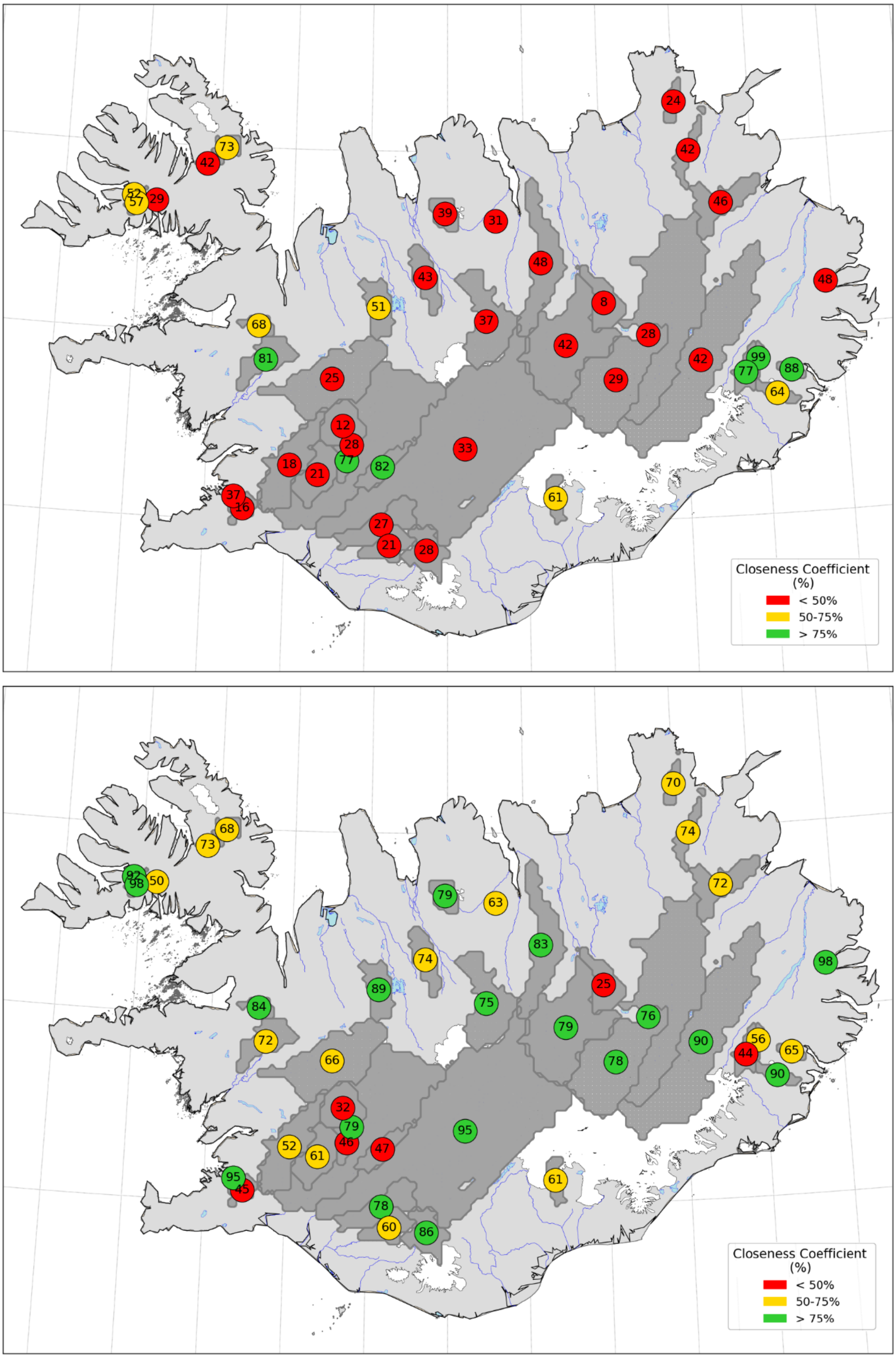

Figure 16 – Closeness Coefficient map comparing 25-year flood return level between observation and ICRA before (top) and after (bottom) applying the correcting factor.

Table 5 – Closeness Coefficient values between measurements and simulated discharge, before and after correction. Results are shown for the 25-, and 200-year return periods for all rivers. Mean CC values are given in bold for each cluster. The cells are coloured in green when the river benefits from the correction, in red when it does not.

		Closeness Coefficient *(%)*			
		25-year return period		**200-year return period**	
		ICRA	**ICRA, corr.**	**ICRA**	**ICRA, corr.**
Cluster A	**VHM 185**	16	45	19	54
	VHM 68	77	46	80	44
	VHM 43	21	61	21	59
	VHM 271	18	52	17	49
	VHM 59	27	78	28	80
	VHM 81	37	95	39	89
	VHM 60	21	60	21	61
	VHM 121	24	70	24	70
	VHM 64	28	79	28	82
	VHM 30	33	95	35	99
	Mean CC	**30**	**68**	**31**	**68**
Cluster B	**VHM 149**	64	90	65	89
	VHM 148	88	65	97	59
	VHM 206	99	56	95	54
	VHM 205	77	44	69	40
	VHM 200	48	83	52	90
	VHM 26	42	74	43	75
	VHM 400	29	50	29	51
	VHM 19	52	92	56	98
	VHM 204	57	98	61	94
	VHM 38	42	73	43	75
	VHM 411	82	47	71	41
	VHM 45	51	89	53	93
	VHM 10	43	74	46	79
	VHM 128	81	72	83	69
	VHM 12	68	84	72	80
	Mean CC	**61**	**72**	**62**	**72**
Cluster C	**VHM 51**	39	79	40	81
	VHM 198	73	68	79	62
	VHM 83	48	98	50	98
	VHM 92	31	63	29	60
	VHM 144	37	75	35	72
	Mean CC	**45**	**76**	**46**	**74**
Cluster D	**VHM 408**	12	32	14	36
	VHM 66	25	66	26	68
	VHM 150	61	61	69	54
	VHM 102	28	76	29	78
	VHM 110	42	90	43	88
	VHM 162	29	78	31	83
	Mean CC	**40**	**67**	**44**	**68**
Cluster E	**VHM 218**	28	86	28	86
	VHM 48	46	72	51	65
	VHM 238	42	79	45	74
	VHM 116	8	25	8	23
	Mean CC	**31**	**65**	**33**	**62**

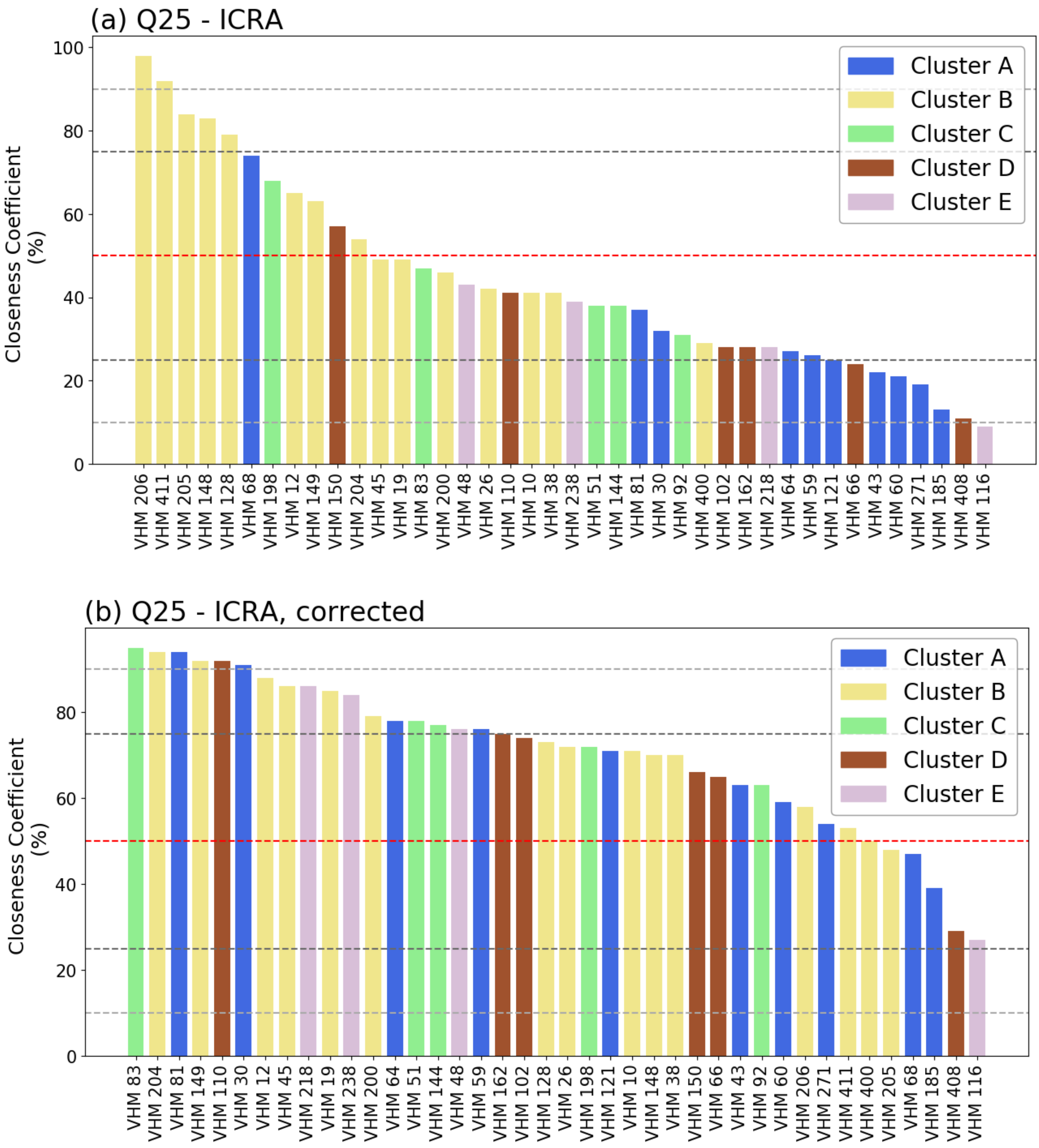

Figure 17 – Histograms presenting ranked CC values for the 25-year flood between observed and simulated discharge before (top) and after (bottom) correction. Horizontal dashed lines show the 10, 25, 50, 75 and 90 % CC thresholds.

5.3.3 Flood analysis for the ungauged catchments

The same methodology is then applied to ungauged areas. For each river, two AMS are created: one based on the simulated discharge from the ICRA runoff, the other based on the same simulated discharge, but scaled down by the corresponding coefficient. The EVA is then carried out on the timeseries, and new daily flood estimates are obtained.

Those results are compiled in Table 6 after applying the correction. For comparison purposes, results before correction are shown in Appendix II. Return-level plots are also produced and shown for rivers Miðfjarðará (Cluster A), Hafralónsá (Cluster E), Hellisá (Cluster B), and Jökulsá í Lóni (Cluster D) in Figure 11. Return-level plots for the other ungauged rivers are shown in Appendix II.

As expected, those results vary significantly whether the correcting factor is applied or not and the lack of reference provided by the measurements for the gauged catchments makes it difficult to assess the quality of the results. However, considering the success of the method for the gauged stations, it is likely that the results after applying the correction are closer to reality than when the AMS from uncorrected discharge is used.

Table 6 – Flood return levels ($m^3 s^{-1}$) for all ungauged rivers. Results are based on the simulated discharge from the ICRA runoff after correction.

	10-year	25-year	50-year	100-year	200-year	500-year
Berufjarðará	24	27	30	33	36	39
Fjarðará	79	90	98	105	113	123
Flókadalsá	51	58	64	69	75	82
Gilsá	41	48	52	57	62	68
Hafralónsá	169	196	217	237	257	284
Hellisá	61	70	76	82	88	96
Hellisfljót	27	32	35	38	41	46
Hornafjarðarfljót	417	474	515	557	598	653
Hrútafjarðará	48	56	62	68	73	81
Jökulgilskvísl	64	73	80	87	94	103
Jökulsá í Lóni	394	450	492	533	574	629
Lágadalsá	53	62	68	74	81	89
Langadalsá	73	87	96	106	116	128
Miðá	78	93	104	115	126	140
Miðfjarðará	105	118	127	136	146	158
Nýjadalsá	19	22	24	26	28	31
Ólafsfjarðará	63	73	80	87	94	103
Sléttuá	47	54	60	65	70	77
Steinavötn	140	157	170	182	195	211
Svínafossá	19	23	26	28	31	34

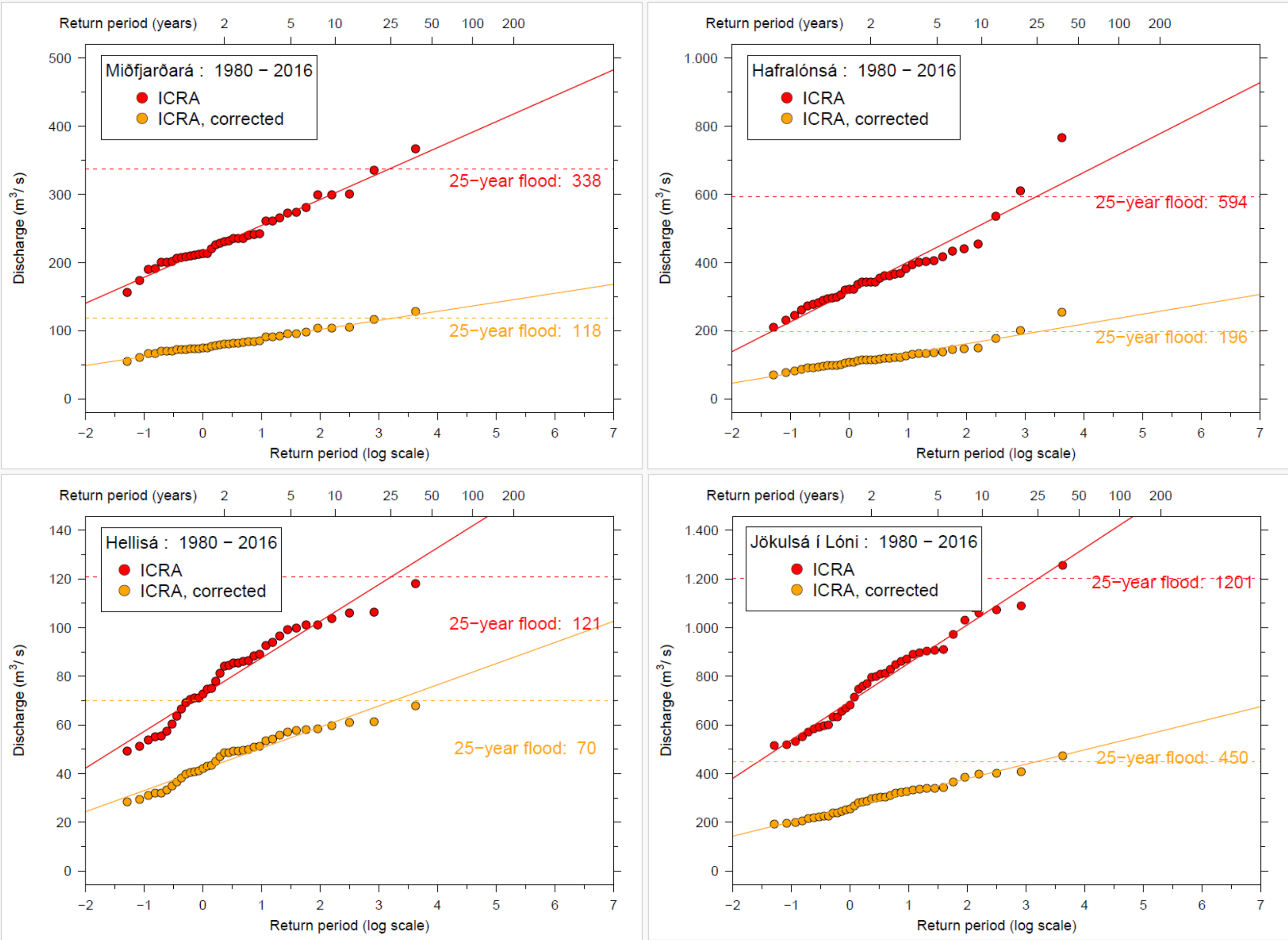

Figure 18 – Return level plot for ungauged rivers Miðfjarðará, Hafralónsá, Hellisá, and Jökulsá í Lóni, based on simulations of daily discharge before (red) and after correction (orange). Dashed-lines show the 25-year return level for the different datasets.

5.4 Flood analysis based on airGR runoff-rainfall model simulations

5.4.1 Model description

5.4.1.1 The GR6J model

airGR is a series of rainfall-runoff models that can be applied either in a lumped or semi-distributed way. The suite of GR hydrological models was developed by INRAE (Institut National de Recherche pour l'Agriculture, l'alimentation et l'Environnement) and the models are available in R packages (Coron *et al.,* 2017; 2020).

In this study, following the works of Atlason *et al.* (2021) and Priet-Mahéo *et al.* (2021), the GR6J model (Pushpalatha *et al.*, 2011) is used along with the CemaNeige module (Valéry, 2010) for handling the simulation of snow accumulation and melt. GR6J runs with a daily time-step and uses six parameters for calibration and optimisation (see Table 7, parameters X1 – X6). Two extra parameters are used for the CemaNeige module (see Table 7, CNX1 and CNX2). All parameters are defined within a range of possible values and are optimised using the automatic ASA (Adaptive Simulated Annealing) optimisation method (Ingber, 2000; Ingber *et al.*, 2012). Upper and lower boundaries for each parameter was kept as default from the model developers to start with, and ranges are shown in Table 7.

When the model runs, both outputs of the CemaNeige module serve as inputs of the GR6J model (Neri *et al.*, 2020). For details about the structure of the GR6J model, a diagram is presented in Pushpalatha *et al.* (2011), illustrating the role of parameters X1 to X6. For further details about the model routines, see Priet-Mahéo *et al.* (2021).

Table 7 – Parameters for the GR6J model and the CemaNeige module, and default ranges tested in this study.

Model	**Parameter**		**Range**
GR6J	**X1**	production store capacity [mm]	[0; 200,000]
	X2	intercatchment exchange coefficient [mm d^{-1}]	[-20; 20]
	X3	routing store capacity [mm]	[0; 6,000]
	X4	unit hydrograph time constant [d]	[0.5; 15]
	X5	intercatchment exchange threshold [-]	[-1; 1]
	X6	exponential store depletion coefficient [mm]	[0; 1,000]
CemaNeige	**X1**	weighting coefficient for snowpack thermal state [-]	[0; 1]
	X2	degree-day melt coefficient [mm °C^{-1} d^{-1}]	[0; 150]

5.4.1.2 Input data

Three types of data are required as inputs to run the airGR model:

- ***Catchment characteristics:*** area and hypsometric curves are needed for each catchment. Those data were previously calculated by Atlason *et al.* (2021) and Priet-Mahéo *et al.* (2021), using ArcGIS.
- ***Meteorological data:*** daily evaporation, precipitation, and temperature timeseries were created using mean or accumulated values of the parameters, as simulated by the ICRA dataset.
- ***Gauge measurements:*** in order to use them as input data, the discharge measurements need to be converted from m^3 s^{-1} into mm day^{-1}, which can easily be done by scaling it with the area of the catchment.

5.4.1.3 Running the model

As previously mentioned, airGR is available as R packages, and is rather straightforward to implement. For this study, one gauged river from each cluster was selected: VHM 43, VHM102, VHM 144, VHM 149, and VHM 238.

The first phase is the calibration phase. In this study, it was decided to use the Nash-Sutcliffe Efficiency coefficient (NSE) as objective function, by analogy with the previous works done at IMO with airGR. Once the NSE reaches its maximum value, the optimisation will stop. The second phase is the validation, where values of the eight parameters corresponding to the highest NSE are retrieved and used to simulate the discharge over the validation period. In some cases, the highest NSE value corresponds to several set of parameters, although it usually does not lead to major differences in the results.

5.4.2 Results

5.4.2.1 Calibration and validation of the selected rivers

For this study, it was decided to calibrate the rivers over a five-year period, from 01.01.2007 to 01.01.2012, with the exception of VHM 149 that was already calibrated from previous unpublished research over a period of six years (2007 – 2013).

For each catchment, validation was then carried over the whole period covered by both measurements and the ICRA dataset. For VHM 43, VHM 144 and VHM 149, this period spans from 01.09.1980 to 31.12.2016, with a spin up between 01.01.1980 to 01.09.1980. For VHM 102, the validation started on 01.02.1985, and for VHM 238 on 01.09.1988, and also ended on 31.12.2016. A spin up from January to September was also used for the latter.

NSE coefficients for the five catchments are shown both for the calibration and the validation periods in Figure 19. On the map, the catchments are coloured according to their cluster, similarly to Figure 7. NSE values appear in green when results are considered very good (above 0.75), in yellow when the results are considered good (between 0.35 and 0.75), and in red when the model fails to simulate the river flows successfully (under 0.35). In this case, all the catchments show good to very good results, both for the calibration and validation period. Best results are obtained for VHM 149, with NSE superior to 0.7 both for the calibration and validation. With a NSE of 0.46 over the validation period, VHM 102 is the river that is the least successfully simulated by the model.

To further illustrate those results, Figure 20 shows the hydrographs for the whole validation period for the five rivers. For VHM 144 and VHM 149, while the simulated discharge follows the general patterns of the measurements, results from airGR underestimate the highest peaks. This is expected to lead to lower flood estimates, as the EVA only focus on the highest discharge peaks. For VHM 43 and VHM 238, the opposite can be seen, with an overestimation by the model. Finally, for VHM 102, the smaller NSE over the validation period (0.46) can be attributed to the model not simulating properly the yearly late-spring peaks. However, the annual maximum, usually happening at the end of the summer, are very well simulated by the model, which is expected to benefit the EVA.

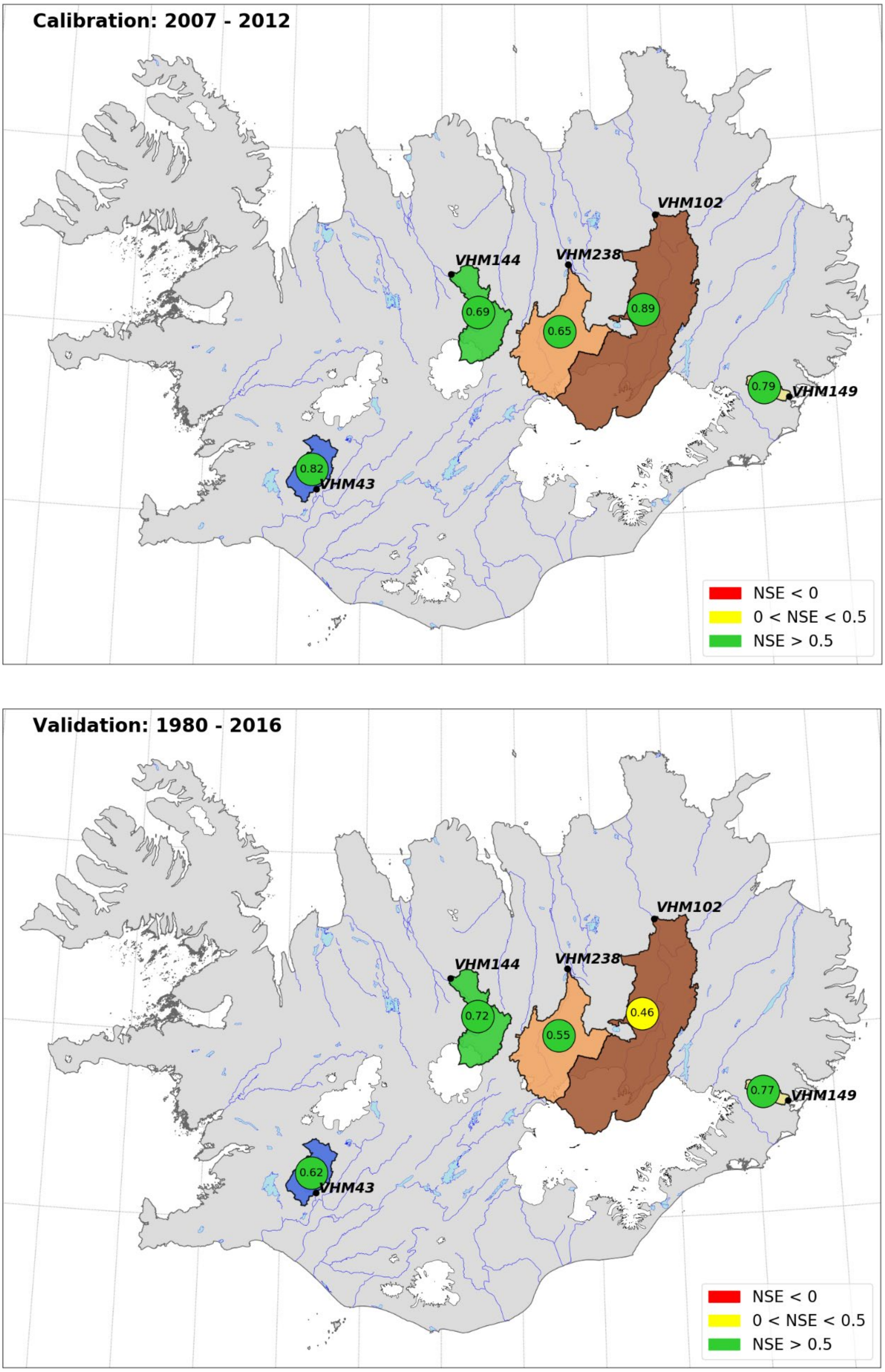

Figure 19 – Maps of Iceland with catchments selected for runoff-rainfall model simulations. NSE values after calibration (top) and validation (bottom) are shown in circles. The colours of the catchments match the colours used for the cluster analysis shown in Figure 4.

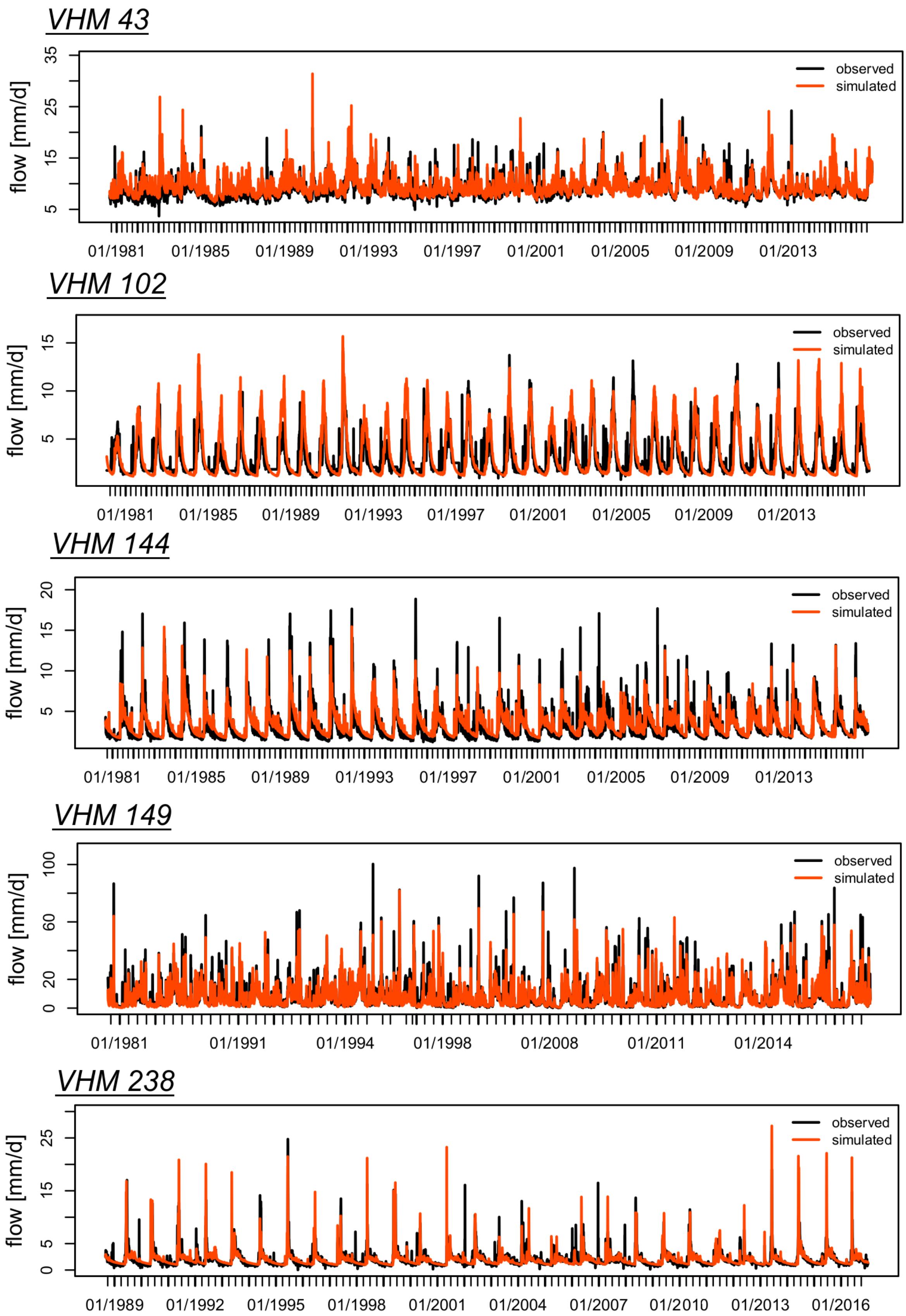

Figure 20 – Measured (black) and simulated (red) discharge for five catchments over the validation periods.

5.4.2.2 Flood estimates from airGR

After running airGR for the five rivers, new discharge timeseries were created. From these timeseries, AMS were calculated, and the Block Maxima method applied to calculate daily discharge with a 10-, 25-, 50-, 100-, 200-, and 500-year return period. Results are shown in Table 8 for the five rivers. The return levels calculated earlier from measurements are also shown.

Results show that for most rivers, the return levels calculated from airGR give values within the same range than from the observations. This is especially true for VHM 43 with a 10-year flood value of 181 $m^3\ s^{-1}$ when running airGR, and a value of 163 $m^3\ s^{-1}$ from the measurements. Another river that gives very good results is VHM 102, with values within 10% from each other for every threshold. This can be explained by the quality of the simulation of the yearly maximum peaks, as previously shown in Figure 20.

These results are further illustrated by Figure 21 which shows return level plots similar to Figure 13, 14, 15, and 18. On the plots, results from airGR are shown in green, and results from the measurements in blue. For comparison purposes, results from the ICRA dataset are also shown in the figure in orange. The coloured dots show the AMS, and for all stations, results from airGR are rather good. There is no trend whether airGR under- or overestimated the AMS compared to the measurements on this selection of rivers. Indeed, airGR overestimated the AMS for three rivers (VHM 43, VHM 102, and VHM 238), and underestimated the series in two cases (VHM 144 and VHM 149).

Table 8 – Flood return levels ($m^3\ s^{-1}$) for all ungauged rivers. Results are based on the simulated discharge from the GR6J model (top part) and from the observed daily discharge (bottom part).

GR6J SIMULATIONS						
	10-year	**25-year**	**50-year**	**100-year**	**200-year**	**500-year**
VHM 43	181	209	230	250	270	297
VHM 102	778	866	931	997	1061	1147
VHM 144	171	195	212	230	247	270
VHM 149	157	180	196	213	230	252
VHM 238	593	716	808	899	990	1109
MEASUREMENTS						
	10-year	**25-year**	**50-year**	**100-year**	**200-year**	**500-year**
VHM 43	163	182	195	209	223	241
VHM 102	730	842	924	1006	1087	1195
VHM 144	222	252	274	296	318	347
VHM 149	202	237	263	288	314	347
VHM 238	468	565	636	708	779	873

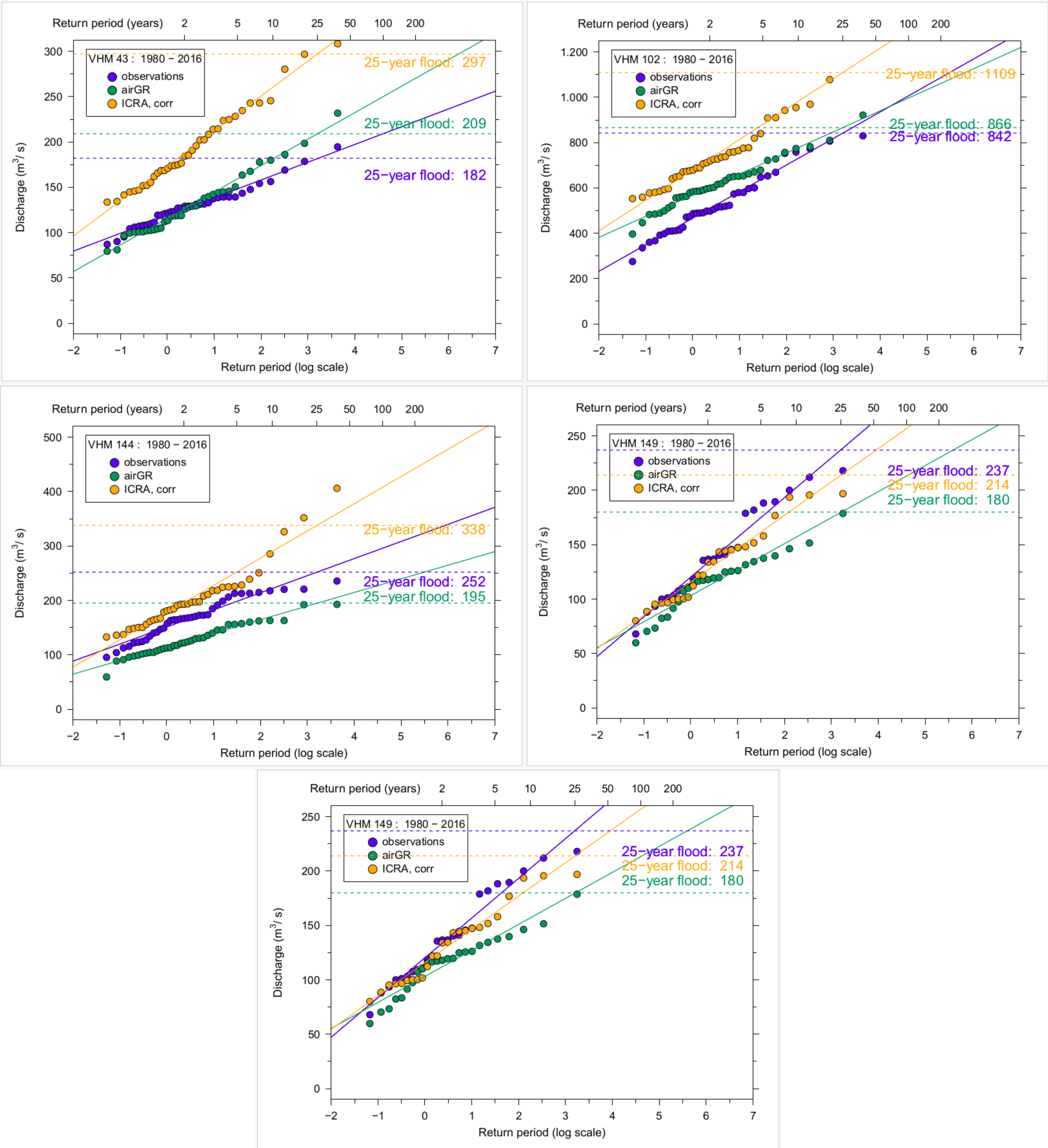

Figure 21 – Flood return level plot for five rivers, based on simulations from the GR6J model (green), measurements (blue), and the corrected ICRA dataset (orange). Dashed-lines show the 25-year return level for the three datasets.

6 Discussion

At the beginning of this study, rivers were classified using a cluster analysis based on various discharge characteristics and physical catchment attributes. This classification was later used to calculate a mean correcting factor based on all rivers within each cluster, which serves as a reference to correct the simulated discharge based on the ICRA dataset from ungauged rivers. It should be noted that if this approach led to catchments being classified according to their type and weather conditions, it could have been improved using other input data for the clustering. Likewise, the choice of only keeping five clusters was practical, and different results could have been expected if a larger number of groups had been picked. However, considering the values of the correcting factors were all within a relatively narrow interval, it can be expected that the final results for the ungauged basins would not change drastically if a different number of clusters would have been selected. Ultimately, while design-flood estimates were obtained for the 20 ungauged rivers, it is difficult to assess the quality of these results without any measurements. Those results should therefore be handled carefully.

Later in this project, five gauged rivers were selected, and extremes were calculated after simulating their discharge with the airGR rainfall-runoff model. Table 9 shows the CC values when comparing 25- and 200-year return levels calculated from the ICRA corrected discharge and the airGR simulation to the values calculated from the measurements. Overall, four out of the five rivers reach higher CC values after calculating the extremes with the GR6J model. While these results show how promising a simple model like airGR is for calculating extremes, it should be noted that those five rivers were scoring high NSE on both calibration and validation periods. This is not the case for all the rivers in Iceland (Atlason *et al.*, 2021; Priet-Maheo, 2021). Moreover, results based on the ICRA corrected discharge, although not as close to the observations, are still good, and this method is not as time-consuming as the airGR option. If airGR was to be used for assessing flood estimates in ungauged basins, the model parameters for each river would need to be averaged over each member of the same cluster, and then used as reference for the ungauged watersheds, depending on how they clustered. This is currently being studied in other research projects carried out at IMO.

Another aspect in this research that was not investigated is the fact that the observed and simulated block maxima of each year do not necessarily occur the same days or even the same seasons. Moreover, a runoff maximum does not always trigger a flood: in case of unsaturated soil for instance, a second, subsequent precipitation event can be the one leading to the flood, although the simulated runoff associated with this is less than the first event. This should be looked and further studied for all catchments in future research projects.

Table 9 – Closeness Coefficient values between measurements and simulated discharge from the ICRA runoff and from the GR6J model. Results are shown for the 25-, and 200-year return periods for the five selected rivers.

	Closeness Coefficient *(%)*			
	25-year return period		**200-year return period**	
	ICRA,corr	**GR6J**	**ICRA,corr**	**GR6J**
VHM 43	61	87	59	83
VHM 102	76	97	78	98
VHM 144	75	77	72	78
VHM 149	90	76	89	73
VHM 238	79	79	74	79

7 Conclusions

In this research, a first attempt to estimate extreme flood values based on simulated data from a reanalysis has been proposed. Firstly, 40 gauging stations that have been recording discharge of the main rivers in Iceland were selected. Runoff for 38-years of the ICRA dataset was extracted and summed daily for all the catchments associated with the selected rivers. The runoff was then converted into daily discharge. In the first place, this conversion was done without the correcting factor *C* that accounts for infiltration and other processes that happen in the catchment. By the end of the first step of the project, two sets of daily discharge series were available, one built on simulated runoff and the other one on observed discharge.

In the second part of the project, it was tested whether the dataset built on the ICRA data would give similar results of hierarchical clusters as the observed dataset. In both cases, discharge timeseries were normalised and combined in different ways to reflect the seasonality, duration curves and mass curves of the rivers. Various catchment characteristics were also added to the analysis and results were presented on two dendrograms. Catchments clustered into five groups, according to river types and geographical location. Most of the catchments (32 out of 40 gauging stations) clustered similarly between the two datasets. Since the data was normalised before performing the cluster analysis, the results do not give any insight into the closeness of the discharge values but showed that the conversion of the runoff successfully kept the general behaviour of the rivers for some clusters.

Thirdly, discharge values from both datasets were compared with a focus on values above the 95^{th} percentile in order to limit the data only to the extremes. In order to correct the discharge overestimation noted in most simulated flow-duration curves of the 5% highest values (38 cases out of 40 rivers), the difference between simulated and observed discharge is quantified using a coefficient of proportionality. This coefficient is then used as the correcting factor *C* from the formula that converts runoff into discharge to account for infiltration and other processes. After being calculated individually for each river, those coefficients were then averaged by cluster and applied to the simulated dataset, which greatly improved the flow-duration curves.

An EVA was then performed using the Block Maxima method on both the observed and simulated timeseries, before and after correction. Closeness Coefficients were calculated and showed a great improvement of the return levels after applying the correction for 33 out of 40 rivers.

In addition to the 40 selected gauged rivers, 20 ungauged basins were hand-picked and thrown in the cluster analysis using simulated runoff from the ICRA and catchment characteristics. The correcting factors calculated for each cluster were then applied individually to each ungauged river, according to its cluster of belonging, and flood estimates based on the corrected ICRA discharge timeseries were obtained after performing the Block Maxima method.

Eventually, for each cluster, one river was selected, and its discharge simulated by the GR6J model with the CemaNeige module. An EVA was carried out on the simulated timeseries, again using the Block Maxima method, leading to very promising results, even when the NSE values calculated over the validation period were low. In the case of these five stations, airGR was able to simulate properly the highest discharge peaks in most cases, making it possible to obtain flood estimates in the same range than when calculated from the observed timeseries.

Overall, these results show that extreme discharge values based on catchment-accumulated runoff from the ICRA dataset is able to estimate the observed high discharge after applying a correcting factor. The findings of this study were then tested on a selection of ungauged rivers to estimate design-flood values in locations where measurements are unavailable. Adding these results to the promising flood estimates calculated using hydrological modelling represent an initial methodology that could be applied to meet the challenges in determining flood characteristics of rivers were no discharge have been recorded.

References

Atlason, H., Þórarinsdóttir, T., Roberts, M. J., Massad, A.-G. R., Priet-Mahéo, M., Björnsson, B. B. (2021). Notkun einfalds vatnafarslíkans á vatnafarslega ólíkum svæðum á Íslandi. *Veðurstofa Íslands*.

Bengtsson, L., Andrae, U., Aspelien, T., Batrak, Y., Calvo, J., de Rooy, W. & Køltzow, M.Ø. (2017). The HARMONIE-AROME model configuration in the ALADIN-HIRLAM NWP system. *Mon. Wea. Rev.,* **145**, 1919–1935

Coles, S. (2001). An introduction to Statistical Modeling of Extreme Values. London; *Springer.*

Coron, L., Thirel, G., Delaigue, O., Perrin, C., & Andréassian, V. (2017). The suite of lumped GR hydrological models in an R package. Environmental Modelling & Software, 94, 166– 171.

Coron, L., Delaigue, O., Thirel, G., Perrin, C. & Michel, C. (2020). airGR: Suite of GR Hydrological Models for Precipitation-Runoff Modelling. R package version 1.4. 3.65.

Crochet, P. (2012). Flood-Duration-Frequency modeling. Application to ten catchments in Northern Iceland. *Veðurstofa Íslands.* VÍ 2012-006.

Crochet, P. & Þórarinsdóttir, T. (2014). Flood frequency estimation for ungauged catchments inIceland by combined hydrological modelling and regional frequency analysis. *Veðurstofa Íslands.* VÍ 2014–001.

Crochet, P., and Þórarinsdóttir, T. (2015). Regional flood frequency analysis: A case study in Eastern Iceland. *Veðurstofa Íslands.* VÍ 2015-007.

Demirel, M., & Kahya, E. (2007). Hydrological determination of hierarchical clustering scheme by using small experimental matrix., (bls. 161-168). doi:10.13140/RG.2.1.1885.6720

Ingber, L. (2000). Adaptive simulated annealing (ASA): Lessons learned. *ArXiv Preprint Cs/0001018.*

Ingber, L., Petraglia, A., Petraglia, M.R. & Machado, M.A. S. (2012). Adaptive simulated annealing. In Stochastic global optimization and its applications with fuzzy adaptive simulated annealing (pp. 33–62). *Springer.*

Hróðmarsson, H. B., & Þórarinsdóttir, T. (2018). Flóð íslenskra vatnsfalla, flóðagreining rennslisraða. *Veðurstofa Íslands*. VÍ 2018-003.

Massad, A.-G. R., Petersen, G. N., Þórarinsdóttir, T., Roberts, M. J. (2020). Reassessment of return levels in Iceland. *Veðurstofa Íslands*. VÍ 2020-008.

Massad, A.-G. R., Þórarinsdóttir, T., and Roberts, M.J. (2022). Design-flood estimates from daily runoff simulations using the Icelandic Reanalysis (ICRA): a first step towards estimating extremes in ungauged catchments. Veðurstofa Íslands. Greinargerð: AGM/ofl/2022-01.

Nawri, N., Pálmason, B., Petersen, G. N., Björnsson, H. & Þorsteinsson, S. (2017). The ICRA atmospheric reanalysis project for Iceland. *Veðurstofa Íslands*. VÍ 2017-005.

Neri, M., Parajka, J., and Toth, E. (2020). Importance of the informative content in the study area when regionalising rainfall-runoff model parameters: the role of nested catchments and gauging station density, *Hydrol. Earth Syst. Sci*., 24, 5149–5171.

Pagneux, E., Jóhannsdóttir, G. E., Þórarinsdóttir, T., Hróðmarsson, H. & Egilson, D. (2017). Flóð á vatnasviðum Eyjafjarðarár, Héraðsvatna, Hvítár í Borgarfirði, Lagarfljóts og Skjálfandafljóts: I. Yfirlit yfir orsakir, stærð og afleiðingar sögulegra atburða. *Veðurstofa Íslands.* VÍ 2017-006.

Pagneux, E., Jónsson, M. A., Þórarinsdóttir, T., Björnsson, B. B., Egilson, D. & Roberts, M. J. (2018). Hættumat vegna jökulhlaupa í Skaftá: Hermun flóðasviðsmynda. *Veðurstofa Íslands*. VÍ 2018-008.

Pagneux, E., Jónsson, M. Á., Björnsson, B. B., Pétursdóttir, S., Reynisson, N. F., Hróðmarsson, H. B., Einarsson, B. & Roberts, M. J. (2019). Hættumat vegna vatnsflóða í Ölfusá. *Veðurstofa Íslands*. VÍ 2019-013.

Priet-Mahéo, M., Massad, A.-G. R., Pétursdóttir, S., Þórarinsdóttir, T., & Egilson, D. (2019). Daglegar rennslisspár með notkun hliðstæðrar greiningar Harmonieveðurgagna. *Veðurstofa Íslands*.

Priet-Mahéo, M., Massad, A.-G. R., Þórarinsdóttir, T., Roberts, M. J. (2020). Veflausn með daglegum rennslisspám sem byggist á hliðstæðri greiningu veðurgagna. *Veðurstofa Íslands*.

Priet-Mahéo, M. (2021). Prófun einfalds vatnafarslíkans á grunnvatnsríkum vatnasviðum. *Veðurstofa Íslands*.

Pushpalatha, R., Perrin, C., Le Moine, N., Mathevet, T. & Andréassian, V. (2011). A downward structural sensitivity analysis of hydrological models to improve low-flow simulation. *Journal of Hydrology*, 411(1–2), 66–76.

Roberson, J. A., Cassidy, J. J., Chaudhry. M. H. (1998). Hydraulic Engineering, 2nd edition. *Wiley.*

Rist, S. (1990). Vatns er þörf. Reykjavík: Bókaútgáfa Menningarsjóðs.

Stefánsdóttir, G., Björnsson, B. B., Magnússon, S., & Egilson, D. (2014). Verklokaskýrsla vegna stjórnar vatnamála - Vinna ársins 2013. *Veðurstofa Íslands.*

Sigurðsson, F. (1990). Groundwater of glacial areas in Iceland. *Jökull* 40: 119-146.

Þórarinsdóttir, T., Roberts, M. J., Wallevik, J. E., Björnsson, B. B., Massad, A.-G., R. (2021). Hættumat vatnasviða: Eyjafjarðará, Héraðsvötn, Hvítá í Borgarfirði, Lagarfljót og Skjálfandafljót. *Veðurstofa Íslands.*

Appendix I. Flood estimates for the gauged catchments

Return levels (m^3 s^{-1}) for all gauged rivers shown in the following tables. Results are based on the measured discharge, simulated discharge from the ICRA runoff, and simulated discharge from the ICRA runoff after correction. Values are given for a 10-, 25-, 50-, 100-, 200-, and 500-year return period.

VHM 10 - Svartá

Return-period	Return levels *(m^3 s^{-1})*		
	Observations	**ICRA**	**ICRA, corrected**
10 years	82	199	115
25 years	96	224	129
50 years	106	242	139
100 years	116	260	150
200 years	127	278	160
500 years	140	302	174

VHM 12 - Haukadalsá

Return-period	Return levels *(m^3 s^{-1})*		
	Observations	**ICRA**	**ICRA, corrected**
10 years	98	150	86
25 years	119	174	100
50 years	134	191	110
100 years	149	209	120
200 years	164	227	131
500 years	184	250	144

VHM 19 - Dynjandisá

Return-period	Return levels *(m^3 s^{-1})*		
	Observations	**ICRA**	**ICRA, corrected**
10 years	29	59	34
25 years	35	67	38
50 years	39	72	42
100 years	43	78	45
200 years	47	84	48
500 years	52	91	52

<u>VHM 26 - Sandá</u>

Return-period	Return levels *($m^3 s^{-1}$)*		
	Observations	**ICRA**	**ICRA, corrected**
10 years	108	259	149
25 years	128	302	174
50 years	143	334	192
100 years	157	365	210
200 years	172	397	229
500 years	191	438	253

<u>VHM 30 - Þjórsá</u>

Return-period	Return levels *($m^3 s^{-1}$)*		
	Observations	**ICRA**	**ICRA, corrected**
10 years	1499	4750	1653
25 years	1775	5391	1876
50 years	1981	5866	2041
100 years	2184	6338	2206
200 years	2387	6809	2369
500 years	2655	7429	2585

<u>VHM 38 - Þverá</u>

Return-period	Return levels *($m^3 s^{-1}$)*		
	Observations	**ICRA**	**ICRA, corrected**
10 years	26	64	37
25 years	32	77	44
50 years	36	86	50
100 years	40	95	55
200 years	45	105	60
500 years	50	117	67

VHM 43 - Brúará

Return-period	Return levels *($m^3 s^{-1}$)*		
	Observations	**ICRA**	**ICRA, corrected**
10 years	163	748	260
25 years	182	853	297
50 years	195	931	324
100 years	209	1109	351
200 years	223	1086	378
500 years	241	1188	413

VHM 45 - Vatnsdalsá

Return-period	Return levels *($m^3 s^{-1}$)*		
	Observations	**ICRA**	**ICRA, corrected**
10 years	107	217	125
25 years	129	252	145
50 years	145	278	160
100 years	160	303	175
200 years	176	329	189
500 years	197	362	209

VHM 48 - Selá

Return-period	Return levels *($m^3 s^{-1}$)*		
	Observations	**ICRA**	**ICRA, corrected**
10 years	191	442	146
25 years	229	496	164
50 years	258	537	177
100 years	286	577	190
200 years	314	617	204
500 years	351	670	221

VHM 51 - Hjaltadalsá

Return-period	Return levels *(m^3 s^{-1})*		
	Observations	**ICRA**	**ICRA, corrected**
10 years	87	226	111
25 years	100	256	126
50 years	110	279	137
100 years	119	301	148
200 years	129	324	159
500 years	141	353	174

VHM 59 – Ytri-Rangá

Return-period	Return levels *(m^3 s^{-1})*		
	Observations	**ICRA**	**ICRA, corrected**
10 years	137	517	180
25 years	161	593	206
50 years	178	650	226
100 years	196	707	246
200 years	213	763	265
500 years	236	837	291

VHM 60 – Eystri-Rangá

Return-period	Return levels *(m^3 s^{-1})*		
	Observations	**ICRA**	**ICRA, corrected**
10 years	101	490	171
25 years	118	567	197
50 years	131	624	217
100 years	144	681	237
200 years	157	737	256
500 years	174	811	282

__VHM 64 - Ölfusá__

Return-period	Return levels *($m^3 s^{-1}$)*		
	Observations	**ICRA**	**ICRA, corrected**
10 years	1386	5109	1178
25 years	1599	5784	2013
50 years	1758	6286	2187
100 years	1916	6783	2361
200 years	2072	7279	2533
500 years	2279	7933	2761

__VHM 66 - Hvitá__

Return-period	Return levels *($m^3 s^{-1}$)*		
	Observations	**ICRA**	**ICRA, corrected**
10 years	347	1432	616
25 years	410	1652	710
50 years	456	1815	781
100 years	503	1977	850
200 years	549	2138	920
500 years	609	2351	1011

__VHM 68 - Tungufljót__

Return-period	Return levels *($m^3 s^{-1}$)*		
	Observations	**ICRA**	**ICRA, corrected**
10 years	168	226	79
25 years	202	264	92
50 years	227	291	101
100 years	252	319	111
200 years	277	347	121
500 years	310	383	133

VHM 81 - Úlfarsá

Return-period	Return levels *(m^3 s^{-1})*		
	Observations	**ICRA**	**ICRA, corrected**
10 years	17	46	16
25 years	20	54	19
50 years	23	60	21
100 years	25	66	23
200 years	28	71	25
500 years	31	79	28

VHM 83 - Fjarðará

Return-period	Return levels *(m^3 s^{-1})*		
	Observations	**ICRA**	**ICRA, corrected**
10 years	37	78	39
25 years	44	92	45
50 years	50	102	50
100 years	56	111	55
200 years	61	121	60
500 years	68	134	66

VHM 92 - Bægisá

Return-period	Return levels *(m^3 s^{-1})*		
	Observations	**ICRA**	**ICRA, corrected**
10 years	17	55	27
25 years	20	65	32
50 years	22	72	35
100 years	24	79	39
200 years	25	86	42
500 years	28	96	47

VHM 102 – Jökulsá á Fjöllum

Return-period	**Return levels *(m^3 s^{-1})***		
	Observations	**ICRA**	**ICRA, corrected**
10 years	730	2618	1126
25 years	842	2958	1272
50 years	924	3210	1380
100 years	1006	3460	1488
200 years	1087	3709	1595
500 years	1195	4038	1736

VHM 110 – Jökulsá á Dal

Return-period	**Return levels *(m^3 s^{-1})***		
	Observations	**ICRA**	**ICRA, corrected**
10 years	870	2125	914
25 years	1026	2461	1058
50 years	1142	2711	1166
100 years	1257	2958	1272
200 years	1371	3205	1378
500 years	1522	3530	1518

VHM 116- Svartá

Return-period	**Return levels *(m^3 s^{-1})***		
	Observations	**ICRA**	**ICRA, corrected**
10 years	32	355	117
25 years	34	410	135
50 years	36	450	149
100 years	38	490	162
200 years	40	530	175
500 years	42	583	192

VHM 121 - Ormarsá

Return-period	Return levels *(m^3 s^{-1})*		
	Observations	**ICRA**	**ICRA, corrected**
10 years	40	162	56
25 years	46	188	66
50 years	51	208	72
100 years	55	227	79
200 years	60	246	86
500 years	66	271	94

VHM 128 - Norðurá

Return-period	Return levels *(m^3 s^{-1})*		
	Observations	**ICRA**	**ICRA, corrected**
10 years	410	522	300
25 years	497	617	356
50 years	561	688	397
100 years	625	759	437
200 years	689	829	478
500 years	773	922	531

VHM 144 – Austari-Jökulsá

Return-period	Return levels *(m^3 s^{-1})*		
	Observations	**ICRA**	**ICRA, corrected**
10 years	222	590	290
25 years	252	686	338
50 years	274	758	373
100 years	296	829	408
200 years	318	900	443
500 years	347	993	489

VHM 148 - Fossá

Return-period	Return levels *($m^3 s^{-1}$)*		
	Observations	**ICRA**	**ICRA, corrected**
10 years	152	184	106
25 years	184	208	120
50 years	208	227	131
100 years	231	245	141
200 years	255	263	151
500 years	285	287	165

VHM 149 - Geithellnaá

Return-period	Return levels *($m^3 s^{-1}$)*		
	Observations	**ICRA**	**ICRA, corrected**
10 years	202	321	185
25 years	237	371	214
50 years	263	409	235
100 years	288	446	257
200 years	314	483	278
500 years	347	532	306

VHM 150 - Djúpá

Return-period	Return levels *($m^3 s^{-1}$)*		
	Observations	**ICRA**	**ICRA, corrected**
10 years	288	508	219
25 years	352	573	246
50 years	400	620	267
100 years	447	668	287
200 years	495	715	397
500 years	557	777	334

<u>VHM 162 – Jökulsá á Fjöllum</u>

Return-period	Return levels *($m^3 s^{-1}$)*		
	Observations	**ICRA**	**ICRA, corrected**
10 years	408	1449	623
25 years	481	1642	706
50 years	536	1785	767
100 years	591	1927	829
200 years	645	2068	889
500 years	716	2255	970

<u>VHM 185 - Hólmsá</u>

Return-period	Return levels *($m^3 s^{-1}$)*		
	Observations	**ICRA**	**ICRA, corrected**
10 years	42	313	109
25 years	56	356	124
50 years	65	389	135
100 years	75	421	146
200 years	85	452	157
500 years	97	494	172

<u>VHM 198 – Hvalá</u>

Return-period	Return levels *($m^3 s^{-1}$)*		
	Observations	**ICRA**	**ICRA, corrected**
10 years	206	301	148
25 years	247	339	167
50 years	277	368	181
100 years	307	396	195
200 years	337	424	208
500 years	376	461	227

VHM 200 - Fnjóská

Return-period	Return levels *($m^3 s^{-1}$)*		
	Observations	**ICRA**	**ICRA, corrected**
10 years	392	859	495
25 years	479	996	574
50 years	543	1098	632
100 years	607	1199	690
200 years	671	1299	748
500 years	755	1432	825

VHM 204 - Vatnsdalsá

Return-period	Return levels *($m^3 s^{-1}$)*		
	Observations	**ICRA**	**ICRA, corrected**
10 years	76	141	81
25 years	91	161	93
50 years	102	175	101
100 years	114	190	109
200 years	125	204	118
500 years	140	223	129

VHM 205 - Kelduá

Return-period	Return levels *($m^3 s^{-1}$)*		
	Observations	**ICRA**	**ICRA, corrected**
10 years	376	316	182
25 years	482	372	214
50 years	560	414	238
100 years	637	455	262
200 years	715	496	286
500 years	817	550	317

VHM 206 - Fellsá

Return-period	**Return levels *(m^3 s^{-1})***		
	Observations	**ICRA**	**ICRA, corrected**
10 years	120	122	70
25 years	147	145	83
50 years	166	161	93
100 years	186	178	103
200 years	206	195	112
500 years	232	217	125

VHM 218 - Markarfljót

Return-period	**Return levels *(m^3 s^{-1})***		
	Observations	**ICRA**	**ICRA, corrected**
10 years	188	662	219
25 years	215	756	249
50 years	234	825	272
100 years	254	893	295
200 years	273	962	317
500 years	299	1052	347

VHM 233 - Kreppá

Return-period	**Return levels *(m^3 s^{-1})***		
	Observations	**ICRA**	**ICRA, corrected**
10 years	456	564	242
25 years	568	637	274
50 years	652	691	297
100 years	735	746	321
200 years	818	799	344
500 years	927	870	374

__VHM 238 - Skjálfandafljót__

Return-period	Return levels *($m^3 s^{-1}$)*		
	Observations	**ICRA**	**ICRA, corrected**
10 years	468	1186	391
25 years	565	1360	449
50 years	636	1490	492
100 years	708	1618	534
200 years	779	1747	576
500 years	873	1916	632

__VHM 271 - Sog__

Return-period	Return levels *($m^3 s^{-1}$)*		
	Observations	**ICRA**	**ICRA, corrected**
10 years	227	1214	422
25 years	250	1386	482
50 years	268	1513	527
100 years	285	1640	571
200 years	303	1766	615
500 years	326	1933	673

__VHM 400 - Vattardalsá__

Return-period	Return levels *($m^3 s^{-1}$)*		
	Observations	**ICRA**	**ICRA, corrected**
10 years	35	122	70
25 years	40	140	80
50 years	45	153	88
100 years	49	166	96
200 years	53	180	103
500 years	59	197	113

VHM 408 - Sandá

Return-period	**Return levels *(m^3 s^{-1})***		
	Observations	**ICRA**	**ICRA, corrected**
10 years	112	1016	437
25 years	140	1155	497
50 years	160	1258	541
100 years	180	1360	585
200 years	200	1463	629
500 years	227	1597	687

VHM 411 – Stóra Laxá

Return-period	**Return levels *(m^3 s^{-1})***		
	Observations	**ICRA**	**ICRA, corrected**
10 years	409	377	217
25 years	533	439	253
50 years	625	485	279
100 years	717	530	305
200 years	808	576	332
500 years	928	636	366

Appendix II. Flood estimates for the ungauged catchments

Return level plot for all the ungauged rivers, based on simulations of daily discharge before (red) and after correction (orange). Dashed-lines show the 25-year return level for the different datasets.

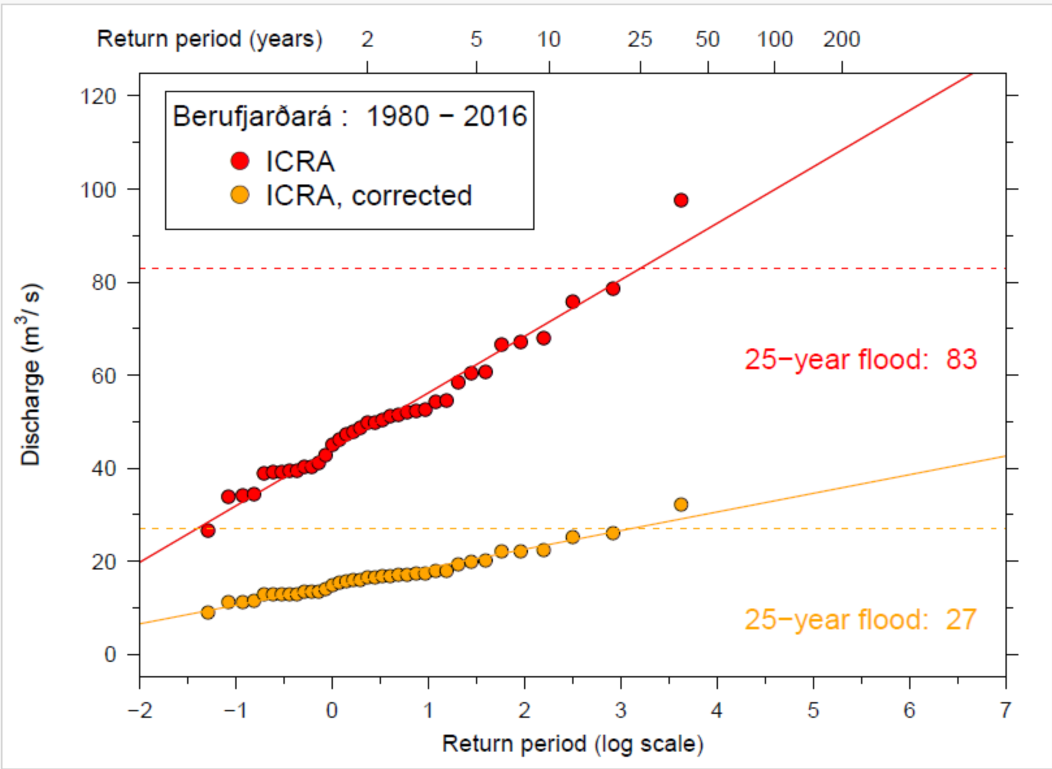

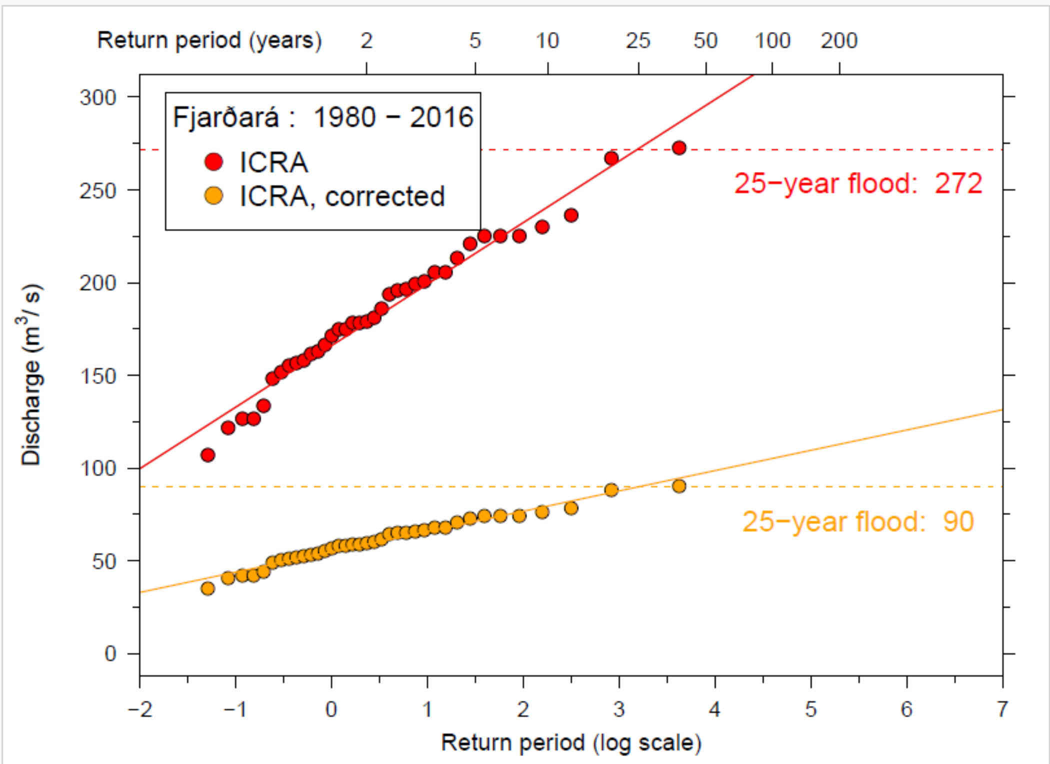

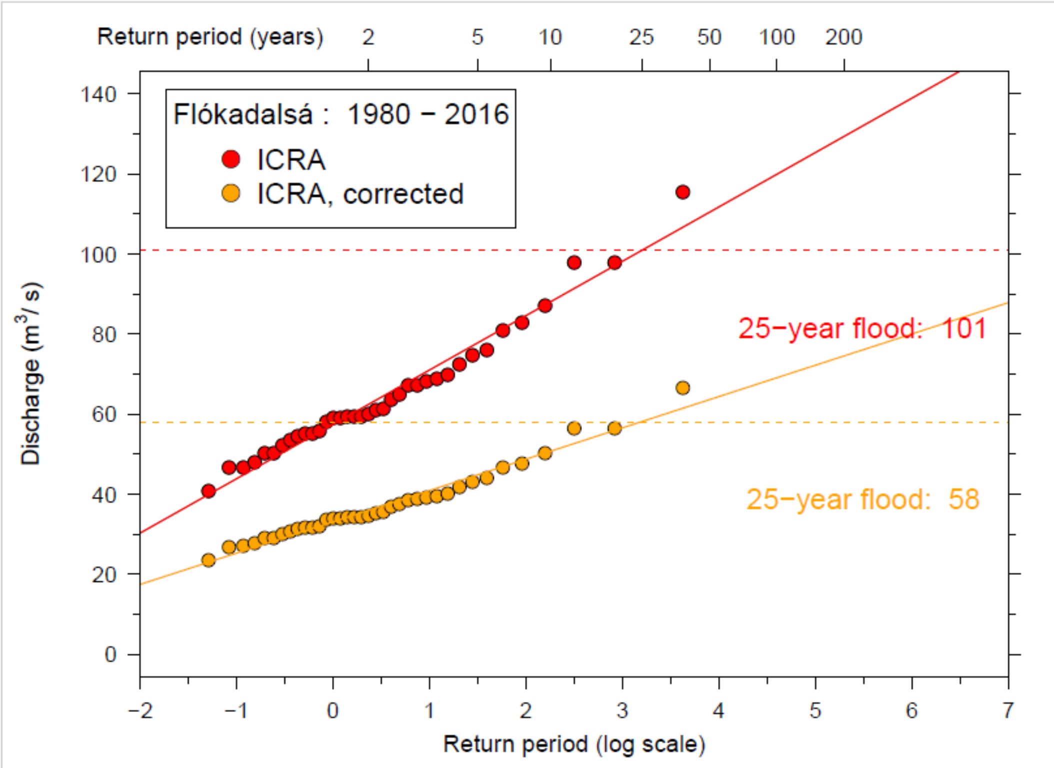

Return period (years)
2
5
10
25
50
100
200
Flókadalsá : 1980 − 2016
ICRA
ICRA, corrected
25−year flood: 101
25−year flood: 58
Discharge (m³/ s)
140
120
100
80
60
40
20
0
−2
−1
0
1
2
3
4
5
6
7
Return period (log scale)

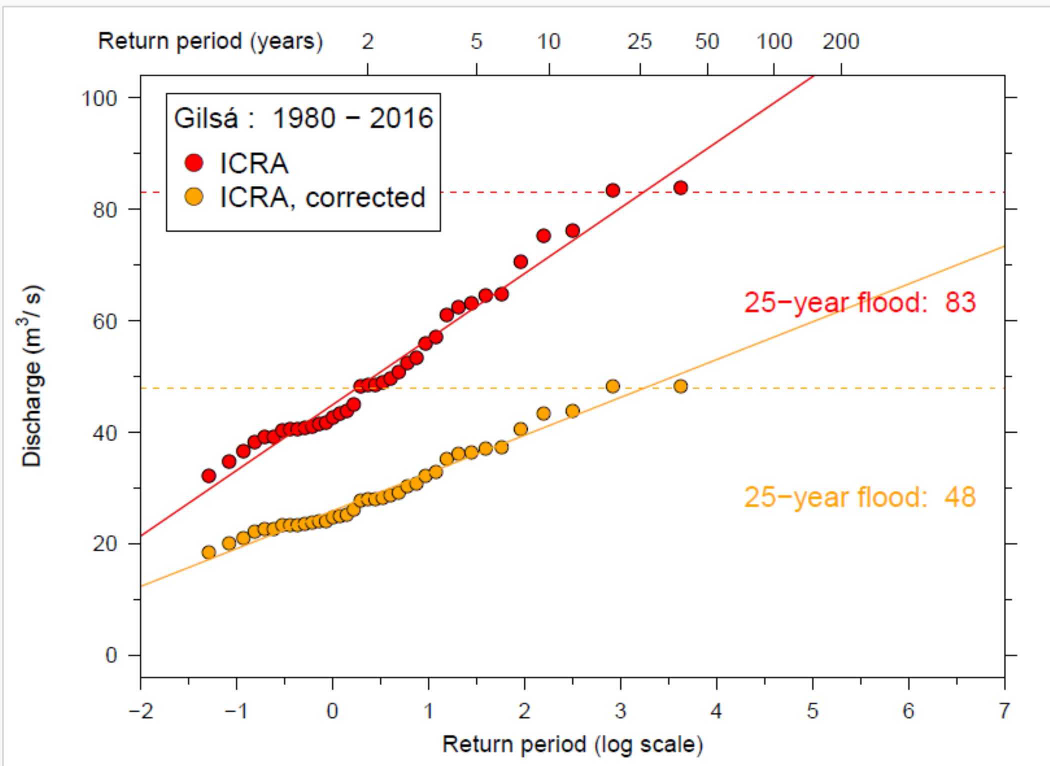

Return period (years)
2
5
10
25
50
100
200
Gilsá : 1980 − 2016
ICRA
ICRA, corrected
25−year flood: 83
25−year flood: 48
Discharge (m³/ s)
100
80
60
40
20
0
−2
−1
0
1
2
3
4
5
6
7
Return period (log scale)

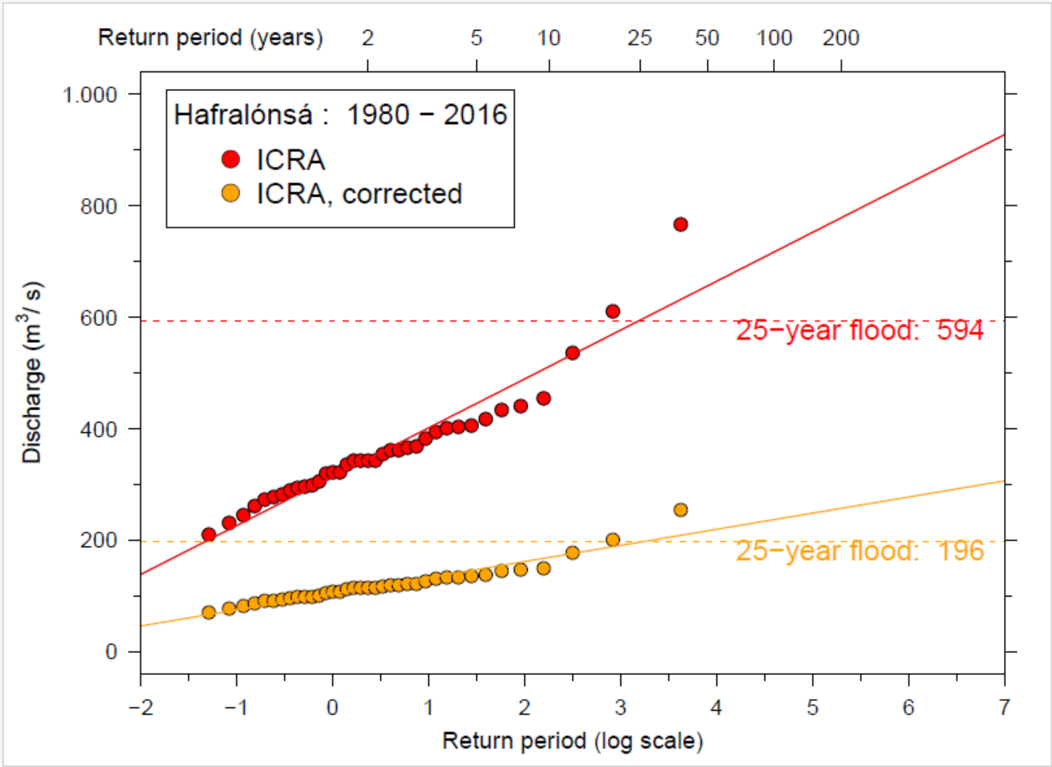

Return period (years)
2
5
10
25
50
100
200
1.000
800
600
400
200
0
Discharge (m^3/ s)
Hafralónsá : 1980 − 2016
ICRA
ICRA, corrected
25−year flood: 594
25−year flood: 196
−2
−1
0
1
2
3
4
5
6
7
Return period (log scale)

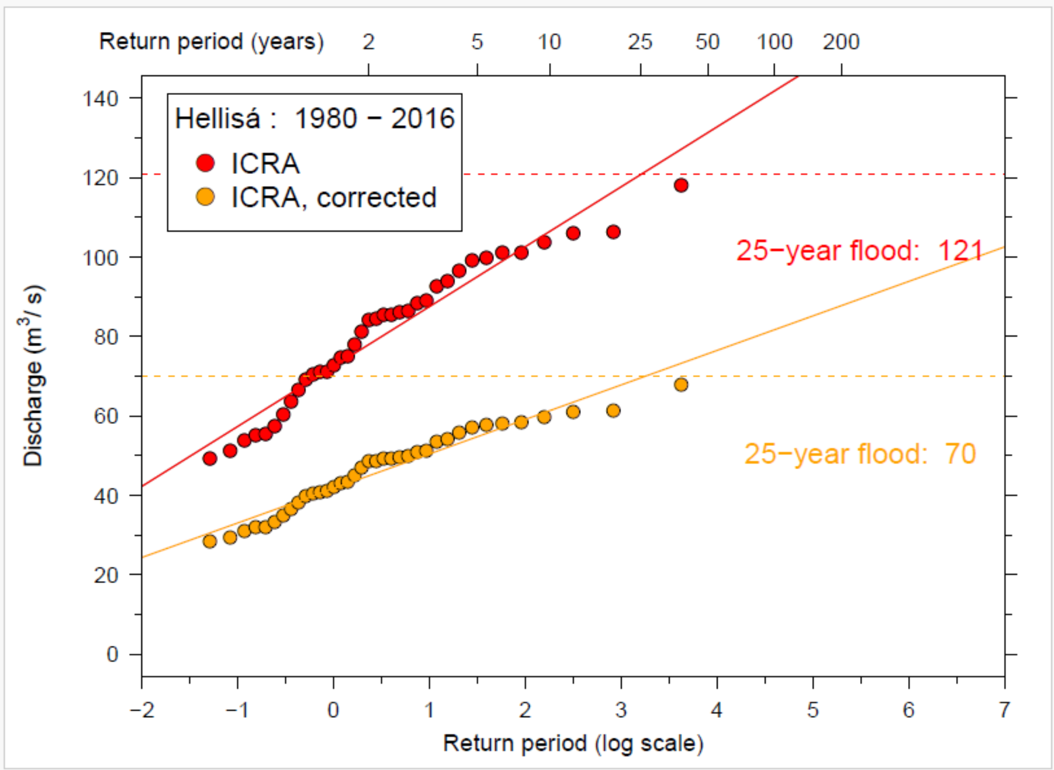

Return period (years)
2
5
10
25
50
100
200
140
120
100
80
60
40
20
0
Discharge (m^3/ s)
Hellisá : 1980 − 2016
ICRA
ICRA, corrected
25−year flood: 121
25−year flood: 70
−2
−1
0
1
2
3
4
5
6
7
Return period (log scale)

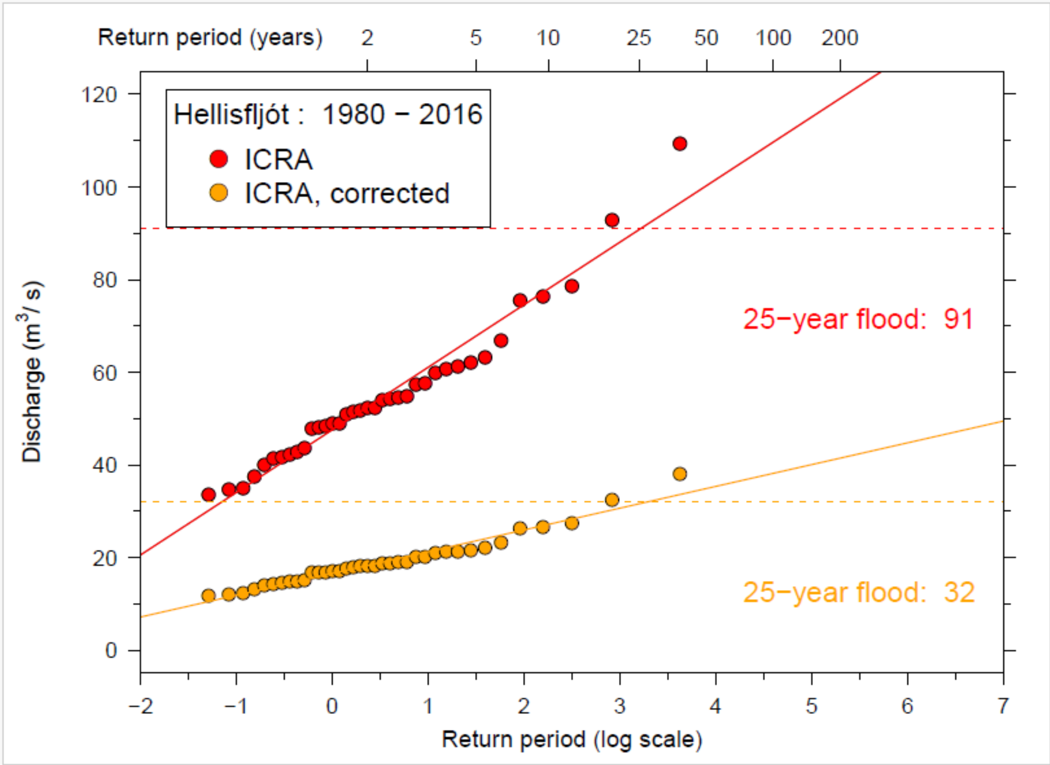
Return period (years)
2
5
10
25
50
100
200
120
100
80
60
40
20
0
Discharge (m3/s)
Hellisfljót : 1980 − 2016
ICRA
ICRA, corrected
25−year flood: 91
25−year flood: 32
−2
−1
0
1
2
3
4
5
6
7
Return period (log scale)

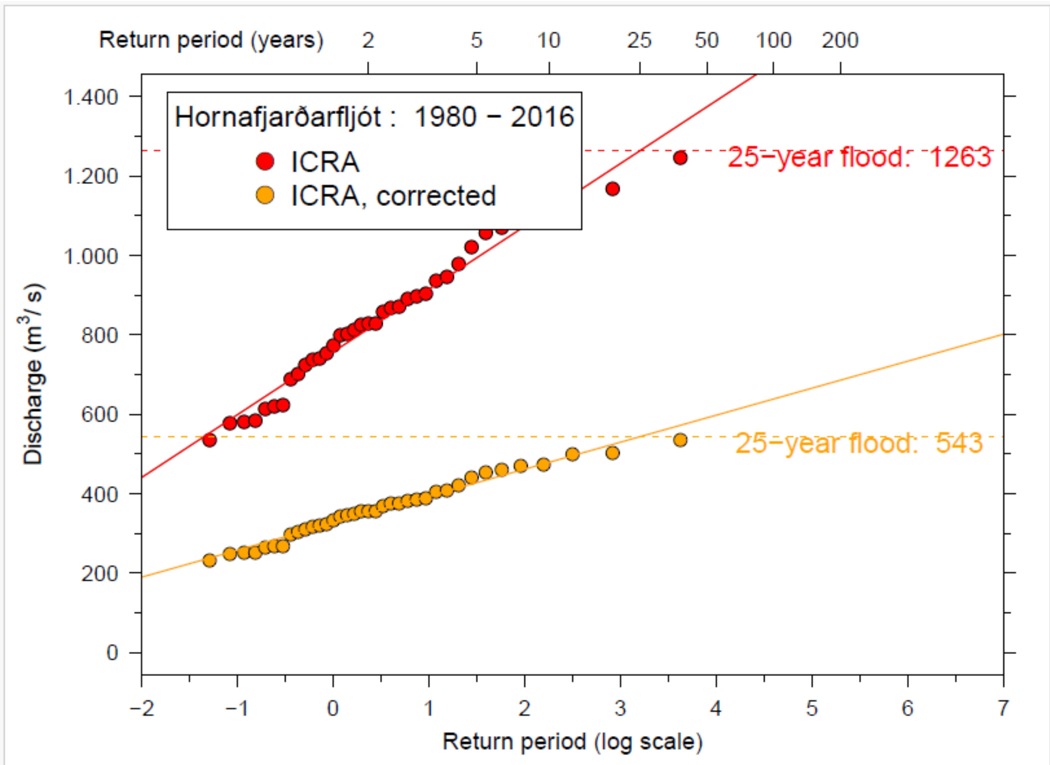
Return period (years)
2
5
10
25
50
100
200
1.400
1.200
1.000
800
600
400
200
0
Discharge (m3/s)
Hornafjarðarfljót : 1980 − 2016
ICRA
ICRA, corrected
25−year flood: 1263
25−year flood: 543
−2
−1
0
1
2
3
4
5
6
7
Return period (log scale)

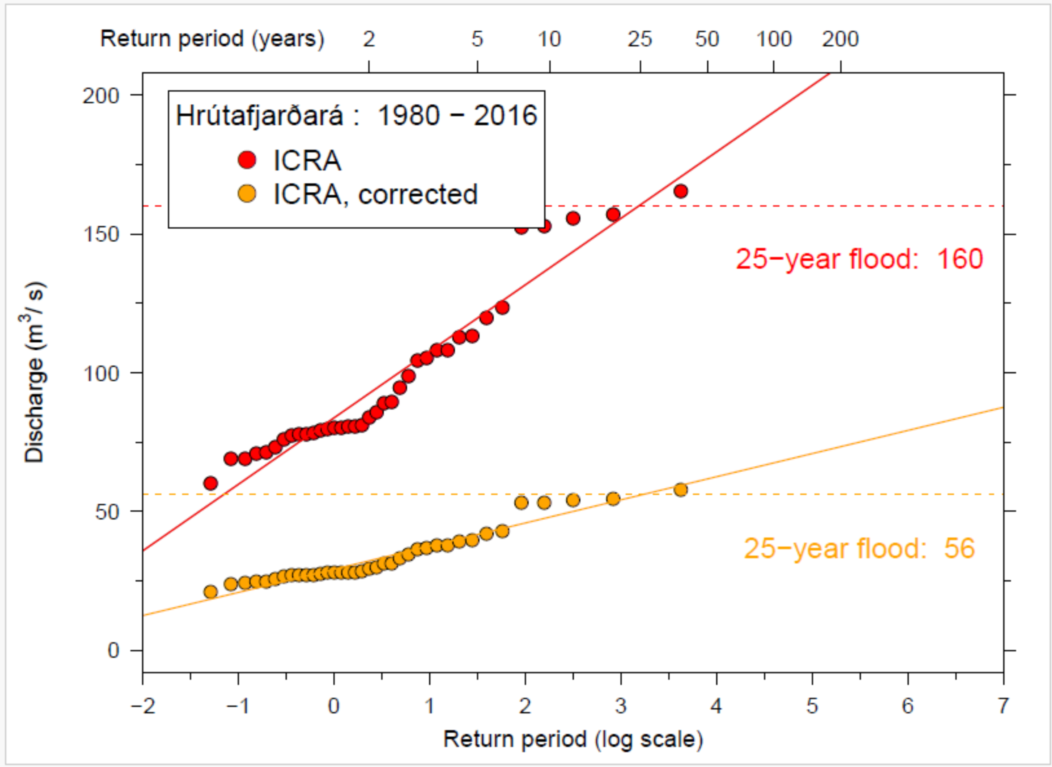

Return period (years)
2
5
10
25
50
100
200
Hrútafjarðará : 1980 − 2016
ICRA
ICRA, corrected
25−year flood: 160
25−year flood: 56
Discharge (m³/ s)
Return period (log scale)

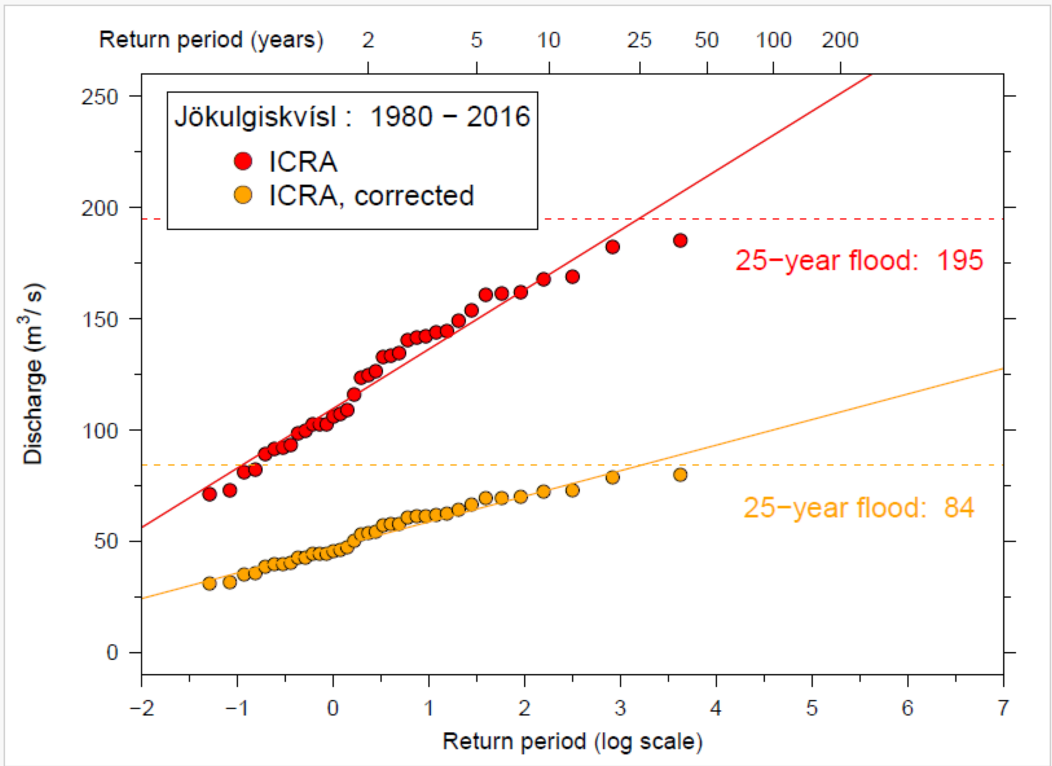

Return period (years)
2
5
10
25
50
100
200
Jökulgiskvísl : 1980 − 2016
ICRA
ICRA, corrected
25−year flood: 195
25−year flood: 84
Discharge (m³/ s)
Return period (log scale)

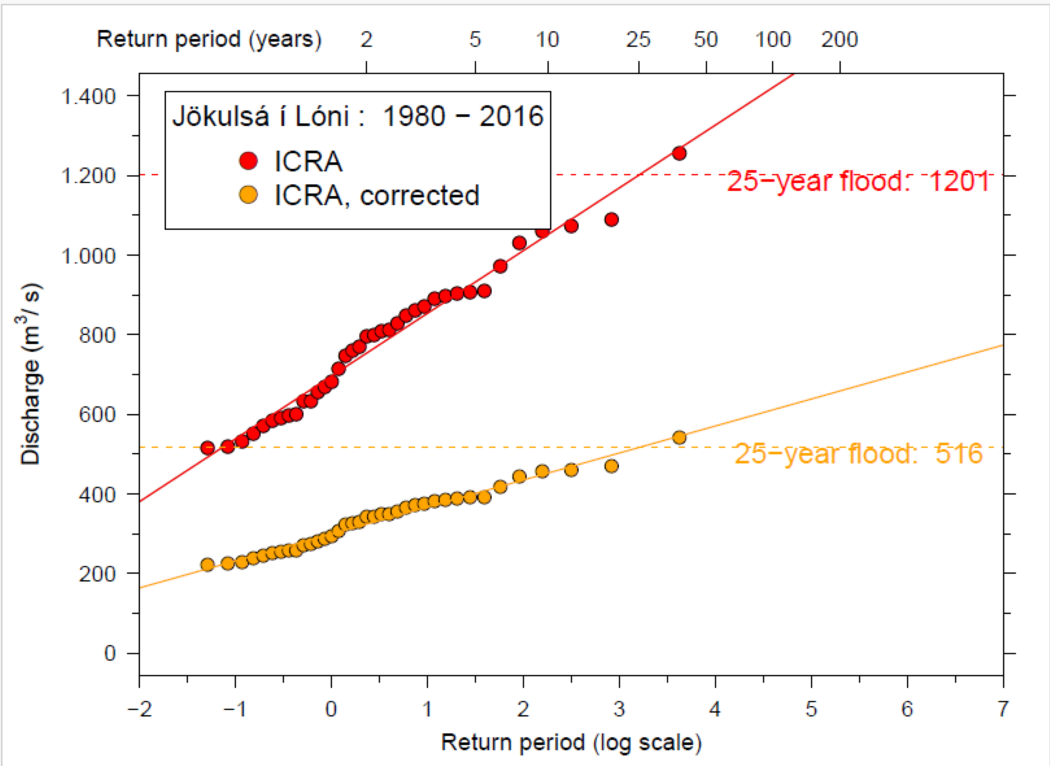

Return period (years)
2
5
10
25
50
100
200
1.400
1.200
1.000
800
600
400
200
0
Discharge (m³/ s)
Jökulsá í Lóni : 1980 − 2016
ICRA
ICRA, corrected
25−year flood: 1201
25−year flood: 516
−2
−1
0
1
2
3
4
5
6
7
Return period (log scale)

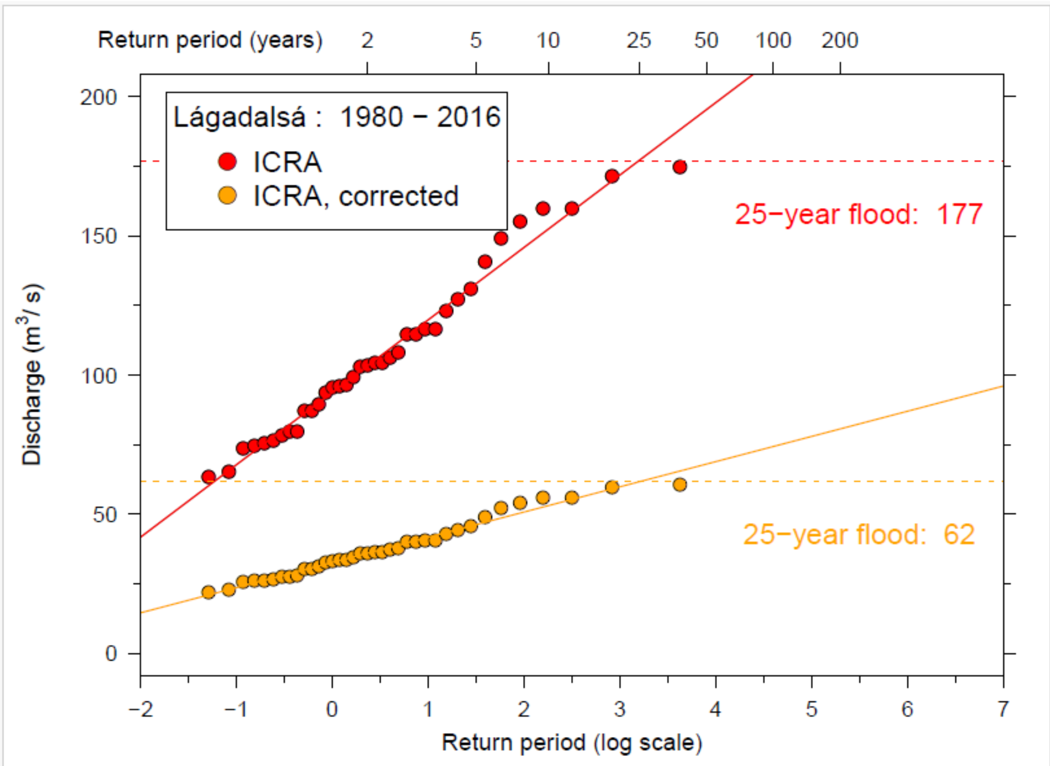

Return period (years)
2
5
10
25
50
100
200
200
150
100
50
0
Discharge (m³/ s)
Lágadalsá : 1980 − 2016
ICRA
ICRA, corrected
25−year flood: 177
25−year flood: 62
−2
−1
0
1
2
3
4
5
6
7
Return period (log scale)

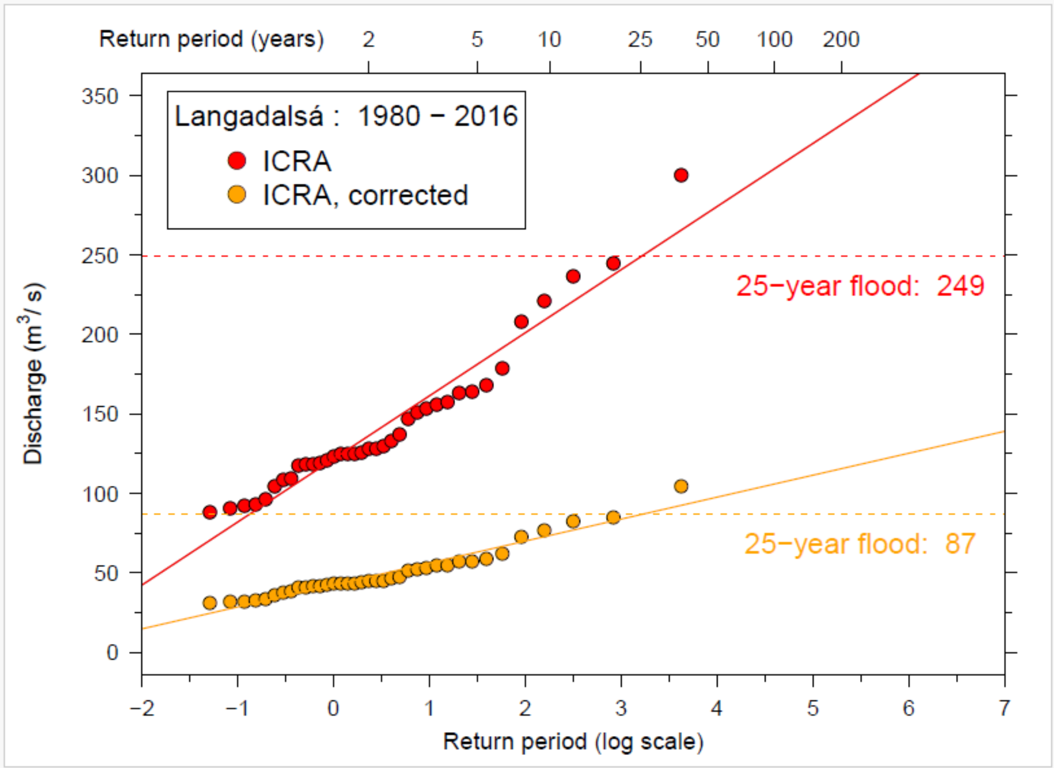

Return period (years)
2
5
10
25
50
100
200
Langadalsá : 1980 − 2016
ICRA
ICRA, corrected
25−year flood: 249
25−year flood: 87
Discharge (m³/ s)
Return period (log scale)

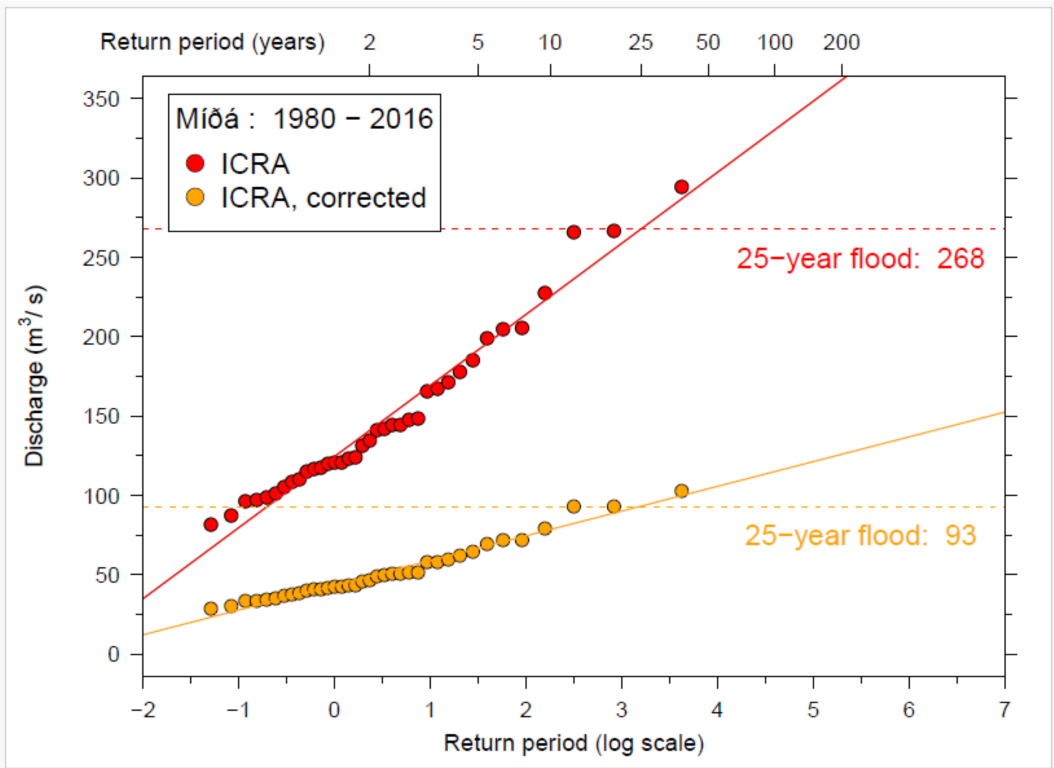

Return period (years)
2
5
10
25
50
100
200
Míðá : 1980 − 2016
ICRA
ICRA, corrected
25−year flood: 268
25−year flood: 93
Discharge (m³/ s)
Return period (log scale)

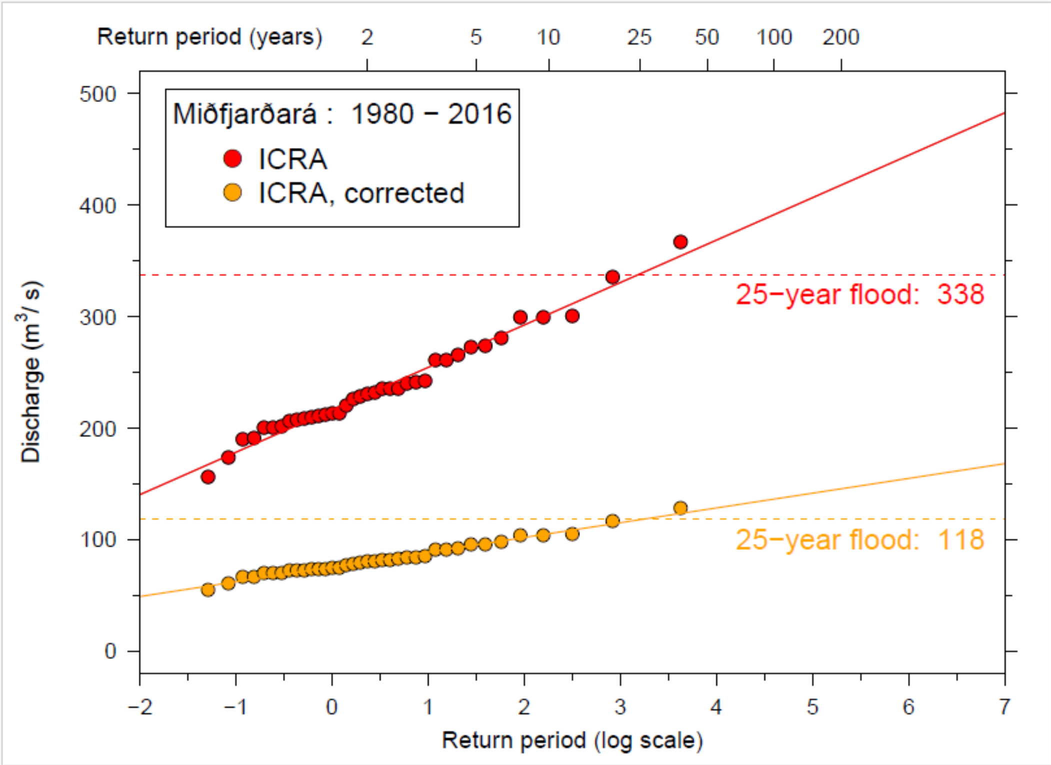

Return period (years)
2
5
10
25
50
100
200
Miðfjarðará : 1980 − 2016
ICRA
ICRA, corrected
25−year flood: 338
25−year flood: 118
Discharge (m^3/ s)
Return period (log scale)

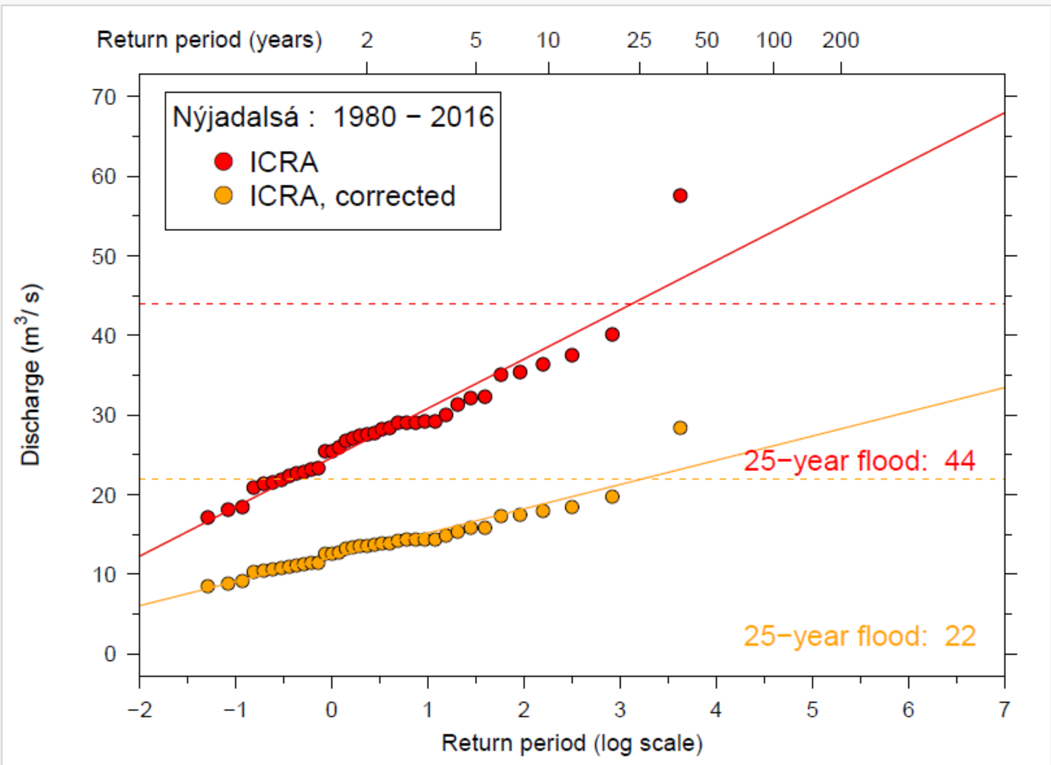

Return period (years)
2
5
10
25
50
100
200
Nýjadalsá : 1980 − 2016
ICRA
ICRA, corrected
25−year flood: 44
25−year flood: 22
Discharge (m^3/ s)
Return period (log scale)

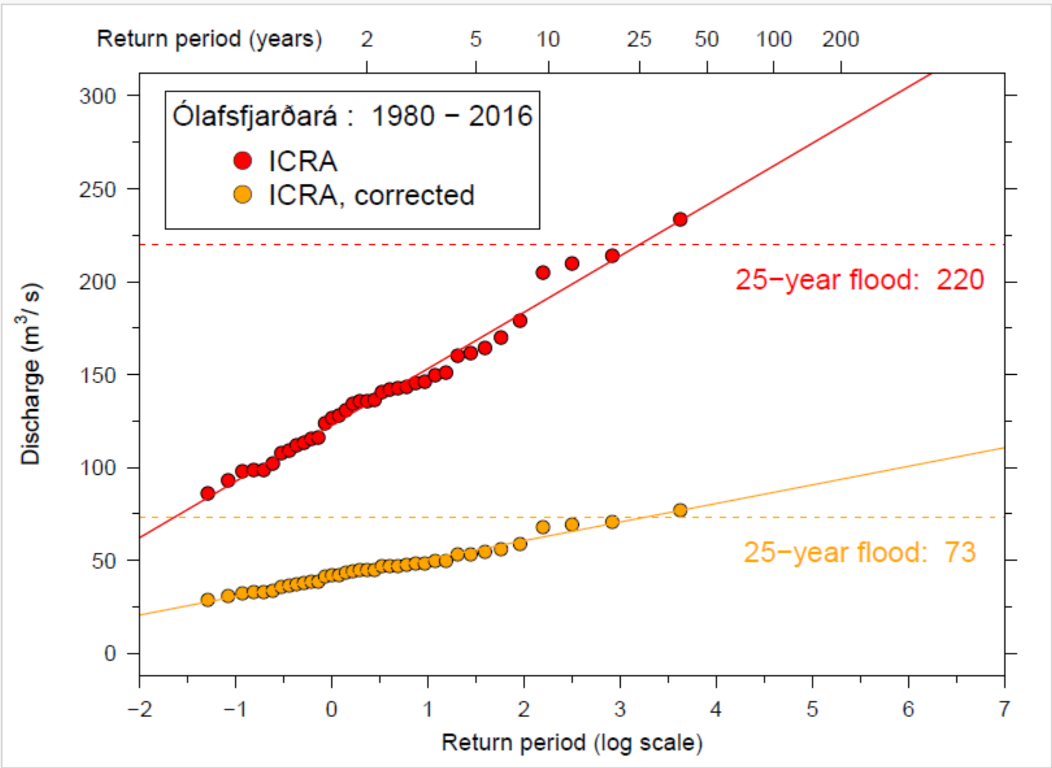
Return period (years)
2
5
10
25
50
100
200
Ólafsfjarðará : 1980 − 2016
ICRA
ICRA, corrected
25−year flood: 220
25−year flood: 73
Discharge (m³/ s)
300
250
200
150
100
50
0
−2
−1
0
1
2
3
4
5
6
7
Return period (log scale)

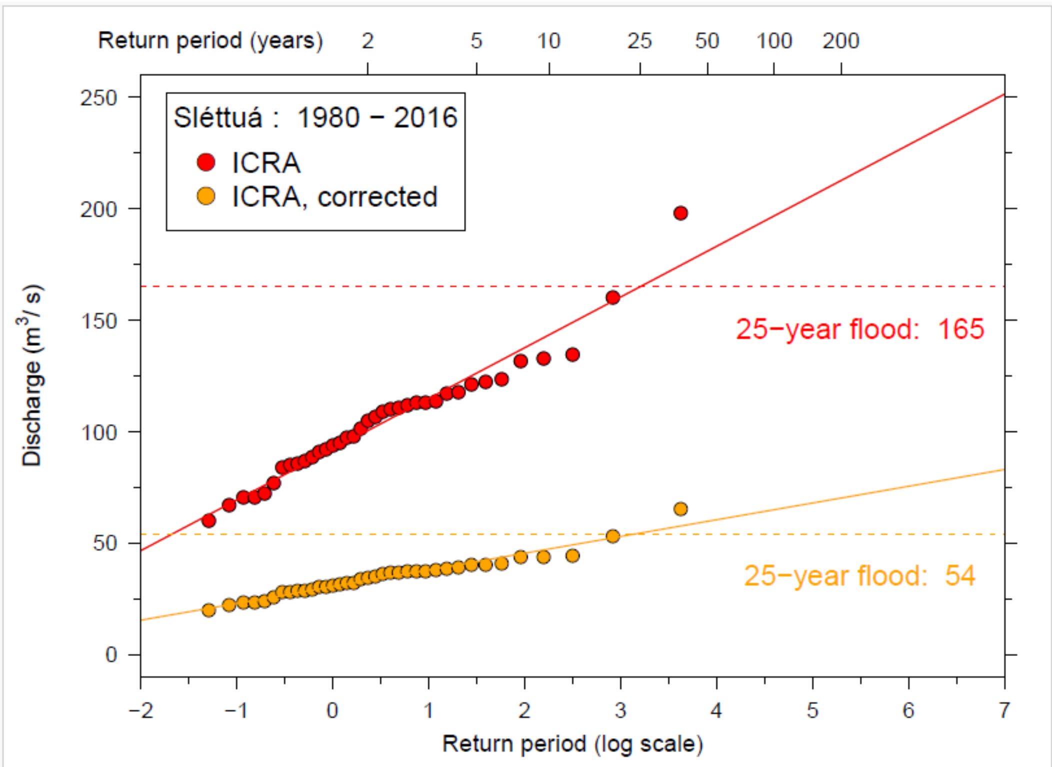
Return period (years)
2
5
10
25
50
100
200
Sléttuá : 1980 − 2016
ICRA
ICRA, corrected
25−year flood: 165
25−year flood: 54
Discharge (m³/ s)
250
200
150
100
50
0
−2
−1
0
1
2
3
4
5
6
7
Return period (log scale)

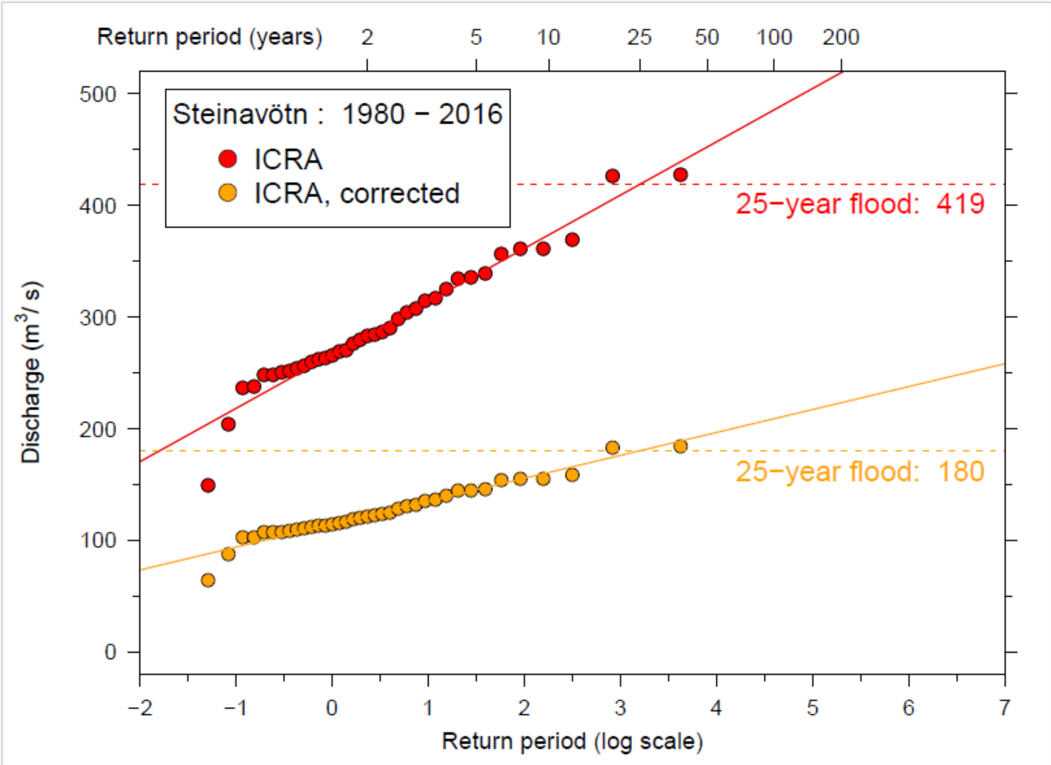

Return period (years)
2
5
10
25
50
100
200
Steinavötn : 1980 − 2016
ICRA
ICRA, corrected
25−year flood: 419
25−year flood: 180
Discharge (m³/ s)
500
400
300
200
100
0
−2
−1
0
1
2
3
4
5
6
7
Return period (log scale)

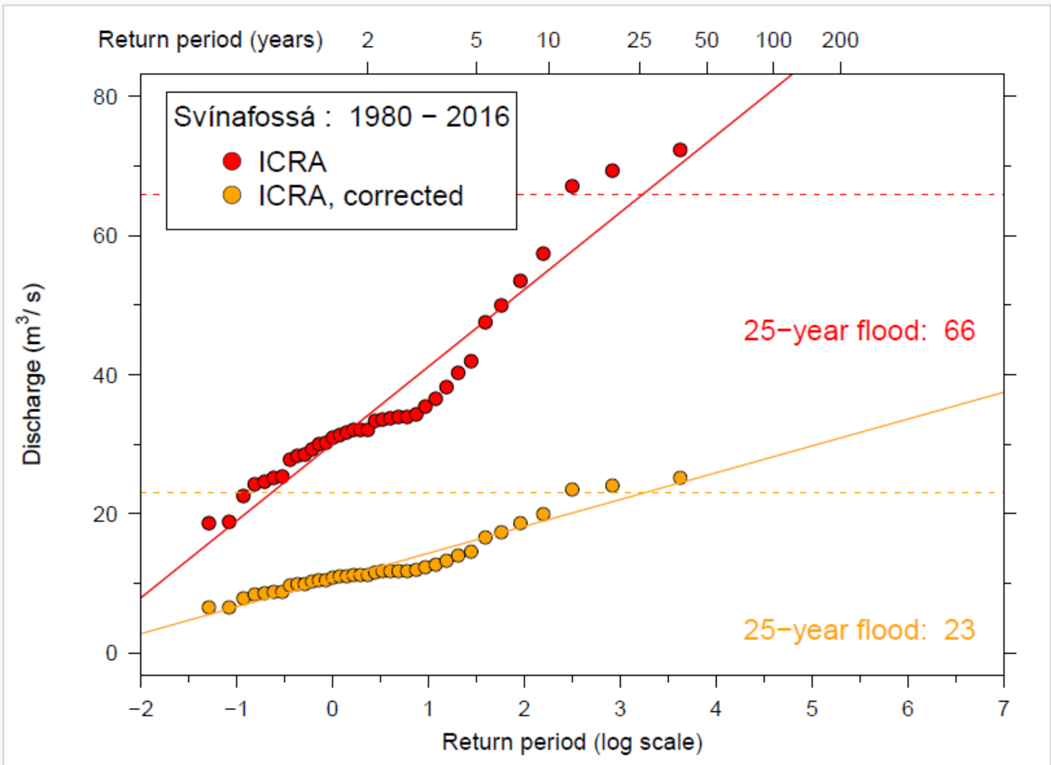

Return period (years)
2
5
10
25
50
100
200
Svínafossá : 1980 − 2016
ICRA
ICRA, corrected
25−year flood: 66
25−year flood: 23
Discharge (m³/ s)
80
60
40
20
0
−2
−1
0
1
2
3
4
5
6
7
Return period (log scale)

Return levels (m3 s-1) for all ungauged rivers. Results are based on the simulated discharge from the ICRA runoff before (top table) and after (bottom table) correction.

<u>*ICRA discharge – before correction*</u>

	10-year	25-year	50-year	100-year	200-year	500-year
Berufjarðará	71	83	91	100	108	120
Fjarðará	241	271	296	319	342	372
Flókadalsá	88	101	110	120	129	142
Gilsá	71	83	91	99	107	118
Hafralónsá	511	594	656	717	779	859
Hellisá	106	121	131	142	152	166
Hellisfljót	78	91	100	110	119	132
Hornafjarðarfljót	1113	1263	1375	1485	1595	1740
Hrútafjarðará	138	160	177	194	211	233
Jökulgilskvísl	170	195	214	233	251	276
Jökulsá í Lóni	1051	1201	1312	1422	1532	1677
Lágadalsá	152	177	195	214	232	256
Langadalsá	211	249	277	304	332	368
Miðá	225	268	299	331	362	403
Miðfjarðará	302	338	365	392	418	453
Nýjadalsá	39	44	49	53	57	63
Ólafsfjarðará	191	220	241	262	284	311
Sléttuá	143	165	181	197	213	234
Steinavötn	374	419	452	486	519	563
Svínafossá	55	66	73	81	89	99

<u>*ICRA discharge – after correction*</u>

	10-year	25-year	50-year	100-year	200-year	500-year
Berufjarðará	24	27	30	33	36	39
Fjarðará	79	90	98	105	113	123
Flókadalsá	51	58	64	69	75	82
Gilsá	41	48	52	57	62	68
Hafralónsá	169	196	217	237	257	284
Hellisá	61	70	76	82	88	96
Hellisfljót	27	32	35	38	41	46
Hornafjarðarfljót	479	543	591	639	686	748
Hrútafjarðará	48	56	62	68	73	81
Jökulgilskvísl	73	84	92	100	108	119
Jökulsá í Lóni	452	516	564	611	659	721
Lágadalsá	53	62	68	74	81	89
Langadalsá	73	87	96	106	116	128
Miðá	78	93	104	115	126	140
Miðfjarðará	105	118	127	136	146	158
Nýjadalsá	19	22	24	26	28	31
Ólafsfjarðará	63	73	80	87	94	103
Sléttuá	47	54	60	65	70	77
Steinavötn	161	180	195	209	223	242
Svínafossá	19	23	26	28	31	34